Norwegian University
of Life Sciences

Development and application of an isomer specific quantification method for perfluoroalkyl carboxylic acids (PFCAs) in Arctic environmental samples

Ada B.H.U. Njerve
Chemistry

Acknowledgements

This thesis would not be possible without several people, and I would like to share my gratitude with them. First, I would like to thank Dr. Roland Kallenborn, my main advisor at the faculty of Chemistry, Biotechnology and Food science for an interesting project, writing advise, and guidance. And for valuable guidance, hands-on training, and support during the project, I also thank my co-advisors Erik Magnus Ræder and Stine Göransson Aanrud at the faculty of Veterinary Medicine.

Second, I would like to show my greatest gratitude to my parents who have always supported me every step of the way. Not coming from a scientific backgrounds themselves, they have always showed interest in what I do – which I really appreciate. Also, thank you to my two siblings for showing support and interest, it means the world to me.

Finally, a special, big thanks to all my amazing friends, including my roommates in Ås, my friends from Billingstad and Chicago, and all the rest. I would not be able to do this without you.

Norwegian University of Life Sciences

May 12th, 2023

Ada Njerve

II

Abstract

Per- and polyfluoroalkyl substances (PFAS) are anthropogenic, persistent pollutants found all over the world. These compounds have the ability to repel both water and oil, and are known for their durability. Since the 1950s perfluoroalkyl carboxylic acids (PFCAs), a group of PFAS, have been used in various industries as e.g., surfactant materials and firefighting foam. PFAS have been found in the environment, both locally and remotely from where they were disposed. These fluorinated substances are known to pose health risks to humans and animals all around the world and are therefore crucial to investigate.

In this project, a HPLC-MS/MS method was developed and validated for isomeric analysis of twelve PFCAs, including linear perfluorooctanoic acid (L-PFOA). To gain a better understanding of the consequences of PFAS abundance in the Arctic, water and soil samples were collected from Ny-Ålesund, Svalbard. The water (n=4) and soil (n=2) samples were collected in June of 2016 close to a fire-fighting training site (FFTS), where PFAS containing firefighting foam had previously been used over 10 years ago. Additional water samples (n=3) were collected from meltwater away from the FFTS. The water samples closest to the FFTS had a mean concentration of target analytes at 40-56 ng/mL, while the soil samples measured between 11-24 ng/mL. The remaining water samples had concentrations of 0.6-14 ng/mL.

Because the electrochemical fluorination process of producing PFAS gives a composition of <80% linear and >20% branched PFAS, it was investigated to gain a further understanding of the source of contamination in Ny-Ålesund. Contrary to firefighting foam, this process was never executed on Svalbard. The water samples close to the FFTS had compositions of L-PFOA at 87-94%, showing local contamination. The soil samples had 91-95% L-PFOA, which also suggests local contamination. The other water samples were at 0-87% L-PFOA, along with other parameters, can suggest remote contamination. Such discoveries can signify source of contamination, as well as giving a greater understanding of the target analytes' abundance in the Arctic.

Sammendrag

Per- og polyfluoralkylstoffer (PFAS) er menneskeskapte, persistente miljøgifter som finnes over hele verden. Disse stoffene har evnen til å avvise vann og olje, og er kjente for sin langsomme nedbrytningstid i naturen. Siden 1950-tallet har perfluoralkylkarboksylsyrer (PFCAer), en gruppe av PFAS, blitt brukt i ulike bransjer som f.eks. overflatebehandlede materialer og brannskum. PFAS er funnet i naturen, både lokalt og ekstern fra der det ble deponert. Disse stoffene er kjent for å være helseskadelig for mennesker og dyr over hele verden, og er derfor viktige å undersøke.

I dette prosjektet ble en HPLC-MS/MS metode utviklet og validert for isomeranalyse av tolv PFCAs, inkludert lineær perfluoroktansyre (L-PFOA). For å forbedre forståelsen av konsekvensene av PFAS-overflod i Arktis, ble det samlet inn vann- og jordprøver fra Ny-Ålesund, Svalbard. Vann (n=4) og jord (n=2) ble samlet inn i juni 2016 ved et brannøvingsfelt (FFTS) hvor PFAS-holdig brannskum har blitt brukt over 10 år tidligere. Ytterligere vannprøver (n=3) ble samlet inn fra smeltevann, ikke i nærheten av FFTSen. Vannprøvene ved FFTSen hadde gjennomsnittlig konsentrasjoner av analyttene på 40-56 ng/mL, mens jordprøvene hadde konsentrasjoner på 11-24 ng/mL. Smeltevannprøvene målte på 0.6-14 ng/mL.

Fordi den elektrokjemiske fluorineringsprosessen for å produsere PFAS gir en sammensetning på <80% lineære PFASer og >20% forgreinede PFASer, ble sammensetning undersøkt for å få en ytterligere forståelse av forurensningskilden av PFCAer i Ny-Ålesund. I motsetning til brannskummet, ble denne prosessen aldri utført på Svalbard. Vannprøvene ved FFTSen hadde sammensetning av L-PFOA på 87-94%, som tyder på lokal forurensning. Jordprøvene hadde sammensetning på 91-95% L-PFOA, som også kan tyde på lokal forurensning. De andre vannprøvene var på 0-87% L-PFOA, som, samt med andre faktorer, kan tyde på ekstern forurensning. Slike funn kan gi ett godt overblikk over forurensningskilde, samt en større forståelse av analyttenes overflod i Arktis.

v

Abbreviation

ACN	Acetonitrile
AFFF	Aqueous film-forming foam
Br-PFCA	Branched perfluoro carboxylic acid
Br-PFOA	Branched
Br-PFOS	Branched PFOS
C	Carbon
C-F	Carbon-fluor bond
CAS	Chemical Abstracts Service
CAV	Cell Accelerator Voltage
CE	Collision energy
ECF	Electrochemical fluorination
ECHA	European Chemicals Agency
ESI-QqQ	Electrospray ionization triple quadrupole
EU	European Union
F	Factor (in PCA)
F	Fluorine
FFTS	Firefighting training site
FTOHs	Fluorotelomer alcohols
FTSAs	Fluorotelomer sulfonic acids
FWHM	Full width at half maximum
g	Gram
HCl	Hydrochloric acid
HF	Hydrofluoric acid
HFOP-DA	Hexafluoropropylene oxide dimer acid
HPLC	High performance liquid chromatography
ISTD	Internal standard
L-PFOS	Linear PFOS
LC	Liquid chromatography
LOD	Limit of detection
LOQ	Limit of quantification
MeOH	Methanol
mL	Milli liter
MRM	Multiple reaction monitoring
MS	Mass spectrometry
MS/MS	Tandem MS
NaOH	Sodium hydroxide
ng	Nanogram
NH_3	Ammonia
NH_4Ac	Ammonium acetate
NMBU	Norwegian University of Life Science
NMR	Nuclear Magnetic Resonance
OSF	octane sulfonyl fluoride
PCA	Principle component analysis
PFCA	Perfluoroalkyl carboxylic acid
PFAS	Per- and polyfluoroalkyl substances
PFHpA	Perfluoroheptanoic acids

PFHxA	Perfluorohexanoic acids
PFOA	Perfluorooctanoic acid
PFOS	Perfluorooctanesulfonic acid
POP	Persistent organic pollutant
RSD	Relative standard deviation
SD	Standard deviation
SPE	Solid phase extraction
ΣPFCA	Sum of PFCA
TFE	tetrafluoroethylene
TIC	Total ion chromatogram
UPLC	Ultra high performance LC
VET	Faculty of Veterinary Medicine
WAX	Weak anionic exchange

Table of contents

1   Introduction

1.1   Per- and polyfluoroalkyl substances

Per- and polyfluoroalkyl substances (PFAS) is a large group of man-made molecules and are classified as persistent organic pollutants (POP). These anthropogenic chemicals are grouped as molecules holding at least one fluoroalkyl moiety (Buck et al., 2011). Since the 1950s the group of chemicals have been produced and used in the industry (Hanssen et al., 2013) and in the early 2000s been found in the environment. PFAS are sought after for their ability to repel both water and oil (Kissa, 2001a) and are therefore found in products such as water-resistant clothing, non-stick cooking pans, food packaging, firefighting foam, and more (Kelly et al., 2009; Kissa, 2001b). The carbon-fluor bond (C-F) is the strongest bond in organic chemistry (Bank et al., 1994), which makes the materials containing PFAS extremely durable and long-lasting. Even though this is beneficial to the industry sector, it also means that when the molecules enter the environment, they do not degrade and thus become persistent pollutants. Due to their extreme environmental stability, this group of chemicals has recently raised concerns in, but not only, the European Union (EU), European Economic Area, and the USA (ECHA, 2023).

In Helsinki, Finland on January 13th, 2023, several countries, including Norway, proposed to prohibit ~10 000 PFAS in the EU to the European Chemicals Agency (ECHA). ECHA is the agency of the EU, responsible for chemical registration and control. ECHA started a consultation of the proposal in March of 2023. This is the largest restriction proposal in history according to ECHA (ECHA, 2023). The main goal of the proposal is to reduce PFAS emission into nature, along with pushing the industries to produce safer products.

Not only are PFAS hazardous for the environment, but they are also toxic to humans and animals. Increased cholesterol and liver damage have been found to be caused by PFAS exposure (Chain et al., 2018). Mice fetuses experience birth defects when exposed to e.g., perfluorooctanoic acid (PFOA), one of many PFAS (Henderson & Smith, 2006). Studies have also found evidence that PFAS have been linked to cancers such as testicular, prostate and kidney cancer (Steenland & Winquist, 2021). Along with being carcinogenic, PFAS have found to decrease response in antibodies from vaccination, especially in children (Grandjean et al., 2017). PFAS impact the health of humans and animals around the globe, it is therefore

important to study these toxins to gain and expand knowledge with the aim to restrict usage and environmental release of PFAS.

1.1.1 Terminology, structure, and properties

In this paper, PFAS, as the acronym for Per- and polyfluoroalkyl substances, will be used as a plural noun because the phrase itself is plural. "PFASs" will therefore not be used.

Even though there is some debate regarding the exact definition of PFAS, the Buck et al. (2011) definition has been used repeatedly throughout the scientific field. That reads, PFAS contain an aliphatic carbon back-bone along with functional group(s) (Buck et al., 2011), and as previously mentioned, PFAS must contain one or more fluoroalkyl groups. That means, at least one of the hydrogens bonded to the carbon chain is substituted with a fluorine atom. Perfluoroalkyl substances, such as the molecules drawn in *Figure 1.1*, are molecules where all carbons are fully saturated with fluorine atoms. The general moiety is therefore C_nF_{2n+1}. Differently, polyfluoroalkyl substances may have some carbons saturated with fluorine, while other carbons are bonded to hydrogens or other functional groups (ITRC, 2022).
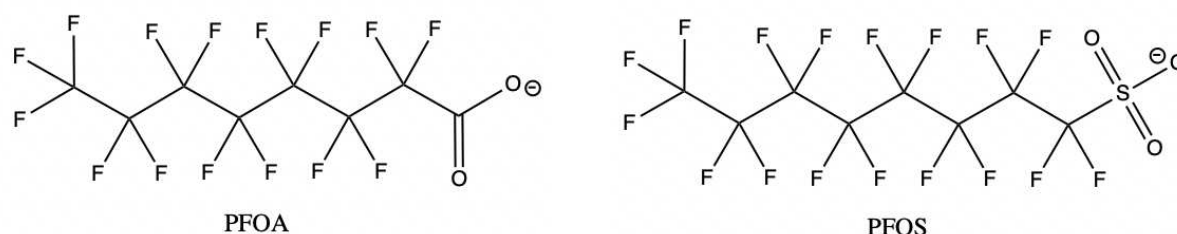
Figure 1.1. *Chemical, anionic structure of L-PFOA and L-PFOS (Ada Njerve 28.09.2022, ChemDraw 21.0.0).*

Perfluorooctanoic sulfonic acid (PFOS) and perfluorooctanoic acid (PFOA) (in *Figure 1.1*) are two of many molecules in the PFAS group. As of 2018, 4730 different PFAS had been identified and registered with each their respective CAS-registration number (OECD, 2018). Two years later, 6330 PFAS were registered (Miljødirektoratet, 2023a), including the previous 4730. The current estimate of PFAS is more than 10 000 different compounds (EPA, 2021), and the number is still growing.

With fluorine being the most electronegative atom, it has been found that the C-F bond is the strongest out of all single carbon bonds (O'Hagan, 2008). Along with having notable stability,

PFAS have a significantly low polarization, which makes the intermolecular forces with other polar and non-polar molecules, weak (O'Hagan, 2008; Rayne & Forest, 2009). As mentioned, this makes PFAS especially hard to degrade in nature. And because of their hydrophobic fluorinated C-chain and hydrophilic functional group, PFAS have the unique ability to repulse water, fats, and oils. Therefore, the amphiphilic molecules work great as surfactant material. However, selected PFAS are also water-soluble, and when the molecules are disposed into nature, they are environmentally mobile and therefore more persistent than other POPs, however PFAS does have a low vapor pressure. (Meegoda et al., 2020).

The length of the backbone determines whether the fluorinated compound is referred to as "long-chained" or "short-chained" PFAS. According to the Organization for Economic Co-operation and Development, OECD, long-chained PFAS are those with seven or more fluorinated carbons, and short-chained are those with less than seven (OECD, 2011). This definition is being used in this current project to differentiate between the two categories of PFAS.

PFAS can also be divided into linear and branched groups. The linear molecules will be referred to as "L-"PFAS, while the branched will be referred to as "Br-"PFAS in this paper. L-PFAS are those molecules where a carbon-atom (C) is only bonded to one or two other C's. n-PFOA and n-PFOS (n: normal, or linear isomer of molecule (same as L-PFOA), seen in *Figure 1.1*) are examples of linear PFAS. Contrary, branched PFAS have C's that can be bonded to more than two C's (Buck et al., 2011). Because there is one linear and several branched compounds of each PFAS, there is a significant issue regarding analyzing, assembling, and quantizing environmental samples. Br-PFOS, as an example, is often found in mixtures of up to ten different branched molecules (Riddell et al., 2009).

It is also worth mentioning that the analytes used in this project are not all isomers of PFOA. The molecular formula of PFOA is $C_8HF_{15}O_2$ and a molecular weight of 414 g/mol. While some are isomers, other target analytes have different molecular formulas and weights. The hypernym for all analytes is therefore perfluoroalkyl carboxylic acids (PFCAs) because they are sharing a carboxyl moiety. While there is only one L-PFOA, there are numerous Br-PFOAs and other Br-PFCAs. The Br-PFCAs used in this study will be called their acronyms according to their chemical names. These acronyms are adapted directly from the manufacturer of the standards

(Wellington Laboratories, Guelph, ON, Canada); all acronyms can be found in *Table A.2* in *Appendix A.* Two Br-PFCAs acronyms are exemplified in *Figure 1.2.*

P3MHpA   P37DMOA

Perfluoro-3-methylheptanoic acid   Perfluoro-3,7-dimethyloctanoic acid

Figure 1.2. Examples of acronyms and names of two PFCAs used in this study.

The two main processes for synthesizing PFAS are telomerization and electrochemical fluorination. These methods differ in that (a) telomerization does not contribute to isomers and (b) electrochemical fluorination (ECF) does (Benskin, De Silva, et al., 2010; Benskin, Yeung, et al., 2010). Through the last-mentioned process, the final products consist of 70-80% linear and 20-30% branched isomers (Paul et al., 2009; Prevedouros et al., 2006). The known Br-PFOAs resulting from ECF are P3MHpA, P4MHpA, P5MHpA, P6MHpA, P44DMHxA, P55DMHxA, P35DMHxA, and P45DMHxA (Benskin, De Silva, et al., 2010). For further understanding, these processes will be discussed in the next subchapter.

1.1.2   Manufacturing and application in industry

PFAS are not naturally occurring in nature and are therefore produced in industry where materials with amphiphilic properties are needed. Two main techniques and methods are used for this:

Telomerization is a three-step process where the first step is mixing a perfluoroalkyl iodide and tetrafluoroethylene (TFE), gaining a longer chained perfluoroalkyl iodide. This product is called Telomer A. Separately, step two includes reacting Telomer A with ethylene. This gains a fluorotelomer iodides, which is an even longer perfluoroalkyl iodide, and this is called Telomer B. The third and last step is to react Telomer A and B. The product is the raw material for "fluorotelomer-based" surfactant (Buck et al., 2011). This process produces some polymers, but few branched compounds and isomers.

Electrochemical fluorination (ECF) is a common technique used in the industry to synthesize PFAS, such as PFOA and PFOS. One example of this is the production of PFOS (see *Reaction 1.1*). Starting with any organic molecule, like octane sulfonyl fluoride (OSF) and adding anhydrous hydrofluoric acid (HF) along with an electric current, will gain

perfluorooctanesulfonyl fluoride (POFS). From the POFS, PFOS is then gained, along with other isomers and starting material ([3M]Company, 1999; Bank et al., 1994).
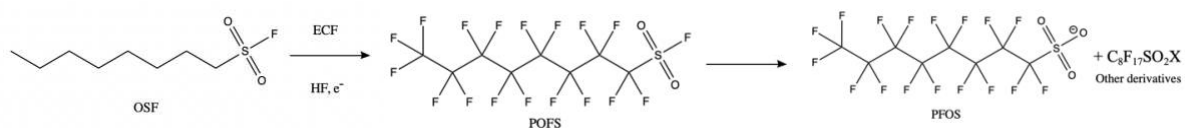
Reaction 1.1. *Electrochemical fluorination of octane sulfonyl fluoride to PFOS. (Ada Njerve 30.09.2022, ChemDraw 21.0.0).*

The 3M Company used the last-mentioned technique to produce materials with PFOA and PFOS until 2001. In collaboration with the United States Environmental Protection Agency, the company stopped their production due to backlash regarding environmental and toxicity concerns (Paul et al., 2009). 3M produced products such as surface treatment products, paper products, performance chemicals, spot cleaners, mining and oil surfactants, firefighting foams, and more ([3M]Company, 1999), which all contain fluorinated alkyls. According to 3M Company's website (https://www.3m.com/), they still produce and market fluorinated products, yet not containing restricted PFAS.

One reason for the growing number of PFAS is the quick development of new fluorinated compounds while the old ones are banned. Countries and regulatory agencies work to understand and research PFAS that are used in industry. When they are found to have a negative impact on the environment or found to be toxic to humans and animals, they are banned and must be phased out in industry. Companies will then produce new, similar compounds which they can use in their production (Lindstrom et al., 2011).

1.1.3   Exposure and global transportation

There are several pathways to PFAS exposure. PFOA and PFOS have been found in waters, lakes, animals, and agricultural sites all over the world (Ghisi et al., 2019). The fluorinated substances enter our food chain through (1) the soil we grow our vegetables in (Lesmeister et al., 2021; Wang et al., 2020), (2) the plants our livestock or we eat (Jha et al., 2021; Liu et al., 2023), (3) the animals carnivores eat (Falk et al., 2012) , or (4) the packaging or processing of our food (De Silva et al., 2021). PFAS bioaccumulate in animals and it has been found that predatory animals have higher levels of PFOS than that of their prey. This suggests that the

level of PFOS, and other PFAS, have a strong positive correlation with increasing tropic level (Giesy & Kannan, 2001).

PFAS are found in water, which is most often contaminated by emissions or waste from the industry sector. Through emissions and waste, PFAS end up in the soil and later in our groundwater. From the groundwater, the substances are transported into rivers and run-offs and will eventually end up in our drinking water reservoirs and oceans. Firefighting foam follows a similar route to this (De Silva et al., 2021).

In our homes we are also exposed to PFAS. Products such as non-stick cooking pans, waterproof make-up products, stain resistant textile, and waterproof apparel all contain PFAS which we are exposed to through inhalation, ingestion, or dermal exposure (De Silva et al., 2021). There are also PFAS accumulated in dust and air found in homes (Shoeib et al., 2005).

Considering the ubiquitous environmental distribution of PFAS, a survey done by Yamashita et al. (2005), showed that PFOS, PFOA, and several other PFAS were found at more than 100 locations worldwide. Comparing the concentration of PFOS in livers of polar bears (*Ursus maritimus*) located in the Canadian Arctic (Martin et al., 2004) and in livers of bottlenose dolphin (*Tursiops truncates*) in the Mediterranean Sea (Kannan et al., 2002), with 1700–4000 ng/g (ww) and <1.4–110 ng/g (ww) respectively, shows a ~200% difference. Finding potent chemicals at remote locations such as the Arctic can suggest the oceanic transportation routes of PFAS. Studies have found PFAS in aerosols in the air, which suggests atmospheric transportation (McMurdo et al., 2008; Sha et al., 2022). Similar to other POPs, PFAS do not only end up in the environment where they are discarded but travel throughout the world with oceanic and atmospheric currents (Yamashita et al., 2005).

Due to PFAS' low vapor pressure, considering atmospheric transportation seems contradictory, however, PFAS has been found in the Arctic despite the absence of local sources (Kannan et al., 2005; Martin et al., 2004). Studies have thus been conducted on how PFAS ends up in the Arctic through the atmosphere. These studies have revealed that the more volatile precursors in PFOA and PFOS production, such as fluorotelomer sulfonic acids (FTSAs) and fluorotelomer alcohols (FTOHs), are released into the air and are subsequently converted into PFOA and PFOS through biotic and abiotic processes (Dai et al., 2020; Shoeib et al., 2006). Formation of PFOA from precursors has been studied, and it has been found that abiotic factors, such as

temperature or oxygen levels, are optimal in the Arctic (Wallington et al., 2006), which may explain the heightened levels of PFOA there.

1.2   PFAS in Arctic water and soil

1.2.1   PFAS at Svalbard

Due to the atmospheric and ocean-borne transportation routes PFAS can be found in the Arctic environment. But even though PFAS can be found remotely, the compounds can also be released by local source into the environment. Svalbard, under Norwegian administration, is an example of that. Svalbard is an archipelago between Norway and the North Pole. Local industries were confined to coal mining during the past 100 years. However, the Norwegian mining activities have been ceased since 1918. Today only Russian coal mining is active in the town of Barentsburg. The Norwegian government has decided to promote the establishment to two professional activities on Svalbard: Tourism, as well as research and education. Firefighting training was regularly conducted at the firefighting training sites (FFTS) of the local airports (in Longyearbyen, Barentsburg, Ny-Ålesund and Svea). For this PFAS-containing aqueous film-forming foam (AFFF) was applied. PFAS-containing AFFF were, hence, used Svalbard Airports for many years until 2002. In 2012 the airport owner, Avinor, restricted all use of PFAS-containing AFFF, but due to the non-degrading nature of the chemicals, PFAS are still found at high levels in the grounds and the run-off waters close to the airport (Miljødirektoratet, 2023b).

The second largest airport at Svalbard is the Ny-Ålesund Airport. According to a 2017 report from the Norwegian Polar Institute, the research site and airport at Ny-Ålesund, has also an established FFTS. With no record of PFAS-containing AFFFs, yet levels of PFAS in the water and ground, it was concluded in the report that AFFFs had most likely been used there (Granberg et al., 2017). A later study from 2019 found elevated levels of PFAS in run-off water and soil near the FFTS, with 113-119 ng/L and 211-800 ng/g, respectively (Skaar et al., 2019). These findings confirm that PFAS-containing AFFF had been used at the site.

Another factor is where the PFAS are found, Skaar et al. (2019) studied 14 different PFAS in seawater, run-off meltwater, and soil from around Ny-Ålesund Airport. The run-off water and soil had elevated levels of PFAS, while the seawater measured at 5-6 ng/L PFAS. This suggests that the contaminants from the FFTS are not contributing to notable seawater contamination.

It is difficult to distinguish the PFAS sources in the Arctic. As mentioned, precursor mediated long-range PFAS transportation has been suggested from many previously reported studies, but also local contamination has been suggested by others. One method used to purpose sources of PFAS, e.g., in Hartz et al. (2023) and Ali et al. (2021), is investigating the PFAS isomeric profile. Because the L- and Br-PFAS ratio (70-80%, 20-30% respectively) is known from the ECF manufacturing process, deviation from the original ratios may indicate remote source, while other ratios, other PFAS, or derivatives of PFAS can suggest local contamination. (Benskin, De Silva, et al., 2010; Benskin, Yeung, et al., 2010). Another method is to investigate precursor, discussed previously in subchapter *1.1.3 Exposure and global transportation.*

1.3   Liquid Chromatography and Mass Spectrometry for Isomeric Specific Analysis

1.3.1   High Performance Liquid Chromatography (HPLC)

As touched upon before, isomeric analysis can be problematic due to the number of Br-PFAS, but relatively recent analytical methods have been developed to fathom the problem. ^{19}F nuclear magnetic resonance spectroscopy (NMR) has previously been used for determination of fluorinated organic compounds but lacked the opportunity for accurate quantification (Kissa, 2001a). ^{19}F NMR has since been improved for quantitation but is still not as sensitive and selective as liquid chromatography (LC).

Separation of PFAS using high performance liquid chromatography has rapidly improved and is currently the most common technique for separation of PFAS. Therefore, HPLC will be used in the study to conduct accurate and clear results. And because several of the target analytes in this study have the same molecular weight or similar structures, the separation can be strenuous. Along with choosing a suitable column, it is important to find the optimal HPLC separation parameters according to the van Deemter equation and plot, which will be further discussed in chapter 2, *Method.*

1.3.2   Mass Spectrometry

Mass spectrometry (MS) is often used as a detector in combination with the HPLC instrumentation. For PFAS isomeric determination, tandem mass spectrometer (MS/MS) is an appropriate fit due to its high sensitivity for small, ionic molecules. A single mass spectrometer usually uses a soft ionization source, in which few or no fragmentations occur. Alternately,

using several mass separators coupled together can gain both molecular ions and fragmentations of those, which will make qualification and quantification reliable. Electrospray ionization (ESI) works well with polar molecules, such as PFAS. Though ESI is a soft ionization source, coupled with tandem MS, it does succeed in fragmentation while also producing molecular ions.

Triple quadrupole (QqQ) is a well-known tandem MS-technique, consisting of quadrupole 1 (Q), collision cell (q) and quadrupole 2 (Q). With two mass spectrometers, along with a collision cell in between, several modes can be used. One example out of several, is product ion scan, where a certain mass is selected in the first quadrupole, fragmented in the collision cell, and then the fragmentations are scanned in the second quadrupole. The diverse ways to utilize the QqQ, gives a broader spectrum of ways to analyze isomers. This will also increase the accuracy and precision for the analysis, along with selectivity of the analyte.

1.4　Purpose of study

PFAS is a raising concern regarding the environment, animal, and human health. The purpose of this study is to develop a HPLC-MS/MS method using a perfluorooctyl column to separate 12 different PFCAs, both short-chained and long-chained; and L-PFOA and Br-PFCAs. Previous methods, such as Skaar et al. (2019), have been able to separate and quantify L-PFAS, but there are several thousand PFAS, and the largest proportion of those are yet to be studied. The more studies obtained regarding PFAS, the greater the knowledge of the consequences of their abundance.

Through method development and comparison for this current study, Skaar et al. (2019) will be used as a reference method. Along with being in a peer-reviewed, respected journal, the reference uses well-known experimental design and analytical methods, which ensures reliability. The reference will be used for guidance, and to ensure propitious outcome. The reference method uses the same sample matrix, but not the same analytes, nor the same column. Therefore, the MS parameters, mobile phases, and gradient program will be optimized manually. Along with developing a method, validation of the method will be done. It is important to statistically prove that the method is usable and robust for further PFCA analysis and improvement. Parameters such as accuracy, precision, selectivity, linearity, and analytical range will be determined.

The HPLC-MS/MS method will be applied to water and soil samples from Ny-Ålesund, Svalbard. Linear PFAS have been found in these samples (Skaar et al., 2019), but Br-PFAS and other specific PFCAs will be investigated in this project. Before 2019, no organized investigation had been conducted in this area. This project will accomplish a further understanding of PFAS sources in the Arctic, along with the comprehension of which and how much of the toxic substances are still present after a decade of the last contamination.

Lastly, along with abundance, an evaluation of contamination source will be done according to composition of linear vs. branched PFAS. Samples from locally contaminated and remote areas will be compared. With the knowledge of the isomeric composition resulting from ECF, the expectation is that the remote samples will have L-PFOA compositions of <80% and Br-PFCAs of >20%, while those samples from contaminated areas have higher L-PFOA compositions.

2 Method and materials

As mentioned in the introduction, the Skaar et al. (2019) method was used as a reference method for comparison and guidance. Along, was sample preparation methods and procedures used according to the Environmental Toxicology Laboratory at the Faculty of Veterinary Medicine at NMBU, Ås, Norway.

2.1 Precautions

Due to PFAS being hazardous, precautions were taken during the experimental procedure. Nitrile gloves were worn during standard and sample handling. All transfers of standards and samples were carried out in fume hoods, and all surfaces were cleaned with ethanol after use. All glass- and plasticware were left in the hood over night or until fully evaporated before being disposed, to ensure safe disposal.

2.2 Reagents and materials

A complete list of all reagents, standards, and materials used in this study is found in *Appendix A*. Internal standard and external standards were purchased from Wellington Laboratories (Guelph, ON, Canada).

All standards came in ampules with a concentration of 50 μg/mL, except for P4MHpA, P5MHpA, P6MHpA, P55DMHxA, P45DMHxA, and P35DMHxA which had concentrations of 2.20 μg/mL, 1.96 μg/mL, 3.10 μg/mL, 1.95 μg/mL, 1.22 μg/mL, and 0.593 μg/mL respectively. All were in separate ampules, except for P45DMHxA and P35DMHxA, which were mixed. All standards are at 98% purity except T-PFOA. T-PFOA is a technical grade standard and contains 96% L-PFOA and branched PFOA isomers, and 4% impurities such as perfluoroheptanoic acids (PFHpA) and perfluorohexanoic acids (PFHxA). The internal standard used was [$^{13}C_4$]-PFOA.

Mobile phase A was prepared by dissolving ammonium acetate (0.077 g, 2 mM) in 50 mL methanol (MeOH) and adding Milli Q water to reach a volume of 0.5 L. The organic mobile phases were prepared by (1) dissolving ammonium acetate (0.077 g, 2 mM) in MeOH to reach a volume of 0.5 L, then filtered with 0.2 μm filter. (2) Mixing formic acid (0.5 mL, 0.1%)

MeOH to reach a volume of 0.5 L. (3) Dissolving formic acid (0.5 mL, 0.1%) in acetonitrile (ACN) to reach a volume of 0.5 L.

2.3   Validation

2.3.1   Samples

The samples for validation were cattle (*Bos taurus*) liver and cod (*Gadus morhua*) filet/muscle. There were two types of "blank" samples, one in the validation matrix and one in water matrix, both not spiked with analyte. The samples called "blind" are liver and filet samples, while the samples called "blank", were Milli-Q water, type 1. The rest were spiked liver and filet according to *Table 2.1*. Internal standard was added to all samples in the beginning except the matrix effect samples, where ISTD was added at the end. The blank, blind, 0.5 ng/mL, 10 ng/mL, 50 ng/mL, and matrix effect samples were analyzed in replicates (*n=3*) to investigate recoveries. The blind, spiked, and matrix effect samples were analyzed to investigate the matrix effect of cattle liver and cod filet in regard to the analytes. The blank samples were analyzed to determine LOD and LOQ.

Table 2.1. Samples for method validation with number of replicates per sample. Top row indicates how much of each analyte the samples were spiked with.

	Blank (water)	Blind	0.1 ng/mL	0.5 ng/mL	1 ng/mL	10 ng/mL	50 ng/mL	100 ng/mL	Matrix effect
Blank	3								
Liver		3	1	3	1	3	3	1	3
Muscle		3	1	3	1	3	3	1	3

2.3.2   Sample preparation

The samples were pre-homogenized by cutting and griding and stored in the freezer. The samples defrosted to room temperature before being weighed out to ~0.5g into 15mL polypropylene centrifuge tubes, except the blank samples, where 0.2 mL water was pipetted into the tubes. Then, 80 µL of 120 ng/mL ISTD (ending concentration 10 ng/mL) was added first, followed by calibration standards according to *Table 2.1*. 5mL methanol was then added, and the tubes were sonicated for one minute each before being shaken on a shaker table for 30 minutes. The tubes were then centrifuged for 10 minutes at 3000 rpm. The liquid layer was transferred to new 15mL centrifuge tubes. 3mL methanol was added to the tubes with the solids left, then stirred with a small spatula, shaken for 30 minutes, and centrifuged for another 10

minutes at 3000 rpm. The liquid layer was transferred to the already transferred liquid in the new tubes. The supernatant liquid was then evaporated to a volume of 2mL.

To further remove fat and other contaminants from the samples, 0.1-0.3g of Superclean™ ENVI-Carb™ (graphitized charcoal) was added to each sample, then mixed using a vortex mixer. The tubes were then centrifuged for 10 minutes at 3000 rpm, and the top layer was transferred to new 15mL centrifuge tubes. The process was repeated, but instead of Envi-Carb, 1mL methanol was added. The supernatant was then evaporated fully, and methanol was added to reach an ending volume of 1mL. The samples were centrifuged one last time for 10 minutes at 3000 rpm, then placed in the fridge overnight to harden any left-over fat. The samples were transferred to HPLC-vials, and 416 μL of 120 ng/mL ISTD (ending concentration 50 ng/mL) was added to the matrix-effect samples before analysis.

2.4 Samples for method application

2.4.1 Samples from Ny-Ålesund, Svalbard

For application of the here developed method, previously analyzed freshwater and soil from Ny-Ålesund, Svalbard (N78.92, E11.92) was chosen. The samples were collected and reported by Skaar et al. (2019). The primary analysis found ranging levels of L-PFOA but did not investigate the remaining analytes used in this project. Advantages of doing a secondary analysis are not only limited to the ability for comparison, but also economic and environmental parameters. Comparison of results, along with validation of the method, can prove the dependability of the method. Using samples several times for different analyses also lowers the cost, time and resources for sampling and sample preparation, as well as decreasing environmental pollution regarding transportation. Disadvantages for using the same samples are that it might not answer the intended research question, or that it might not be specific enough to the research. The lack of control over the sampling and sample preparation is also a disadvantage.

The samples were collected on the 22nd and 23rd of June 2016. *Table 2.2* presents the samples and their locations, while *Figure 2.1* visualized where the samples were collected. Field blank NÅ-B-01, -02, and -03 were collected from about 1km from Ny-Ålesund away from the sea, about 20m from the FFTS, and in the sea about 60m from the shoreline, respectively. Freshwater sample NÅ-W-02 was collected the same place as NÅ-B-02, from a small pond

close to the FFTS. NÅ-W-01, -08, and -16 were collected in three different run-off streams. The soil samples NÅ-S-01 and -02 were collected about 40 and 60m from the FFTS, respectively. All water samples were collected in duplicates, except NÅ-W-16, -S-01, and –S-02.

Table 2.2. *List of samples analyzed with sample name, and coordinates for sampling.*

Sample	Sample name	Position collected
Field blank	NÅ-B-01	N78.91738 E11.86061
Field blank	NÅ-B-02	N78.92851 E11.91476
Field blank	NÅ-B-03	N78.92860 E11.92930
Freshwater	NÅ-W-01A	N78.92694 E11.91112
Freshwater	NÅ-W-01B	N78.92694 E11.91112
Freshwater	NÅ-W-02A	N78.92851 E11.91476
Freshwater	NÅ-W-02B	N78.92851 E11.91476
Freshwater	NÅ-W-08A	N78.92445 E11.90311
Freshwater	NÅ-W-08B	N78.92445 E11.90311
Freshwater	NÅ-W-16	N78.92619 E11.94336
Soil	NÅ-S-01	N78.92877 E11.91242
Soil	NÅ-S-02	N78.92880 E11.91109

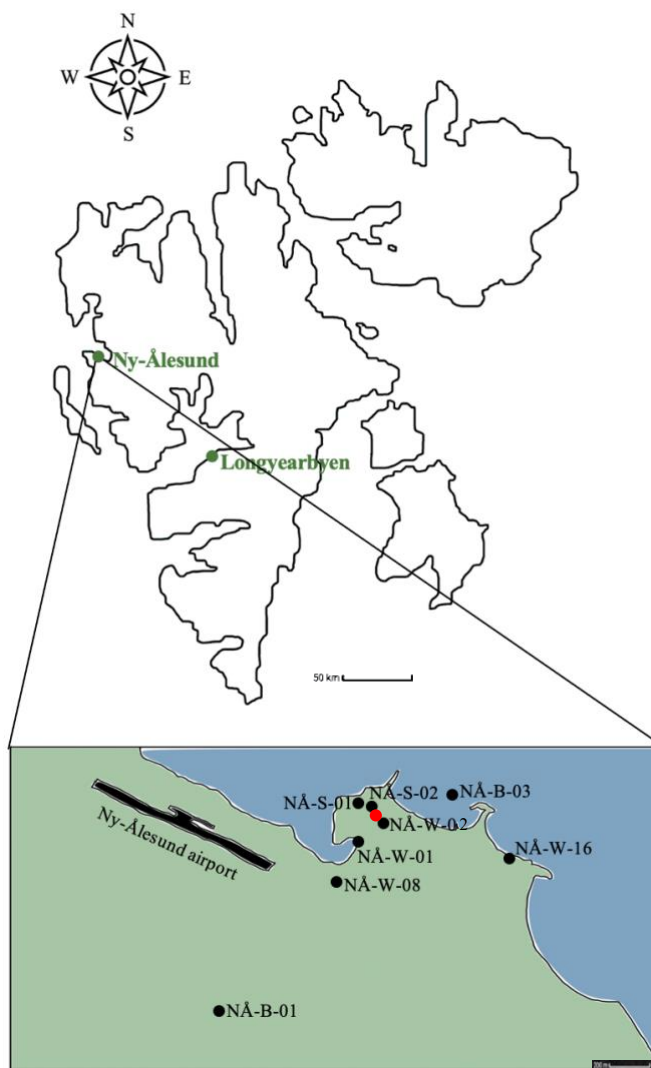***Figure 2.1.*** *Map of Svalbard including Longyearbyen, Svalbard's administration center and Ny-Ålesund, the location of sampling for this project. Zoomed-in map (approx.) of Ny-Ålesund with positions of where samples were collected. The red location is the FFTS. NÅ-B-02 is collected at the same coordinates as NÅ-W-02 and is therefore not marked in the map (Drawn by Ada Njerve, Incscape 1.2 and Microsoft Word, 14.04.23)*

2.4.2   Sample preparation and clean-up

The water samples were transported to the Faculty of Veterinary Medicine, Ås, Norway in polypropylene containers, free of PFAS to avoid cross-contamination. The samples were stored in the fridge at 4°C until sample preparation and then in the freezer until quantitative analysis.

The freshwater samples were subject to solid-phase extraction (SPE). The mode was mixed reverse phase/weak anion exchange (WAX) resin with the use of Waters Oasis® WAX (500 mg, 6 cc, 60 μm, Waters, Milford MA, USA) cartridges. The cartridges were first conditioned with 4 mL 0.1% ammonia (NH_3) in MeOH, 4 mL MeOH, and lastly 4 mL Milli Q, type 1 water. After the cartridges were placed on a manifold vacuum, 4 mL MeOH was added to the cartridges to prevent drying of the resin and reservoir adapter was placed on top. 50 μL of 200 ng/mL ISTD (ending concentration 20 ng/mL) was added to all the samples and field blanks, before being placed at a level above the vacuum. Polypropylene tubes were connected from the samples to the SPE cartridges. The vacuum was turned on, and a loading speed of maximum 5 mL/min was set. After all samples were flushed trough the cartridges, 4 mL of acetate buffer was added. This was done to clean out salts and other contaminants, while also enhancing adsorption. The remaining solvent was eluted before the cartridges were centrifuged for 2 minutes at 1500 rpm. Then the nonionic analytes were washed out with 4 mL MeOH into 15 mL polypropylene tubes, and the ionic analytes were extracted with 4 mL 0.1% NH_3 in MeOH into another set of 15 mL tubes. The extracts were evaporated using a Zymark Turbovap LV Evaporator to about 0.25 mL. MeOH was added to reach an ending volume of 0.5 mL, and the extraction solution was transferred to HPLC-vials.

The soil samples were first dried until complete dryness in an oven at 30°C, before ~2.5g of each sample was weighed out into 50 mL polypropylene tubes. 1 mL of 200 mM sodium hydroxide (NaOH) was added and sat still for 30 minutes. Then, 50 μL of 200 ng/mL ISTD (ending concentration 20 ng/mL) and 10 mL of MeOH was added before being shaken on a shaker table for 30 minutes. 100 μL hydrochloric acid (HCl) was mixed in. The tubes were centrifuged for 20 minutes at 3000 rpm. The top layer was transferred into new 15 mL tubes. 3 mL MeOH was added to the tubes from the beginning, the centrifugation was repeated, and the top layer was again transferred to the new 15 mL tubes. The supernatants were evaporated to 5 mL. To remove fat and other contaminants, 0.25 g of Envi-Carb was added and mixed in, the tubes were centrifuged again before the extract was transferred to new 15 mL polypropylene

tubes. Finally, 2 mL MeOH was added, evaporated to 0.5 mL using a Zymark Turbovap LV Evaporator, and transferred to HPLC-vial.

2.5   Band broadening

Distillation has historically been used as a method for separating analytes, where actual plates collected the distillate. More plates meant better separation. Theoretically, each plate should therefore be shortened to increase the number of plates. Height equivalent to theoretical plates (HETP), as a model, has therefore been used in chromatography to understand the efficiency and resolution of separation. However, this model alone does not sufficiently account for band broadening. Band broadening is often deteriorating the chromatographic resolution during long chromatographic separation runs and should therefore be considered during method development. Jan van Deemter developed a model where the van Deemter equation (*Equation 2.1*) considers three parameters causing band broadening in relations to HETP.

$$H = A + \frac{B}{u} + Cu$$

Equation 2.1*. The van Deemter equation.*

The H in the van Deemter equation describes a dimensionless measure for HETP. For the chromatographic peaks to be as narrow as possible, this measure must be as low as possible. The A term refers to Eddy diffusion. This means that, in a packed column, molecules that enter at the same time will exit at separate times. This is due to different pathways though the particles in the column. To improve the A term, the particles should be as uniform and small as possible. The B term describes longitudinal diffusion, which comes from the analyte wanting to move from an area in the column with high concentration to low concentration. To improve this, in addition to using a more viscous mobile phase, increasing the flowrate will allow the analyte to not broaden as much. The C term is mass transfer, which describes processes such as some of the analytes interacting with the stationary phase and therefore moving slower other components in the mobile phase. Increasing the flowrate can improve this measure. The u term is the linear flowrate of the method. The equation gives the van Deemter plot shown in *Figure 2.1*, which helps determine the optimal flowrate for the method. The x is at the lowest point on the H curve, where the method is most ideal (van Deemter et al., 1956).
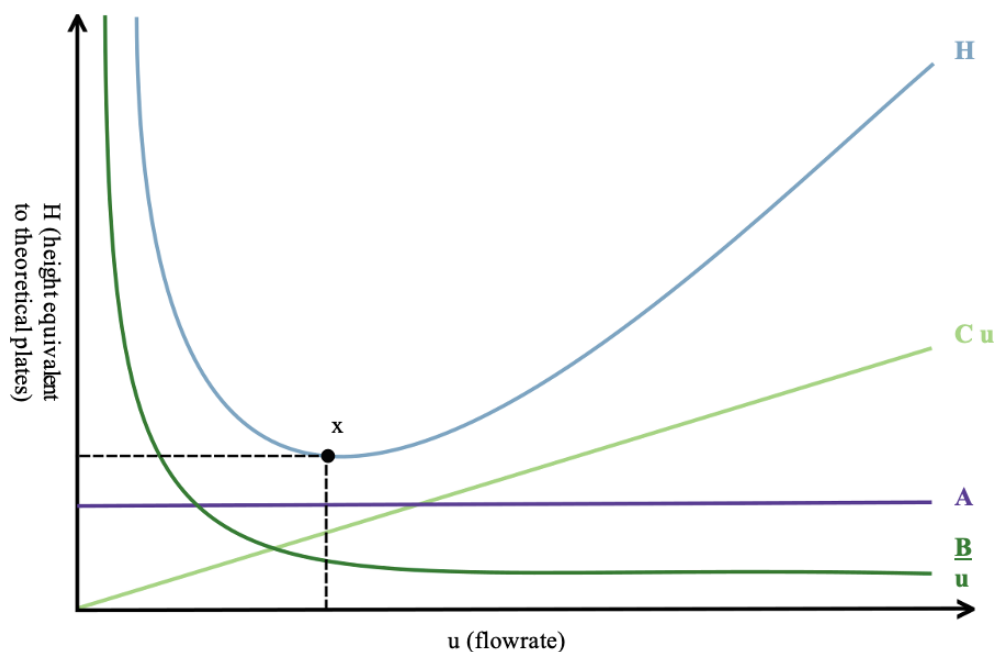
Figure 2.1. *Generalized van Deemter plot where x is optimal flowrate (drawn by Ada Njerve in Inkscape 1.2, 16.11.22).*

2.6 HPLC-MS/MS method development

Method development and quantitative analysis were conducted at the Faculty of Veterinary Medicine at the Norwegian University of Life Sciences (NMBU) in Ås, Norway. The instrumentation used was Agilent Series 1200 Gradient HPLC System combined with Agilent 6460 Triple Quad Mass Spectrometer System. The column utilized was Ascentis® Express F5 Column (2.7 μm, 10 cm x 2.1 mm) from Merck (Darmstadt, Germany).

2.6.1 Mass spectrometry parameters

To begin with, the MS parameters were optimized. No column was used during the MS optimization procedure. This was done by first running all the target analytes in separate vials through the MS using an MS2-scan in negative mode. The mode was negative due to all literature regarding PFAS analysis used in this study, uses negative mode. The expected *m/z*'s of the analytes were found in the mass spectra, which was the mass minus 1. The second step was running product ion scan, while also determining the approximate collision energy (CE) for each standard. Two or three product ions were collected from the mass spectra, along with whether the standards were optimal in high CE (20-35eV) or low CE (0-15eV). With this information, a multiple reaction monitoring method (MRM) was developed for each fragmentation of each analyte, to find the exact CE. The same procedure was done to find the

Cell Accelerator Voltage (CAV) and Fragmentor Voltage for each standard, testing all voltages and determining the highest responses. The last step was to determine Dwell, which was finding the highest dwell time that would give a cycle time closest to 500 ms.

2.6.2 Column

For this project, rather than using the well-known C_8 or C_{18} columns, a fluorine column was used. C_8 and C_{18} columns are widely used in PFAS detection and separation, but for isomeric separation, these columns are yet to be amended. Therefore, a fluorinated stationary phase was investigated to achieve separations. The Ascentis Express F5 HPLC column (Merck), containing a pentafluoro phenylpropyl stationary phase, was used in this project. The manufacturer claims the column has polar and non-polar properties, which allows the stationary phase to retain polar and non-polar compounds. C_8 and C_{18} columns do not have this property. This is significant due to PFAS's amphiphilic properties, and it will therefore aid separation.

Considering Eddy diffusion (term *A* in the van Deemter equation), the particles in the column should be as small and uniform as possible. The column is only sold with one particle size, 2.7μm, which is on the smaller side of particles available from the manufacturer. The particles also have fused core, which makes the particles heavier than porous particles and more like fully porous particles, yet smaller. This makes the particles easier to manufacture uniform and will assist to improve Eddy diffusion.

For the temperature of the column compartment, it was recommended by the manufacturer of the column (Merck) to use <60°C to prolong the column life. As well as lowering the power usage of the instrument, holding a stable temperature was important to ensure constant results. This led to choosing a starting temperature of 30°C, which was higher than that of the room temperature (fluctuating between 20 - 21°C). 30°C worked for the method, and increasing the temperature was therefore not necessary.

2.6.3 Mobile phase and gradient program

One of the most consequential parameters to separating isomers and similar compounds in chromatography is the mobile phases and their gradient program. Zhang et al. (2017), which uses the same column for PFAS-isomeric separation, used 20 mM ammonium formate in water and 100% methanol as mobile phases. The manufacturer of the column suggests using

acetonitrile or methanol as the organic phase. Therefore, there were several mobile phases and gradient programs tried to conduct the optimal separation during this development. The different trials are separated into five stages underneath. The aqueous mobile phase stayed consistent during all the stages as 2 mM ammonium acetate (NH_4Ac) in water and 10% MeOH (mobile phase A). MeOH was added to prevent bacterial growth in the water.

Stage 1: The first organic phase (mobile phase B) tested was MeOH with 2mM NH_4Ac buffer. Because the Br-PFCAs were different than that of the reference method, it was important to conduct a scouting gradient, rather than adapting the same gradient program. The scouting program started with 90% A and 10% B, and this was held for 5 minutes. During the next 10 minutes B went from 10% to 90%. 90% B was held for 5 minutes before ramping up to 100% B, which was held for 3 minutes to elute anything that was left in the column. Lastly, B was brought back to 10% and held for 5 minutes to re-stabilize binary pressure. This program was done with all standards in separate vials, except P45DMHxA and P35DMHxA.

Stage 2: With the same organic mobile phase as in *Stage 1,* several gradient programs were tested to elongate the elution of the standards. Similar to *Stage 1*, this program also started with 90% A and 10% B. B was increased to 90% over 15 minutes, then to 100% over 5 minutes. 100% B was held for 5 minutes. B was brought back to 10% and held for 4 minutes.

Stage 3: To further extend the separation, a stepwise gradient was tested. The program started with 60% A and 40% B, which was held for 2 minutes. Within the next minute B was ramped up to 45% and held for 2 minutes. B was increased by 5% four more times, ending at 65% B, all held for 2 minutes each. B was then ramped up to 100% for 3 minutes, then back to 40% B for 7 minutes to ensure that the binary pressure equilibrated.

Stage 4: The same gradient program as in *Stage 3* was used in this stage, but with 0.1% formic acid in acetonitrile (ACN) as the organic mobile phase.

Stage 5: With the same program as in *Stage 3* and *4,* the organic mobile phase was now 0.1% formic acid in MeOH. The program was slightly modified by adding a step of 70% B for 2 minutes between 65% B and 100% B.

2.6.4 Flowrate

Longitudinal diffusion (B) and mass transfer (C) are both improved by increasing the flowrate. However, The Ascentis® Express F5 Column had never been used prior to this project's method development; it was therefore important to find a flowrate that would not exceed the pressure in which it would disturb the column. Ensuring that the analyte had enough time to interact with the stationary phase was another reason to keep the flowrate at a low rate. Hence, finding a middle-ground was necessary. The MS parameters were optimized with a flowrate of 0.5mL/min without a column. The flowrates 0.3mL/min and 0.4mL/min were thus tried with the *Stage 5* gradient program.

3   Quality assurance

To ensure that the current method is valid for analysis of PFOA isomers and PFCAs for future studies, several measures of validation will be used and examined, as listed underneath. Validation parameters and criteria are according to the Environmental Toxicology Laboratory at the Faculty of Veterinary Medicine at NMBU, Ås, Norway.

3.1   Standards

3.1.1   External standard

External standards are solutions containing only the target analyte. The standards are used to conduct a calibration curve for the method. The calibration curve is a two-dimensional relationship of signal and concentration, which is used to calculate the concentration from the obtained unknown analyte's signal.

3.1.2   Internal standard

Due to volume errors, solvent evaporation, and matrix effects, loss of the analyte can happen during sample preparation and analysis. To account for these losses, internal standards can be added at known concentration. The internal standard (ISTD) is different from the analyte, but similar enough that changes to the analyte and the standard are synchronous. Usually, the internal standard has an isotopic difference from the analyte.

3.2   Linearity and range

Linearity is the ability of the calibration curve to assure that the obtained signal of the analyte is corresponding to the correct concentration. The R^2- value of the slope should be as close to 1 as possible to assure the linearity. The criterion is >0.985. Analytical range is the range in which the analyte can be detected using the calibration curve. The analyte must have a signal between those of the lowest and highest standards. If the signal is outside of the range, the results are uncertain.

3.3   Selectivity

Selectivity is a measure of the instrument's ability to chemically differentiate between analytes. To measure this, the selectivity factor, α, will be used and calculated as shown in *Figure 3.1* and *Equation 3.1*. If there is no t_0, it will be omitted from the calculation. The higher the value

of the factor, the better separation of the analytes. If the α value is 1, the chromatographic peaks are co-eluting. To increase this measure, changing solvents, changing pH of mobile phases, and changing temperature can help, but the most efficient method is to change the stationary phase. Selecting the HPLC-column for this project was therefore important, as discussed in the Method chapter.

$$\alpha = \frac{t_B - t_0}{t_A - t_0}$$

(Equation 3.1)
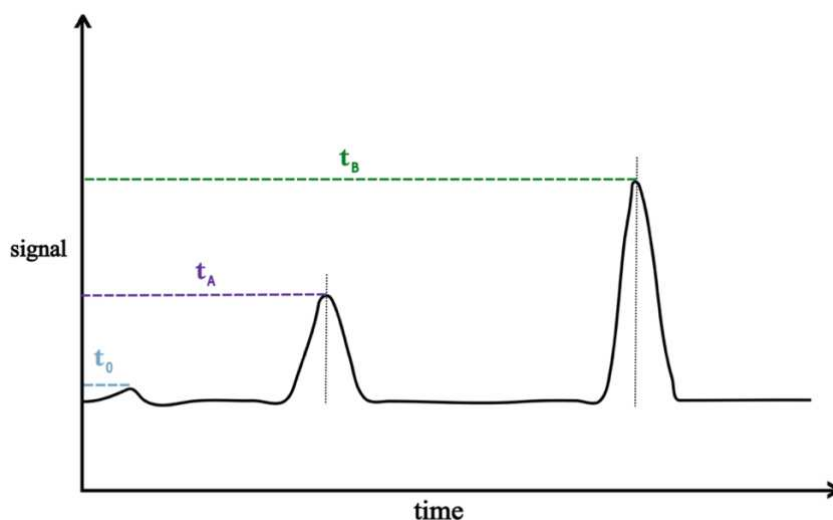
Figure 3.1. *Exemplified chromatogram and the selectivity factor, α, formula (drawn by Ada Njerve in Inkscape 1.2, 30.11.23).*

3.4   Precision

When analyzing the same analyte more times, the results should be the same each time. It is therefore important to inspect to see if they are. Precision is a measure of how distant the results are from one another. Percent relative standard deviation (% RSD) is a measure of precision, and the lower the value is, the closer the results are. The criterion is <20% for all samples, except for those samples with a concentration less than 1 ng/mL, where the criterion is <30%.

3.5   Accuracy

Accuracy is a measure of how close the analyte is to the expected value. Spiked and unspiked samples were analyzed to calculate this measure. The spiked samples have known concentration added to them, while the unspiked does not have any standards added. Using *Equation 3.2,* the percent recovery can be calculated. The closer to 100%, the better the accuracy. The criterion is 40-120%.

$$\% \, recovery = \frac{conc_{spiked} - conc_{unspiked}}{expected\ value} \times 100\% \qquad \textit{(Equation 3.2)}$$

3.6   Limit of detection and quantification

The limit of detection (LOD) and limit of quantification (LOQ) are two measurements to determine at which point the results are still tracible. LOD measures the observation of analyte, while LOQ measures the amount of analyte. When the results are below LOD and LOQ, distinguishing between the analyte and the noise is statistically impossible. There are several ways to calculate this parameter, yet in this project LOD and LOQ will be calculated from the blank samples. According to the ICH Harmonized tripartite guidelines Q2(R1) the LOD is calculated as in *Equation 3.3,* and LOQ as in *Equation 3.4,* where s and *S* are the standard error of the blanks and the slope of the calibration curve, respectively (ICH Expert Working Group, 1994).

$$LOD = \frac{3.3\sigma}{S} \qquad \textit{(Equation 3.3)}$$

$$LOQ = \frac{10\sigma}{S} \qquad \textit{(Equation 3.4)}$$

3.7   Robustness

Robustness for a method is to what degree the method upholds results over time even with small varying factors. This is especially important for methods used for repeatable, routine, and highly important analyses, such as in the pharmaceutical industry. These factors can differ, not by intent, but due to humans' natural inaccuracy. Typical factors to investigate in liquid chromatography, according to the ICH Harmonized tripartite guidelines Q2(R1), are (ICH Expert Working Group, 1994):

- Variation in pH in the mobile phase
- Variation in mobile phase composition
- Same columns, but different supplier/lots
- Temperature
- Flowrate

4 Results

4.1 Method development

4.1.1 MS parameters

All expected precursor ions for each standard were found during the MS2 scan in method development. Along with product ions, CE was optimized by choosing the highest responsive ions. This resulted in each analyte having ≥2 transitions. CAV and Fragmentor Voltage were also optimized. All optimized parameters for all the analytes are presented in *Appendix B, Figure B.1*. In *Appendix D, Figure D.1-D.5* chromatograms and mass spectra for MS optimization for ipPFNA are presented. All analytes underwent the same procedure.

4.1.2 Mobile phase gradient

The chromatograms of all the five stages can be found in *Appendix D, Figure D.6-D.10.* For the mobile phase gradient, four parameters are investigated to determine which gradient program was superlative. The time from the first eluted analyte to the last eluted analyte was calculated and is called the delta time (Δt). The greater the Δt, the better the possibility for separation. With that said, there are other factors to a good separation as well. In *Table 4.1*, the Δt from each stage is listed. The greatest time is 6.6 minutes, resulting from *Stage 5*.

Table 4.1. *Delta t from each gradient stage tested for method development.*

Stage	Δt (min)
1	1.3
2	2.1
3	6.1
4	4.5
5	6.6

Peak shape is another parameter, which, along with Δt, better determines the gradient program. The peaks are most ideal when they are Gaussian shaped, which is a representation of the Gaussian function, $f(x) = \exp(-x^2)$, and means perfect symmetry. There are several ways to investigate peak shape, but in this project full width at half maximum (FWHM) will be used. This measures the skinniness of the peaks in minutes and is significant to determine the performance of the separation. FWHM for all analytes and stages tested are presented in *Table 4.2.*

Lastly, it is important to look at whether the PFCAs are completely separated. To first investigate this, the number of peaks shown in the chromatogram were counted. Because twelve standards were used, twelve peaks are expected. Secondly, the number of co-elutions were counted, meaning where two analytes have a selectivity factor of $\alpha = 1.00$. The numbers are presented in *Table 4.2*.

Table 4.2. *Number of peaks detected, co-elutions, and mean FWHM in the chromatogram of each stage in gradient program optimization. Results are collected from the TICs (Total Ion Chromatograms).*

Stage	Number of peaks	Number of co-elutions	Mean FWHM
1	8	4	0.679 sec
2	8	4	1.048 sec
3	9	3	2.178 sec
4	10	2	1.678 sec
5	10	2	3.323 sec

4.1.3 Flowrate

Stage 5 from the gradient program optimization was tested with two different flowrates, 0.300 mL/min and 0.400 mL/min, to see if separation improved with increased flowrate. Δt for the 0.300 mL/min flowrate was 6.6 minutes, while the 0.400 mL/min flowrate was 6.7 minutes. The co-eluting analytes P37DMOA and ipPFNA fully co-eluted with the 0.400 mL/min flowrate, while the analytes with the 0.300 mL/min flowrate partially co-eluted. In *Figure 4.1* the arrows point to the P37DMOA and ipPFNA co-eluted peak(s).
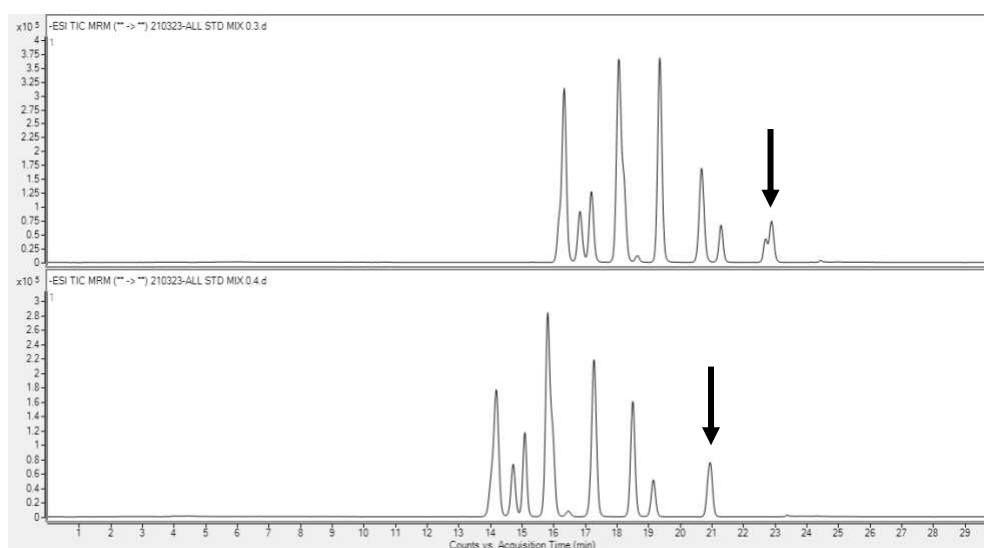

Figure 4.1. *Comparison of 0.300 mL/min and 0.400 mL/min flowrates. Top chromatogram shows the 0.300 mL/min flowrate and bottom chromatogram shows the 0.400 mL/min flowrate.*

4.1.4 Overall

Using the optimized MS parameters, optimized flowrate, and *Stage 5* gradient program the twelve PFCAs did not fully separate. *Figure 4.2* shows the chromatogram. The two analytes, P45DMHxA and P35DMHxA, which came in the same ampule from the supplier, were never distinguished and are counted as one analyte during method development, validation, and application. P4MHpA and P5MHpA were also not separated, while P37DMOA and ipPFNA were partially separated.
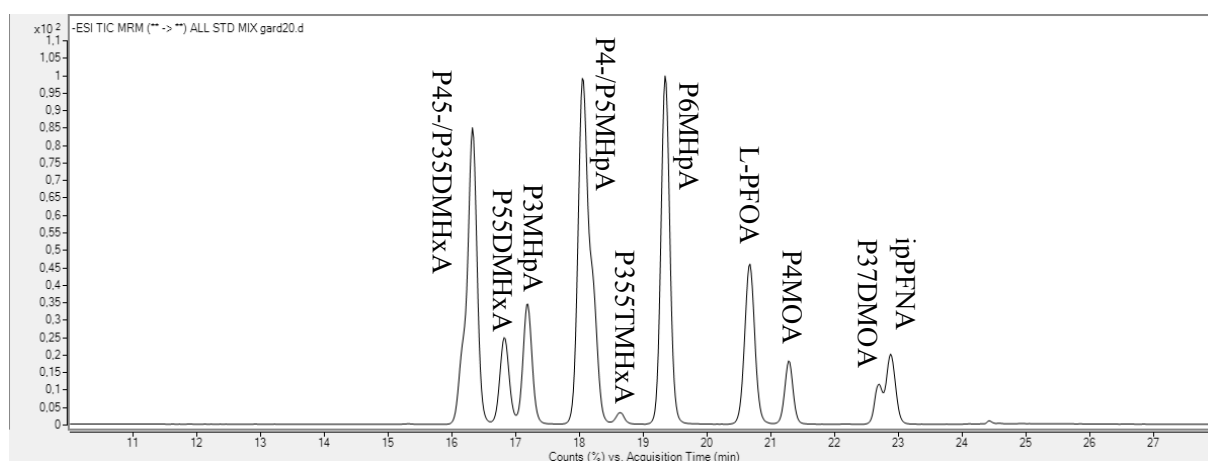
Figure 4.2. Chromatogram of twelve PFCAs, optimized with HPLC-MS/MS parameters in this project.

The selectivity factor, α, was calculated for all peaks, where t_A is any peak and t_B is the peak next to it on the right side, see *Table 4.3*. Because there was no t_0 visible in the chromatogram, the variable was omitted. The selectivity factor for the fully co-eluting peaks were not calculated and are considered to have $\alpha = 1$.

Figure 4.3. The selectivity factor of peaks and the one to the right of it.

t_A	P45-/35DMHxA	P55DMHxA	P3MHpA	P4-/P5MHpA	P355TMHxA	P6MHpA	L-PFOA	P4MOA	P37DMOA
t_B	P55DMHxA	P3MHpA	P4-/5MHpA	P355TMHxA	P6MHpA	L-PFOA	P4MOA	P37DMOA	ipPFNA
α	1.030	1.022	1.050	1.033	1.038	1.069	1.029	1.067	1.008

4.2   MS troubleshooting

In the first run of the method validation, the responses in signal were unpredictably low. The mean response of the internal standard (ISTD) for L-PFOA was 3452, and the response for the 100ng/mL calibration standard was 647. After cleaning the ion source, the signal improved.

Because this worked, the capillary was also cleaned, to ensure optimal results. The mean responses of the ISTD improved to 29224 and the 100ng/mL to 37194. A leak in the nitrogen generator was also found, causing air to enter the instrument without being noticed by any leak detectors. The problem was fixed by a professional, and it improved the mean ISTD and 100ng/mL responses to 55098 and 474275, respectively.

4.3   Method validation

Due to lack of standard solutions, the final validation was only applied to L-PFOA, P3MHpA, ipPFNA, P37DMOA, P4MOA, and P355TMHxA, in which there are only two analytes partially co-eluting: ipPFNA and P37DMOA.

Linearity and linear range of the calibration curves are presented in *Table 4.4*. To gain the results from the lowest calibration standards, all the curves were weighted 1/x. The r^2-value for all the calibration curves is within the >0.985 criterion, with the lowest being 0.988 (P37DMOA), and the highest 0.994 (P4MOA). The recovery of 0.1ng/mL in the L-PFOA, P3MHpA, P4MOA, ipPFNA, P355TMHxA, and P37DMOA calibration curves are 164%, 145%, 174%, 161%, 143%, and 139% respectively, which are all outside the range of acceptance (40-120%). The linear range for all the analytes is therefore LOQ-1000ng/mL. LOD and LOQ are also presented in *Table 4.4*.

Table 4.4. Linear range, linearity as r^2-value, weight of calibration curves, LOD and LOQ for the analytes validated.

Analyte	Linear range (ng/mL)	r^2-value	Weight	LOD (ng/mL)	LOQ (ng/mL)
L-PFOA	0.92-1000	0.992	1/x	0.30	0.92
P3MHpA	0.41-1000	0.990	1/x	0.14	0.41
P4MOA	0.22-1000	0.994	1/x	0.07	0.22
ipPFNA	0.08-1000	0.993	1/x	0.03	0.08
P355TMHxA	0.12-1000	0.990	1/x	0.04	0.12
P37DMOA	0.12-1000	0.988	1/x	0.06	0.19

In *Table 4.5* and *Table 4.6,* the recoveries of the spiked samples are presented. Those results outside of acceptance are marked in blue. The samples spiked with 0.5 ng/mL were all within the acceptance range, except P3MHpA and P4MOA. P4MOA have >120% for all spiked

samples, both cattle liver and cod muscle, except 0.5 ng/mL cod muscle. ipPFNA were outside range for cod muscle spiked with 50 ng/mL analyte. ipPFNA, P355TMHxA and P37DMOA were all outside of the ranges for the matrix effect samples.

Table 4.5. Accuracy as mean percent recoveries and standard deviation (SD) for cattle liver samples for method validation. Values in blue are outside of the acceptance range (40-120%).

Analyte	Spiked 0.5ng/mL (n=3)		Spiked 10ng/mL (n=3)		Spiked 50ng/mL (n=3)		Matrix effect 50ng/mL (n=3)	
	Mean	SD	Mean	SD	Mean	SD	Mean	SD
L-PFOA	82.6	3.6	70.6	12.9	85.9	2.2	101.1	5.0
P3MHpA	69.6	18.5	80.9	25.3	92.8	7.5	115.2	3.6
P4MOA	134.1	34.9	152.2	9.6	163.1	11.7	100.8	5.5
ipPFNA	67.3	6.0	58.1	11.7	45.0	39.4	133.0	5.9
P355TMHxA	80.0	10.1	83.4	10.4	92.2	3.8	125.8	2.6
P37DMOA	74.9	6.5	62.4	1.3	69.9	5.1	135.7	3.4

Table 4.6. Accuracy as mean percent recoveries and standard deviation (SD) for cod muscle samples for method validation. Values in blue are outside of the acceptance range (40-120%).

Analyte	Spiked 0.5ng/mL (n=3)		Spiked 10ng/mL (n=3)		Spiked 50ng/mL (n=3)		Matrix effect (n=3)	
	Mean	SD	Mean	SD	Mean	SD	Mean	SD
L-PFOA	61.5	8.1	76.8	1.8	87.2	1.7	103.4	2.1
P3MHpA	37.5	5.2	71.9	6.5	85.2	3.6	110.4	3.8
P4MOA	108.9	20.0	152.6	7.2	193.8	6.5	104.3	2.1
ipPFNA	86.6	8.6	91.0	1.3	131.5	1.4	146.2	12.9
P355TMHxA	59.6	8.5	71.4	3.3	86.6	1.5	136.2	3.2
P37DMOA	92.8	9.8	80.6	6.5	87.8	1.7	123.9	1.2

Figure 4.3 shows the means of all analytes for the samples analyzed in method validation. The green bars represent mean analyte concentration in cattle liver, and the blue bars, in cod muscle. These are divided to get an insight on how the analytes interact with each sample matrix. The cod muscle generally has higher concentrations, but only for 10 ng/mL, 50 ng/mL, and 100 ng/mL. Cattle liver has higher concentration in the 0.1 ng/mL and 0.5 ng/mL samples, however there is no significant difference in cattle liver and cod liver in the five lowest concentrations, including blank and blind.
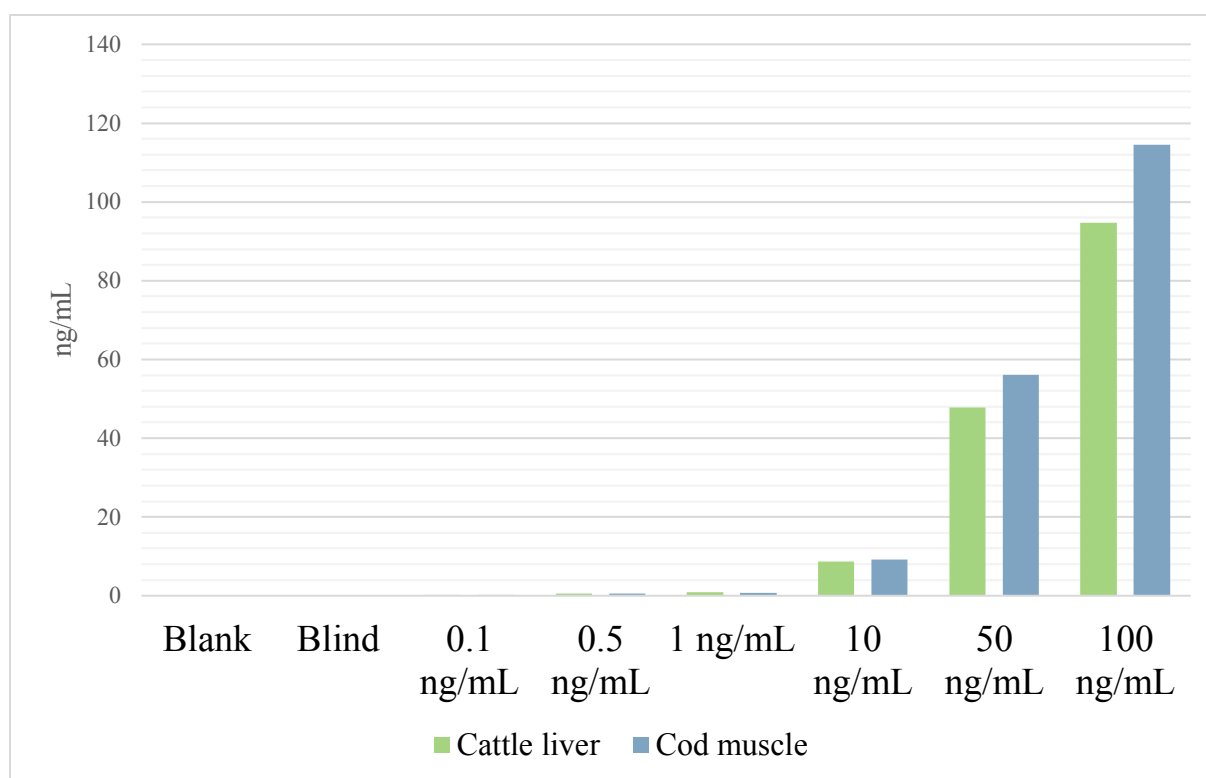
Figure 4.3. *Calculated mean concentration of all target analytes of blanks, blinds, and spiked samples.*

The precision for all spiked samples and matrix effect samples were within acceptance (<20%), see *Table 4.7,* except blank L-PFOA and P3MHpA, P3MHpA in the blind cattle liver sample, and the 10ng/mL cattle liver spiked sample for P3MHpA, marked in blue.

Table 4.7. *Precision as % relative standard deviation, here: L=cattle liver, M=cod muscle. Values in blue are outside of acceptance range (<20%).*

Analyte	Blank (n=3) %		Blind (n=3) %		Spiked 0.5ng/mL (n=3) %		Spiked 10ng/mL (n=3) %		Spiked 50ng/mL (n=3) %		Matrix effect (n=3) %	
		L	M	L	M	L	M	L	M	L	M
L-PFOA	35.0	7.9	17.3	3.2	7.9	17.9	2.3	2.6	1.9	4.9	2.0
P3MHpA	83.2	48.2	-	19.7	13.8	30.8	9.2	8.0	4.2	3.1	3.5
P4MOA	12.2	6.1	4.6	19.8	13.7	6.2	4.7	7.2	3.4	5.4	2.0
ipPFNA	5.0	2.9	8.9	5.9	7.1	19.5	1.4	5.2	1.1	4.4	8.8
P355TMHxA	6.7	24.2	3.4	8.5	9.5	12.2	4.6	4.1	1.8	2.1	2.4
P37DMOA	11.4	7.4	9.0	6.1	7.8	2.1	7.9	7.3	2.0	2.5	0.9

4.4   Findings from Ny-Ålesund

The results were analyzed, and the final concentrations were calculated based on the volume or weight of samples. Since the ISTD concentration in the calibration curve and samples differed, 10 ng/mL and 20 ng/mL, respectively, the concentrations of the samples were multiplied by 2. This was done with the assumption that the ISTD responses were linear.

The findings from Ny-Ålesund, Svalbard are presented in *Table 4.8,* and all chromatograms of blanks, calibration standards, and samples are presented in *Appendix D, Figure D.11-D.18.* The results marked in blue are below LOD and LOQ and are therefore considered not detected, while those marked in green are below LOQ and above LOD. These results are not included in the total sum of PFCAs (ΣPFCA) due to them not being able to be quantized. L-PFOA was detected in all samples, with quantizable concentration of 6.38-52.61 ng/mL. P3MHpA was detected in water samples 01A, 01B, 02A, and 02B with consistent concentrations around 2.4 ng/mL (SD=0.23), along with being detected in 08A at 0.26 ng/mL. P4MOA was detected in all samples except S-02, but only quantized in 02B. ipPFNA was found in all samples at ranging concentrations of 0.23-3.20 ng/mL. P355TMHxA and P37DMOA were detected in all the samples, yet all <0.7 ng/mL. In *Figure 4.4,* a visual representation of data is presented. The NÅ-W-02 samples are those with the largest amount of ΣPFCA, followed by NÅ-W-01, NÅ-S-02, NÅ-W-08A, NÅ-S-01, NÅ-W-16 and NÅ-W-08B, chronologically.

Table 4.8. *Results of samples from Ny-Ålesund, Svalbard (all samples have NÅ- in front). Values in blue are considered not detected, values in blue are below LOQ, but above LOD.*

Analyte	W-01A (ng/mL)	W-01B (ng/mL)	W-02A (ng/mL)	W-02B (ng/mL)	W-08A (ng/mL)	W-08B (ng/mL)	W-16 (ng/mL)	S-01 (ng/mL)	S-02 (ng/mL)
L-PFOA	40.98	34.93	52.61	51.63	13.38	0.57	6.38	10.88	23.37
P3MHpA	2.57	2.35	2.06	2.53	0.26	0.12	0.44	0.51	0.91
P4MOA	0.21	0.20	0.20	1.23	0.19	0.15	0.16	0.19	0.05
ipPFNA	3.20	2.64	0.39	0.35	0.29	0.26	0.35	0.23	0.28
P355TMHxA	0.17	0.19	0.40	0.26	0.15	0.14	0.17	0.24	0.07
P37DMOA	0.27	0.22	0.22	0.68	0.26	0.23	0.23	0.10	0.10
ΣPFCA	47.19	40.33	55.68	56.68	14.08	0.63	7.57	11.69	24.56

Figure 4.5 shows the composition of the target analytes, where all samples, except NÅ-W-08B, mostly consists of L-PFOA. In the NÅ-W-01A, -01B, -02A, -02B samples, L-PFOA are at ~87%, ~87%, ~94%, and ~91%, respectively. Sample NÅ-W-08A has an L-PFOA composition

of ~87%, while -08B is at 0%. NÅ-W-16 is at ~84% L-PFOA. The soil samples are at 91-95% L-PFOA.

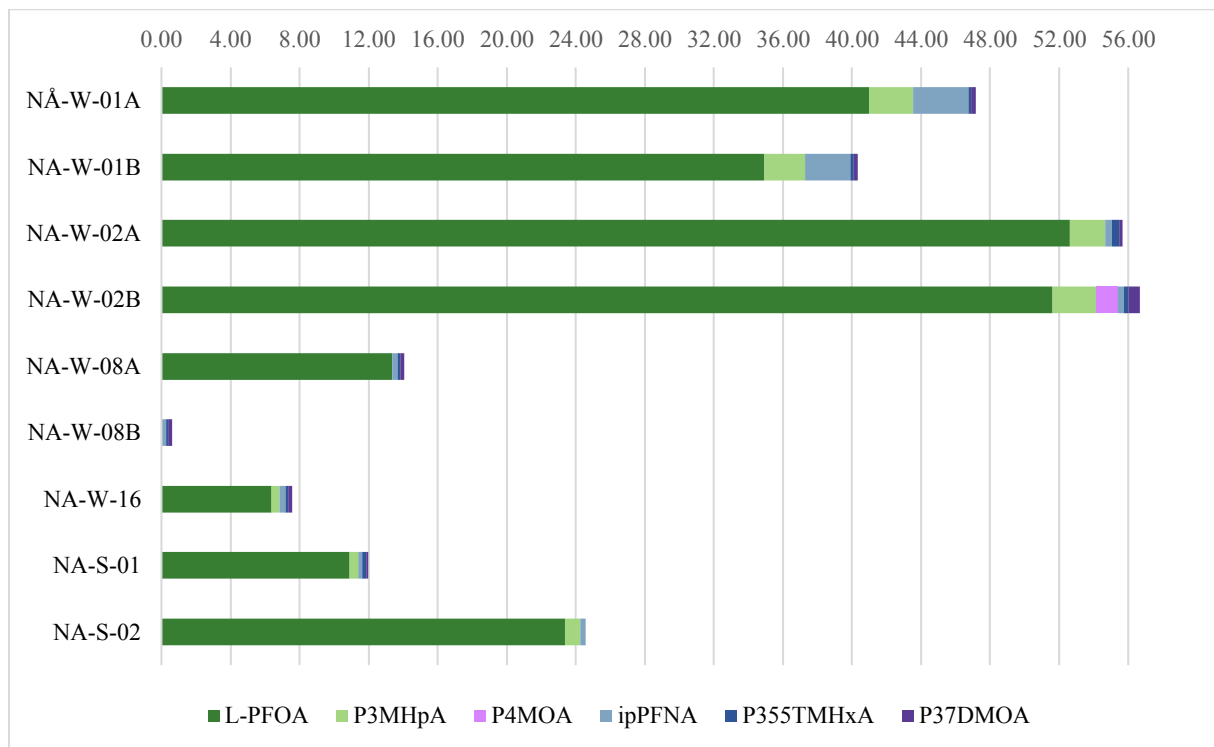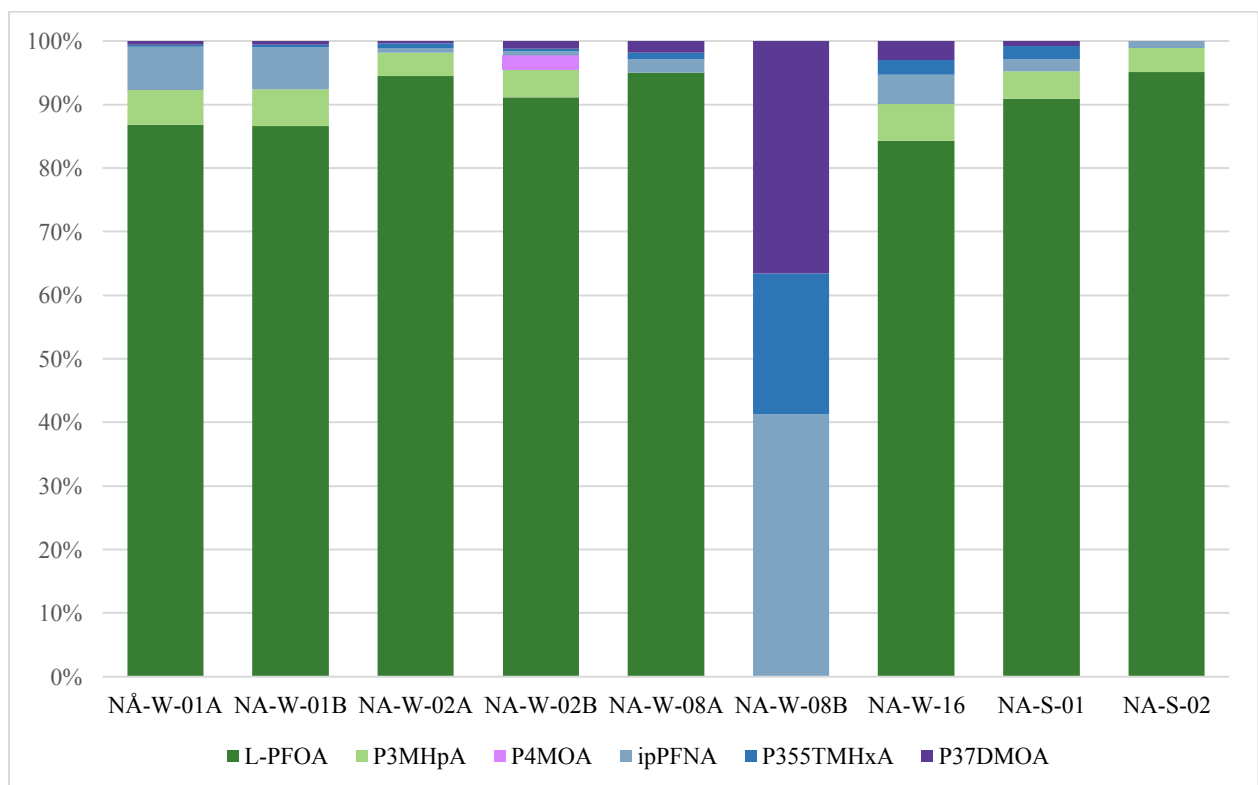**Figure 4.4.** *Representation of results of detected analytes present at sampling sites.*

Figure 4.5. *Composition of target analytes at each sampling site where analyte was detected.*

4.5   Statistical analysis of the results

Multivariate statistics are often used in scientific data analysis to recognize patterns in data sets. Principle component analysis (PCA), a type of multivariate statistic, will be used to analyze the correlations between the target analytes, while also considering the sampling sites. The main goal of PCA is to reduce the number of variables while retaining as much information as possible, and one way to achieve this is by transforming the original variables into a new set of linearly uncorrelated variables called principal components or here; factors (F). The first factor (F1) is a linear combination of the original variables that explains the largest amount of variation in the data. The second (F2) is the next largest, and so on. F1 is the linear line in which the sum of squared distances from the original variables to the origin, is the largest. F2 is the orthogonal line to F1. The Eigenvalue, in *Figure 4.6* is the average of the sum of squared distances. The Eigenvalue is also used in PCA to determine the relative importance of each factor. The percentage variability indicates the proportion of the total variance in the data accounted for by each factor, also presented in Figure 4.6.

Figure 4.6 shows the factors in a scree plot, where the black dots (with a connecting line) are the cumulative variability of each factor. F1 accounts for 55.29% of the total variation in the Fs, and F2 accounts for 25.06% of the variations. F1, F2 and F3 account for 95.81% of variation of all the data. With F1, F2, and F3 accounting for >95%, most of the total variance is accounted for by the first few factors.

When interpreting the PCA plots it is important to investigate three parts. (1) The distance between two samples. The distance is a measure of their similarity in terms of the original variables. Samples that are close together on the plot are more similar than samples that are far apart. And samples on the opposite side of the origin from each other, are inversely correlated. (2) Recognizing outliers. Outliers in PCA plots can indicate samples that are significantly different from the rest of the data. These samples should be investigated further to determine the reason for their deviant behavior. (3) PCA plots can reveal groupings or clusters of samples that are alike. These groups can be identified by their proximity to the plot and are significant in the evaluation of PFCA composition and sample position of the Ny-Ålesund samples.
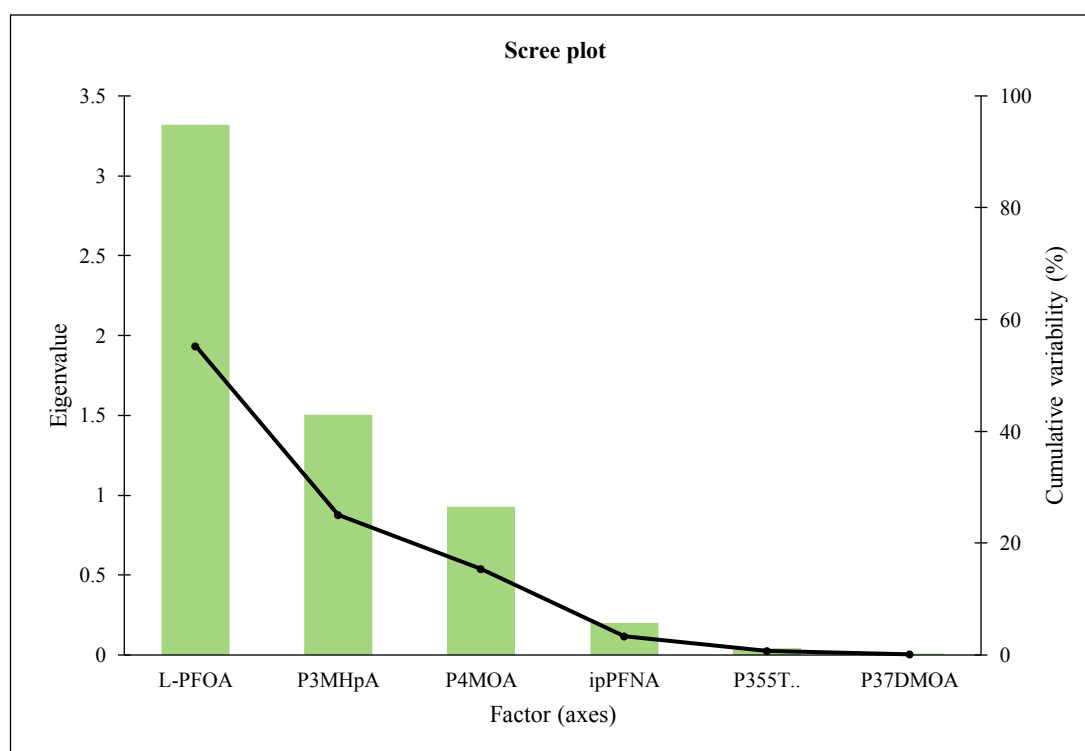
Figure 4.6. *Scree plot of the factors in the principal component analysis for the Ny-Ålesund samples.*

The F1 v F2 PCA plot is presented in *Figure 4.7.* The NÅ-W-01A and -01B samples are grouped towards the top right, while NÅ-W-02A and -02B are plotted further to the right bottom, yet more spread out than -01A and B. The remaining samples are clustered towards the left middle. The soil samples are close to each other, however -S-01 is closer to water sample -16 and -08A, meaning -S-02 and -08B are slightly further away from the cluster. As seen in the plot, the -01 and -02 samples are somewhat spread away from the -08, -16, and soil samples.

In *Figure 4.8,* the F2 v F3 plot is presented, accounting for 40.52% of the variation. Here, all the samples are closer together than in *Figure 4.7.* The NÅ-W-01A and -01B are still grouped together, yet towards the lower right. NÅ-W-02A and -02B are significantly further apart from each other than in the other plot. The remaining water samples are still clustered together, towards the middle left. The soil samples -01 and -02 are in towards the top left and towards the bottom right, respectively, meaning they are on the opposite side of each other from the origin.

In both plots, the variables are shown in blue (with vectors from the origin). This type of representation is called loading plot. The vectors help visualize angles between two analytes. The smaller the angle, the more positively correlated the analytes are, e.g., L-PFOA and

P3MHpA in *Figure 4.7*. If the angle is 90°, the analytes are not correlated, like P4MOA and ipPFNA in *Figure 4.7*. And if the angle is close to 180°, e.g., P4MOA and ipPFNA in *Figure 4.8,* the analytes are negatively correlated.

Figure 4.7. *Plot of principle component analysis for F1 and F2. Samples (observations) are presented in green, while the analytes (variables) are presented in blue, with linear vectors to the origin. Here: 01A=NÅ-W-01A, 02A=NÅ-W-02A, S-01=NÅ-S-01, and so on.*
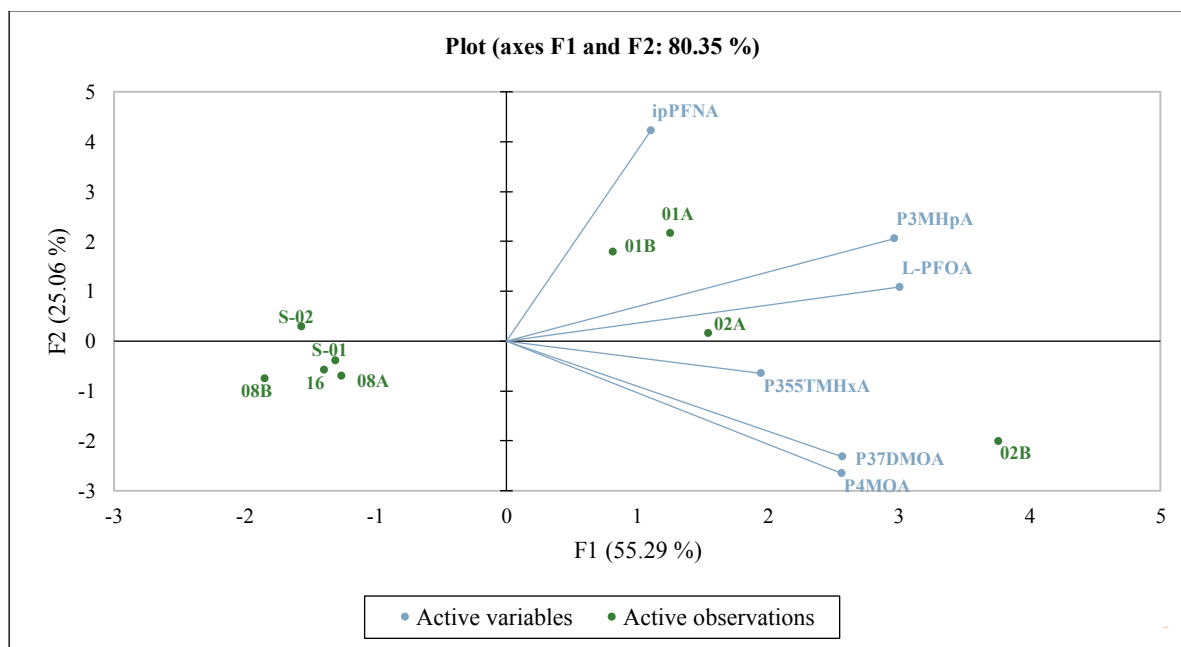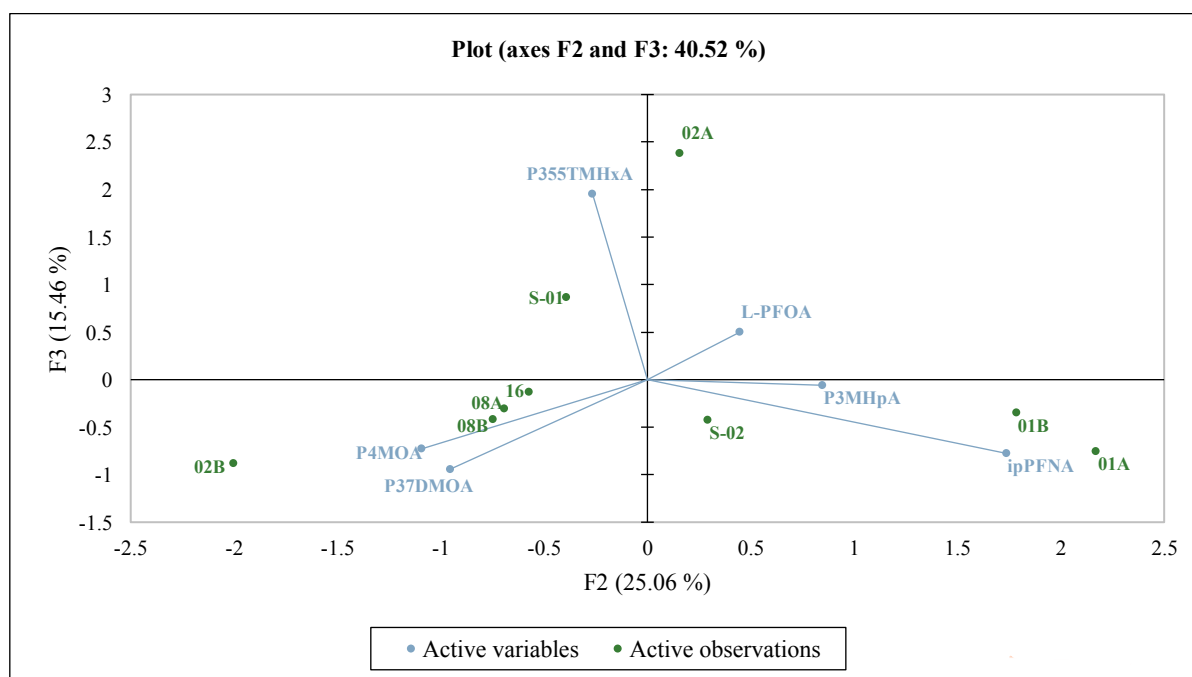

Figure 4.8. *Plot of principle component analysis for F2 and F3. Samples (observations) are presented in green, while the analytes (variables) are presented in blue, with vectors to the origin. Here: 01A=NÅ-W-01A, 02A=NÅ-W-02A, S-01=NÅ-S-01, and so on.*

5 Discussion

5.1 Method development

5.1.1 MS parameters

Half of the analytes had precursor ions at *m/z* 413 with similar product ions and 5 out of 12 analytes had precursor ions at *m/z* 463. With similar product ions, as well as the precursor ions, separation was strenuous, as expected. Investigating if there were unique patterns for the different analytes, could have been tested to further distinguish the isomers/different Br-PFCAs and improved the separation. But due to time and instrument availability this was not done.

During the product ion scan, the analytes that came in the same ampule, P35DMHxA and P45DMHxA were never distinguished. The two analytes had the same precursor ion and similar structures. It was not possible to know which product ion belonged to which analyte, it was therefore counted as one analyte during the rest of the method development and analysis. Some of the PFCA isomers were still distinguishable during gradient optimization, and it was desired to separate P35DMHxA and P45DMHxA then as well. With more time, the two analytes could have been investigated further, and possibly separated.

5.1.2 Gradient program

The gradient optimization improved as the increasing stages were conducted. In *Stage 1* all the target analytes eluted between 87% and 90% B, and the stage had a Δt of 1.256 minutes. Because 7 of the 11 standards have the same molecular weight and similar fragmentation patterns, they eluted at the same time. Due to the standards eluting at 87% B in *Stage 1*, starting with a higher %B was tried in *Stage 2*. At an initial percentage of 50% B, the L-PFOA and P3MHpA both eluted within the first minute of the gradient. This might have been caused by the heightened %B not allowing the analytes to interact with the stationary phase. This starting percentage was therefore not tested further. Even though the separation improved in *Stage 2,* six of the standards (P4MHpA and P5MHpA, P45-/35DMHxA and P55DMHxA, and ipPFNA and P37DMOA) were still co-eluting. In *Stage 3* the step gradient improved the separation with both the Δt and number of peaks, yet there were still six (P3MHpA, P4MHpA and P5MHpA, P45-/35DMHxA and P55DMHxA) that co-eluted. In *Stage 4* and *5,* different organic mobile phases were tested to resolve the problem. *Stage 4,* using acetonitrile, improved the co-eluting peaks in *Stage 3,* but had a 26% decrease in Δt-value. *Stage 4* was run simultaneously with

Stage 5, and with the same number of peaks and co-elutions, *Stage 4* was therefore ruled out due to the shorter Δt. This could have been caused by acetonitrile having a lower viscosity than MeOH at 30°C, which impair longitudinal diffusion in the van Deemter equation. Along with being more viscous, the mobile phase in *Stage 5* had a lower pH (due to added formic acid), which improved the separation. *Stage 5* had the greatest Δt with 6.6 minutes, as well as the most peaks visible and the least amount of co-elutions. Even though the mean FWHM for *Stage 5* was the worst out of all the stages, all the FWHMs were of good rate and this parameter did not play an influential role in gradient program optimization.

Stage 5 was chosen as the most efficient gradient program for separating the PFCAs. Due to the similar structures and fragmentation patterns, not all 12 PFCAs were separated, but for this project the program was considered sufficiently efficient. *Stage 5* had a similar Δt as *Stage 3,* but the two programs were able to separate different analytes. *Stage 3 s*eparated e.g., ipPFNA and P37DMOA, but not P45-/35DMHxA and P55DMHxA. *Stage 5* accomplished the opposite. With all the parameters, *Stage 5* was the most adequate gradient program that was conducted.

The selectivity factor for all the analytes not co-eluting was $\alpha > 1$, meaning they are not co-eluting, as seen in *Table 4.3*. Yet the P37DMOA and ipPFNA are partially co-eluting which explains why their α closer to 1 than the rest. This parameter could have been improved by a more optimal gradient program with a desire to have $\alpha \geq 2$.

5.1.3 Flowrate

The flowrates tried during method development were 0.300 mL/min and 0.400 mL/min, and as seen in *Figure 4.1,* the chromatograms are similar. Increasing the flowrate will improve separation according to the van Deemter equation, yet the ipPFNA and P37DMOA did not improve its separation with a higher flowrate. This suggests that 0.300 mL/min is the highest flowrate in which the column is working optimally. Therefore, increasing or decreasing the flowrate would worsen the separation.

5.1.4 Overall separation

With only two fully co-eluted sets of analytes, the separation for determination of L-PFOA and Br-PFACs to then investigate sources of PFAS contamination in Ny-Ålesund, Svalbard, was somewhat accomplished. Considering all the target analytes used in this project, seven are

known to result from ECF, where L-PFOA, P3MHpA and P6MHpA were completely separated and can therefore be quantized. P4- and P5MHpA, and P35- and P45DMHxA were not separated, but could still be quantified to determine L-PFAS and Br-PFAS ratio. P44DMHxA and P55DMHxA were never investigated, which will be considered during sample analysis. L-PFOA, however, is the most significant analyte to quantify for composition determination.

5.2 Method validation

5.2.1 Calibration curves and linear range

The calibration curves for each analyte were all conducted from 0.1-1000 ng/mL but because the lowest calibration standard is not within validation parameters, it is omitted. 0.1 ng/mL is a significant low concentration of PFAS, which suggests the high % recoveries. With all the r^2-values being above the criterion, >0.985, it is concluded that within the linear range, the signals obtained will correspond to the correct concentration.

5.2.2 Accuracy and matrix effect

Several of the spiked samples used to determine accuracy are outside of acceptance range, meaning either there are significant matrix effects, addition of analyte was wrongfully done, or that the method is not accurate enough. The P4MOA recoveries are all >130%, meaning the results are consistently above acceptance, which can signify that too much analyte was added to all the samples. The results for all other analytes in the spiked samples are <100%, which can indicate significant chemical interference for both cattle liver and cod muscle. Chemical interference is a type of matrix effect, where components in the matrix interact with the analytes, causing reduction of analyte signal. Additionally, the matrix effect samples, where the standard solutions are added after sample preparation, are all >100%, which amplifies the occurrence of this matrix effects.

In *Figure 4.3,* the cod muscle appears to recover more analyte than cattle liver, meaning the liver has a greater matrix effect than muscle. However, this is only true for the three highest concentrations, while the lower concentrations along with blanks and blinds are insignificantly different from liver to muscle (p>0.05). Yet, because the blank, blind and three lowest concentrations are not within range of linearity and are therefore considered not detected, cattle liver does have a greater matrix effect.

5.2.3 Precision

The precision of the samples is mostly within range of acceptance (<20%), as seen in *Table 4.7*. However, the blank and blind samples, at 35-83% precision, are not spiked with analyte and are therefore prone to having high %RSD due to background noise and other matrix effects. The 10ng/mL liver sample for P3MHpA had one of the replicates at 5.37ng/mL and by omitting this result the mean %RSD for P3MHpA would decrease to 8.2%. Because the rest of the results are within acceptance, it can be concluded that the odd result was due to sample preparation error, e.g., too little analyte added was to the sample.

5.3   Findings

The sample matrices differ in the method validation and application, which makes the comparison of matrix effect difficult. Both cattle liver and cod muscle have matrix effect, such as chemical interference, but water and soil are uncertain due to lack of validation. Therefore, no matrix effect will be considered for the calculation of results from the Ny-Ålesund samples. The calibration standards are not in matrices, meaning the calibration curve is independent of matrix effects. After SPE treatment, water too is known to have little matrix effect compared to other complex matrices. Soil, however, is a complex mixture of minerals, dirt, and other contaminants. Even though the matrix effect will not be considered when calculating the results, it will be considered when discussing them.

5.3.1   Source of contamination in Ny-Ålesund

The sample with the lowest PFCA concentration is NÅ-W-08B at 0.63 ng/mL. Though this should not be ignored, source of contamination will not be discussed further due to the low abundance and no trace of L-PFOA. The highest ΣPFCA levels are in the NÅ-W-02A and -B samples, at 55.68 and 56.68 ng/mL, respectively. These samples were collected closest to the FFTS in Ny-Ålesund compared to the other water samples. It was therefore expected to find elevated levels of PFAS in that area. The two samples also have L-PFOA compositions of 91-94%, which can suggest a local source of PFAS contamination. By considering that not all Br-PFCAs resulting from ECF were analyzed, the L-PFOA percentage could be closer to the composition from the ECF process at <80%. However, since the area is known to have been used as a FFTS, and AFFF was used there, the PFOA and PFCAs contamination is caused by that.

The second most contaminated sample is NÅ-W-01A and -B, with 47.19 and 40.33 ng/mL, respectively. Compared to the previous samples, NÅ-W-02A and -B, the compositions of L-PFOA are here 87%. With the not analyzed Br-PFCAs resulting from ECF, there is a greater chance that this percentage of L-PFOA is lower than 87%. This can suggest that the contamination comes from the ECF manufacturing process and has entered the Arctic through atmospheric transport. Contradictory, these samples were collected from a small downstream close to the FFTS in Ny-Ålesund, which can suggest that this downstream is contaminated from AFFF and not remote sources.

The other samples collected from meltwater near Ny-Ålesund, NÅ-W-08A and -16, have lower concentrations of ΣPFCA, at 14.08 and 7.57 ng/mL, respectively. Similar to the previous discussed samples, these samples also have L-PFOA >80%, at 84-95%, which suggest that these do not result from the ECF process. Additionally, these samples were collected from meltwater from the mountains where no AFFFs have been used. These samples do not follow the predicted trend of having <80% L-PFOA resulting from ECF and long-range transportation. Yet it is also difficult to conclude that there is local contamination, due to the sampling locations. However, the other process of producing PFAS, telomerization, is known to not produce isomers or derivatives. It is therefore a possibility that remote contamination is a source for PFCAs in the -08A and -16 samples. Because this is a longer route than from the FFTS, it can suggest why the concentrations are significantly lower than in NÅ-W-01 and -02.

Lastly, the soil samples, NÅ-S-01 and -02 have generally lower concentrations of ΣPFCA than the water samples from the same area, NÅ-W-02. With concentrations of 11.96 and 24.56 ng/mL, and 91-95% L-PFOA, these samples also suggest local contamination. The reason for the lower concentration can be due to chemical interference, which is not accounted for. The affinity of PFAS in soil, where PFAS bind stronger to soil than to water, is causing the analyte extraction to be more strenuous for soil samples.

5.3.2   Principal component analysis

Considering the Eigenvalue and the cumulative variability of the transformed data accounting for 95% of all variances, only using the first three factors will be considered a good approximation of the original data.

In the F1 v F2 plot, the samples can be grouped together by sample type and where they were sampled. The grey circles in *Figure 5.1,* are groups of (1) soil samples near FFTS, (2) water samples from meltwater, and (3) water samples near FFTS. The grey circle "Water near FFTS", is grouped because of their high concentration of ΣPFCA, with more than four times higher than the rest of the samples. The samples are also more influenced by P3MHpA, and NÅ-W-01A and -01B are the most influenced by ipPFNA than the other samples, shown by the distance between the samples and the vectors. The (1) soil near FFTS circle is grouped due to the samples' similar compositions, yet NÅ-S-02 is more influenced by L-PFOA, P3MHpA and ipPFNA than -01, and is therefore higher up in the plot. The (2) water from meltwater samples are clustered, not being related to the FFTS and are therefore on the opposite side of the origin than -01 and -02 water samples.

The blank circles represent clusters of (a) water from meltwater and soil samples, and (b) water samples near FFTS. These are grouped in comparison of their ΣPFCA concentrations, where (a) has lower concentrations than (b). NÅ-W-02B, is here an outlier, which is a result of the high concentration of P4MOA, being six times higher than the rest of the samples. The (a) samples also have higher compositions of P355TMHxA and P37DMOA and are therefore correlated.
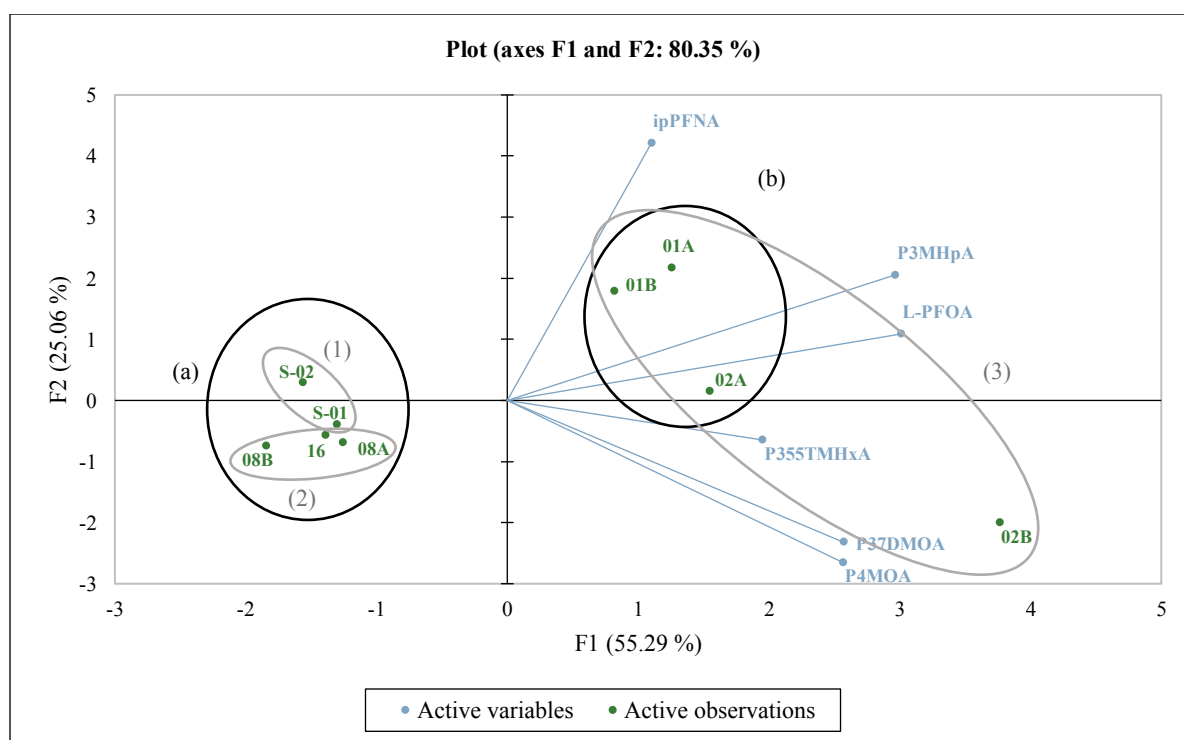

Figure 5.1. *Cluster analysis of PCA plot (F1 v F2).*

The plot F2 v F3 (*Figure 5.2*) shows similar traits to the previous plot. NÅ-W-01A and -01B are still clustered together (ii) and influenced by L-PFOA, P3MHpA and ipPFNA. The NÅ-W-08 samples and NÅ-W-16 are also grouped here (i); however, the soil samples are further apart from this cluster. The soil samples are also further apart from each other and on opposite sides of the origin, meaning that they are inversely correlated in this plot. S-01 has a 3.5 times higher concentration of P355TMHxA than S-02, which suggests the distance between the two. The NÅ-W-02 samples are the furthest apart, which again shows the influence P4MOA has on -02B.

Plot (axes F2 and F3: 40.52 %)
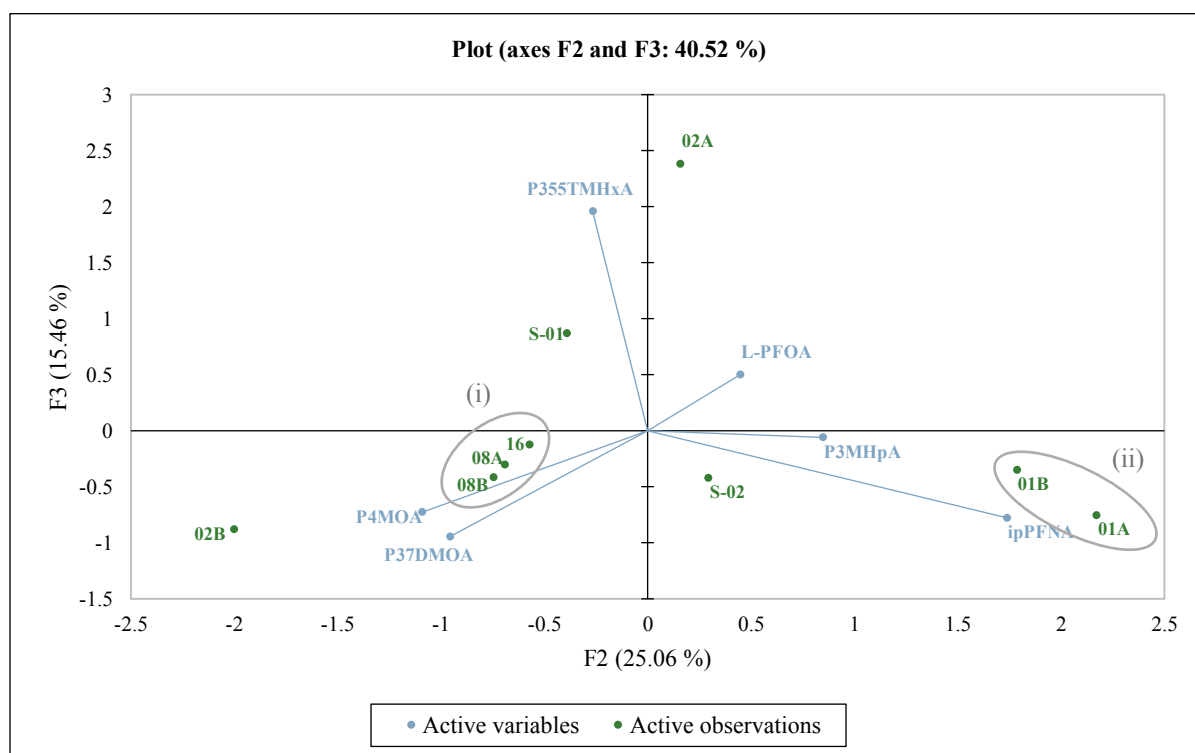
Figure 5.2. Cluster analysis of PCA plot (F2 v F3).

With the objective of finding patterns using principal component analysis, the two plots, accounting for >95% of the variables, five categories can be demonstrated, see below. Though the plots look different, they account for the same variables and show similar traits of the samples, and the categories are concluded from both plots. Importantly, all samples contain mostly L-PFOA, except NÅ-W-08B. The categories are therefore grouped in comparison to each other, not themselves. E.g., when the NÅ-W-08A is categorized as mostly influenced by P355TMHxA, it does not contain mostly P355TMHxA, but is more influenced by this analyte than the other samples.

Overall, the samples can be categorized as such:

1. Samples mostly influenced by L-PFOA, P3MHpA and ipPFNA
2. Samples mostly influenced by P4MOA and P37DMOA
3. Samples mostly influenced by P355TMHxA
4. Samples with high concentration of ΣPFCA
5. Samples with low concentration of ΣPFCA

The first and fourth categories include the water samples -01A, -01B, and -02A, all mostly influenced by the analytes in category 1. The outlier, sample NÅ-W-02B, is also included in category 4, but is more influenced by the analytes in category 2. -02A is also included in category 3.

Category 2 also includes the three water samples from downstream meltwater. Because these are not associated with the FFTS, these were expected to cluster together. The samples are also included in the fifth category, along with the soil samples. Both groups of samples have lower concentrations of ΣPFCA, but distinct reasons for this. As discussed, the meltwater samples have lower concentrations due to the long-range transportation of PFAS. On the other hand, the soil samples are most likely low in concentration due to affinity of PFAS to soil and matrix effects. The soil samples are also influenced by P355TMHxA and are included in category 3, while NÅ-S-02 is also included in category 1 in comparison to NÅ-S-01.

The categories from PCA also match up with the source of contamination. Again, the samples having higher concentrations likely are a result of AFFF contamination, while the other water samples are likely contaminated by atmospheric transportation and accumulation in the Arctic. The soil samples are low due to the matrix. Samples from the FFTS are more influenced by L-PFOA, P3MHpA, ipPFNA, while those samples from meltwater are more influenced by P4MOA and P37DMOA. P355TMHxA is overlapping in both categories of contamination. The PCA plots suggest several patterns in the results and is another factor in future analysis of source of PFAS contamination.

Though the sources of contamination are discussed regarding L-PFOA composition, there are no significant trends. Those samples from local contamination (NÅ-W-01, -02, -S-01, and -S-02) have >80% L-PFOA, but so the samples from remote contamination (NÅ-W-08A and -16).

The PCA is therefore not used to categorize the samples regarding isomeric composition but is still valuable for future investigation of patterns in different PFAS in the Arctic.

5.3.3 Comparison of results

L-PFOA was the only analyte parallel to the reference method, Skaar et al. (2019). *Table 5.1* shows the compared results and when comparing the water samples, no significant difference is found ($p=0.47$, $p>0.05$). The most notable differences are in the soil samples. More than 50% more L-PFOA is detected in the NÅ-S-01 and -02 samples in this project. As discussed before, this can be due to the matrix effects that are not counted for. Because the soil samples are different from the reference method, it can signify that soil does have a larger matrix effect than water.

The comparison of compositions is significantly different. *Table 5.1* also shows the composition of L-PFOA, but the Br-PFOAs and other PFCAs used to calculate the percentages are different from this project to Skaar et al. (2019). The L-PFOA percentage from Skaar et al. is overall lower than in this project, which is likely due to the different Br-PFASs used. However, comparing the results for L-PFOA shows no significant difference, which makes the composition comparison uncritical to consider. It rather shows that this project investigates a different part of the same samples and shows the importance of secondary analyses.

Table 5.1. *Comparison of results for L-PFOA and L-PFOA composition between this project and Skaar et al. (2019). Here: N=Njerve (this project), S=Skaar.*

		W-01A	W-01B	W-02A	W-02B	W-08A	W-08B	W-16	S-01	S-02
L-PFOA	**N**	40.98	34.93	52.61	51.63	13.38	<LOQ	6.38	10.88	23.37
(ng/mL)	**S**	39.73	31.84	38.28	40.27	10.93	<LOD	6.87	4.68	9.92
L-PFOA	**N**	87	87	94	91	95	0	84	91	95
(%)	**S**	24	26	37	38	57	-	41	32	28

Overall, it is important to note that there are some inaccuracies, discussed in method validation. Though not a full separation was accomplished, most target analytes were able to be quantized. Unfortunately, not all initial analytes were able to be validated and those validated in cattle liver and cod muscle were outside of the acceptance range of validation parameters. Nevertheless, with the comparison of results from the reference method, this project's results are not significantly incorrect.

6   Conclusion

A greater understanding of PFAS, their source of contamination, abundance in the Arctic, and their analytical separation was desired in this project. With the aim of separating twelve PFCAs with a new HPLC-MS/MS method, this project was conducted, evaluated, and concluded. The MS parameters were optimized manually, along with mobile phase gradient, flowrate, band broadening, and temperatures for the HPLC. As the project went on, the separation of twelve target analytes improved. Six analytes (L-PFOA, P3MHpA, P4MOA, P355TMHxA, P6MHpA, and P55DMHxA) were fully separated, while two were partially separated (ipPFNA and P37DMOA). A validation was conducted for six analytes, showing opportunities for improvements in the method. Though some parameters, such as accuracy and desired analytical range, were flawed, selectivity factor, linearity and precision were adequate. Comparison of results of the water samples with the reference method shows insignificant differences, which again shows that the method is reasonable.

The target, validated analytes were found in the Ny-Ålesund samples at various concentrations. The water samples had ranging concentrations of ΣPFCAs from 7.57 ng/mL – 56.68 ng/mL (excluding NÅ-W-08B, where 0.63 ng/mL was detected). The soil samples had generally lower concentration at 11.96 ng/mL – 24.56 ng/mL. With the aim to distinguish source of contamination with isomeric compositions of the target analytes, no significant trends were found. The samples taken near the FFTS, regardless of their composition, are likely a result of AFFF contamination, while the samples from meltwater run-offs can demonstrate atmospheric transportation, resulting from the ECF process.

With rising concerns regarding the persistent, fluorinated compounds, it is important to conduct more research about them. PFAS are not only damaging for humans and animals, but the planet as well. PFAS are one of many POPs, which are one of many concerns we humans have in respect to global warming and the environmental crisis. Finding selected few PFAS in Ny-Ålesund is concerning because it amplifies the persistence of the compounds. It also magnifies the possibility for global transportation, not only for PFAS, but perhaps for other POPs and toxins as well.

7 Future Perspectives

In regard to finding contamination source and understanding long-range, atmospheric transportation of PFAS, analyzing the precursors from the ECF process would be an interesting addition to this project. It would also be engaging to analyze all isomers of ECF to give a complementary outline of where the fluorinated substances come from and how they ended up on Svalbard.

Because the limits of detection and quantification were relatively high, along with the analytical range, using a more sensitive instrument would be attractive. Conducting a method using an ultra high performance liquid chromatography (UPLC) instrument would increase sensitivity, and lower LOD and LOQ. This would be beneficial when analyzing samples with low concentration of PFAS. PFAS can be found all over the world and recognizing them regardless of their low abundance would expand the understanding of the compounds. Additionally, being able to analyze all ~10,000 PFAS would also expand the overall comprehension of fluorinated contamination in nature. PCA showed patterns in the results for this project, which can be expanded to analyze all PFAS, which can then further guide future analyses on which analytes to investigate.

This project gained further understanding of the hardship of analyzing similar PFAS, as well as their continuous abundance in the Arctic. The compounds were found to be contaminated locally and remotely, which again gives a larger picture on how PFAS travel throughout the world. For further investigation, analyzing other PFAS and their isomeric composition in the Arctic would expand the knowledge about them. Continuous surveys should be conducted, not only in the Arctic but other places in the world, of PFAS contamination, their persistence, and source of contamination. However, not only is research regarding observance of PFAS important, but how can we clean up the contaminated areas? Finding effective and inexpensive methods for this is a new challenge, but essential in the fight against the environmental crisis.

References

[3M]Company. (1999). *Fluorochemical use, distribution and release overview.* USEPA Administrative Record AR226-0550. Retrieved from www.regulations.gov as document EPA-HQ-OPPT-2002-0051-0003.

Ali, A. M., Langberg, H. A., Hale, S. E., Kallenborn, R., Hartz, W. F., Mortensen Å, K., Ciesielski, T. M., McDonough, C. A., Jenssen, B. M., & Breedveld, G. D. (2021). The fate of poly- and perfluoroalkyl substances in a marine food web influenced by land-based sources in the Norwegian Arctic. *Environ Sci Process Impacts*, *23*(4), 588-604. https://doi.org/10.1039/d0em00510j

Bank, R., Smart, B., & Tatlow, J. (1994). *Organofluorine Chemistry: Principles and Commercial Application* (1st ed.). Plenum and Elsevier, New York. https://link.springer.com/book/10.1007/978-1-4899-1202-2

Benskin, J. P., De Silva, A. O., & Martin, J. W. (2010). Isomer profiling of perfluorinated substances as a tool for source tracking: a review of early findings and future applications. *Rev Environ Contam Toxicol*, *208*, 111-160. https://doi.org/10.1007/978-1-4419-6880-7_2

Benskin, J. P., Yeung, L. W., Yamashita, N., Taniyasu, S., Lam, P. K., & Martin, J. W. (2010). Perfluorinated acid isomer profiling in water and quantitative assessment of manufacturing source. *Environ Sci Technol*, *44*(23), 9049-9054. https://doi.org/10.1021/es102582x

Buck, R. C., Franklin, J., Berger, U., Conder, J. M., Cousins, I. T., de Voogt, P., Jensen, A. A., Kannan, K., Mabury, S. A., & van Leeuwen, S. P. (2011). Perfluoroalkyl and polyfluoroalkyl substances in the environment: terminology, classification, and origins. *Integr Environ Assess Manag*, *7*(4), 513-541. https://doi.org/10.1002/ieam.258

Chain, E. Panel o. C. i. t. F., Knutsen, H. K., Alexander, J., Barregård, L., Bignami, M., Brüschweiler, B., Ceccatelli, S., Cottrill, B., Dinovi, M., Edler, L., Grasl-Kraupp, B., Hogstrand, C., Hoogenboom, L., Nebbia, C. S., Oswald, I. P., Petersen, A., Rose, M., Roudot, A.-C., Vleminckx, C., . . . Schwerdtle, T. (2018). Risk to human health related to the presence of perfluorooctane sulfonic acid and perfluorooctanoic acid in food. *EFSA Journal*, *16*(12), e05194. https://doi.org/https://doi.org/10.2903/j.efsa.2018.5194

Dai, Y., Guo, X., Wang, S., Yin, L., & Hoffmann, M. R. (2020). Photochemical transformation of perfluoroalkyl acid precursors in water using engineered nanomaterials. *Water Research*, *181*, 115964. https://doi.org/https://doi.org/10.1016/j.watres.2020.115964

De Silva, A. O., Armitage, J. M., Bruton, T. A., Dassuncao, C., Heiger-Bernays, W., Hu, X. C., Kärrman, A., Kelly, B., Ng, C., Robuck, A., Sun, M., Webster, T. F., & Sunderland, E. M. (2021). PFAS Exposure Pathways for Humans and Wildlife: A Synthesis of Current Knowledge and Key Gaps in Understanding. *Environmental Toxicology and Chemistry*, *40*(3), 631-657. https://doi.org/https://doi.org/10.1002/etc.4935

ECHA. (2023). The PFAS Restriction Proposal (ECHA/NR/23/04). https://echa.europa.eu/registry-of-restriction-intentions/-/dislist/details/0b0236e18663449b

EPA. (2021, 10.08.2021). *PFAS Master List of PFAS Substances*. United States Environmental Protection Agency. https://comptox.epa.gov/dashboard/chemical-lists/pfasmaster

References

Falk, S., Brunn, H., Schröter-Kermani, C., Failing, K., Georgii, S., Tarricone, K., & Stahl, T. (2012). Temporal and spatial trends of perfluoroalkyl substances in liver of roe deer (Capreolus capreolus). *Environmental Pollution*, *171*, 1-8. https://doi.org/https://doi.org/10.1016/j.envpol.2012.07.022

Ghisi, R., Vamerali, T., & Manzetti, S. (2019). Accumulation of perfluorinated alkyl substances (PFAS) in agricultural plants: A review. *Environ Res*, *169*, 326-341. https://doi.org/10.1016/j.envres.2018.10.023

Giesy, J. P., & Kannan, K. (2001). Global distribution of perfluorooctane sulfonate in wildlife. *Environmental Science & Technology*, *35*(7), 1339-1342. https://doi.org/10.1021/es001834k

Granberg, M. E., Ask, A., & Gabrielsen, G. W. (2017). *Local contamination in Svalbard: Overview and suggestions for remediation actions* (044). https://nyalesundresearch.no/2017_npi_brief-report-series-no-044_local-contamination-in-svalbard/#gallery

Grandjean, P., Heilmann, C., Weihe, P., Nielsen, F., Mogensen, U. B., Timmermann, A., & Budtz-Jørgensen, E. (2017). Estimated exposures to perfluorinated compounds in infancy predict attenuated vaccine antibody concentrations at age 5-years. *J Immunotoxicol*, *14*(1), 188-195. https://doi.org/10.1080/1547691x.2017.1360968

Hanssen, L., Dudarev, A. A., Huber, S., Odland, J., Nieboer, E., & Sandanger, T. M. (2013). Partition of perfluoroalkyl substances (PFASs) in whole blood and plasma, assessed in maternal and umbilical cord samples from inhabitants of arctic Russia and Uzbekistan. *Sci Total Environ*, *447*, 430-437. https://doi.org/10.1016/j.scitotenv.2013.01.029

Hartz, W. F., Björnsdotter, M. K., Yeung, L. W. Y., Hodson, A., Thomas, E. R., Humby, J. D., Day, C., Jogsten, I. E., Kärrman, A., & Kallenborn, R. (2023). Levels and distribution profiles of Per- and Polyfluoroalkyl Substances (PFAS) in a high Arctic Svalbard ice core. *Science of The Total Environment*, *871*, 161830. https://doi.org/https://doi.org/10.1016/j.scitotenv.2023.161830

Henderson, W. M., & Smith, M. A. (2006). Perfluorooctanoic acid and perfluorononanoic ccid in fetal and neonatal mice following In utero exposure to 8-2 fluorotelomer alcohol. *Toxicological Sciences*, *95*(2), 452-461. https://doi.org/10.1093/toxsci/kfl162

ICH Expert Working Group. (1994, 27.10.1994). *Validation Of Analytical Procedures: Text And Methodology Q2(R1)* International Conference On Harmonisation Of Technical Requirements For Registration Of Pharmaceuticals For Human Use, https://database.ich.org/sites/default/files/Q2%28R1%29%20Guideline.pdf

ITRC. (2022). *ITRC (Interstate Technology & Regulatory Council). 2022. PFAS Technical and Regulatory Guidance Document and Fact Sheets PFAS-1. Washington, D.C.: Interstate Technology & Regulatory Council, PFAS Team. https://pfas-1.itrcweb.org/.*

Jha, G., Kankarla, V., McLennon, E., Pal, S., Sihi, D., Dari, B., Diaz, D., & Nocco, M. (2021). Per- and polyfluoroalkyl substances (PFAS) in integrated crop-livestock systems: Environmental exposure and human health risks. *International Journal of Environmental Research and Public Health*, *18*(23), 12550. https://doi.org/10.3390/ijerph182312550

Kannan, K., Corsolini, S., Falandysz, J., Oehme, G., Focardi, S., & Giesy, J. P. (2002). Perfluorooctanesulfonate and related fluorinated hydrocarbons in marine mammals, fishes, and birds from coasts of the Baltic and the Mediterranean seas. *Environmental Science & Technology*, *36*(15), 3210-3216. https://doi.org/10.1021/es020519q

Kannan, K., Yun, S. H., & Evans, T. J. (2005). Chlorinated, Brominated, and Perfluorinated Contaminants in Livers of Polar Bears from Alaska. *Environmental Science & Technology*, *39*(23), 9057-9063. https://doi.org/10.1021/es051850n

References

Kelly, B. C., Ikonomou, M. G., Blair, J. D., Surridge, B., Hoover, D., Grace, R., & Gobas, F. A. (2009). Perfluoroalkyl contaminants in an Arctic marine food web: trophic magnification and wildlife exposure. *Environ Sci Technol*, *43*(11), 4037-4043. https://doi.org/10.1021/es9003894

Kissa, E. (2001a). *Fluorinated surfactants and repellents* (Vol. 97). CRC Press.

Kissa, E. (2001b). *Fluorinated surfactants and repellents* (2nd Revised and Expanded ed.). Marcel Dekker.

Lesmeister, L., Lange, F. T., Breuer, J., Biegel-Engler, A., Giese, E., & Scheurer, M. (2021). Extending the knowledge about PFAS bioaccumulation factors for agricultural plants – A review. *Science of The Total Environment*, *766*, 142640. https://doi.org/https://doi.org/10.1016/j.scitotenv.2020.142640

Lindstrom, A. B., Strynar, M. J., & Libelo, E. L. (2011). Polyfluorinated compounds: Past, present, and future. *Environmental Science & Technology*, *45*(19), 7954-7961. https://doi.org/10.1021/es2011622

Liu, S., Liu, Z., Tan, W., Johnson, A. C., Sweetman, A. J., Sun, X., Liu, Y., Chen, C., Guo, H., Liu, H., Wan, X., & Zhang, L. (2023). Transport and transformation of perfluoroalkyl acids, isomer profiles, novel alternatives and unknown precursors from factories to dinner plates in China: New insights into crop bioaccumulation prediction and risk assessment. *Environment International*, *172*, 107795. https://doi.org/https://doi.org/10.1016/j.envint.2023.107795

Martin, J. W., Smithwick, M. M., Braune, B. M., Hoekstra, P. F., Muir, D. C. G., & Mabury, S. A. (2004). Identification of long-chain perfluorinated acids in biota from the Canadian Arctic. *Environmental Science & Technology*, *38*(2), 373-380. https://doi.org/10.1021/es034727+

McMurdo, C. J., Ellis, D. A., Webster, E., Butler, J., Christensen, R. D., & Reid, L. K. (2008). Aerosol enrichment of the surfactant PFO and mediation of the water−air transport of gaseous PFOA. *Environmental Science & Technology*, *42*(11), 3969-3974. https://doi.org/10.1021/es7032026

Meegoda, J. N., Kewalramani, J. A., Li, B., & Marsh, R. W. (2020). A review of the applications, environmental release, and remediation technologies of per- and polyfluoroalkyl substances. *Int J Environ Res Public Health*, *17*(21). https://doi.org/10.3390/ijerph17218117

Miljødirektoratet. (2023a, 04.01.2023). *Perfluorerte stoffer (PFOS, PFOA og andre PFAS-er)*. Miljødirektoratet. Retrieved Sept. 2022 from https://miljostatus.miljodirektoratet.no/tema/miljogifter/prioriterte-miljogifter/perfluorerte-stoffer-pfos-pfoa-og-andre-pfas-er/

Miljødirektoratet. (2023b, 10.02.2023). *Svalbard Lufthavn: Må rydde opp PFAS-forurensning*. Miljødirektoratet. https://www.miljodirektoratet.no/aktuelt/nyheter/2023/februar-2023/svalbard-lufthavn-ma-rydde-opp-pfas-forurensning/

O'Hagan, D. (2008). Understanding organofluorine chemistry. An introduction to the C–F bond [10.1039/B711844A]. *Chemical Society Reviews*, *37*(2), 308-319. https://doi.org/10.1039/B711844A

OECD. (2011). Organisation for Economic Co-operation and Development. OECD portal on perfluorinated chemicals. https://www.oecd.org/chemicalsafety/portal-perfluorinated-chemicals/.

OECD. (2018). *Toward a new comprehensive global database of per- and polyfluoroalkyl substances (PFASs): Summary report on updating the OECD 2007 list of per- and polyfluoroalkyl substances (PFASs)* (Series on Risk Management, Issue 39). H. a. S. P. OECD Environment.

References

https://www.oecd.org/officialdocuments/publicdisplaydocumentpdf/?cote=ENV-JM-MONO(2018)7&doclanguage=en

Paul, A. G., Jones, K. C., & Sweetman, A. J. (2009). A first global production, emission, and environmental inventory for perfluorooctane sulfonate. *Environmental Science & Technology*, *43*(2), 386-392. https://doi.org/10.1021/es802216n

Prevedouros, K., Cousins, I. T., Buck, R. C., & Korzeniowski, S. H. (2006). Sources, fate and transport of perfluorocarboxylates. *Environmental Science & Technology*, *40*(1), 32-44. https://doi.org/10.1021/es0512475

Rayne, S., & Forest, K. (2009). Perfluoroalkyl sulfonic and carboxylic acids: a critical review of physicochemical properties, levels and patterns in waters and wastewaters, and treatment methods. *J Environ Sci Health A Tox Hazard Subst Environ Eng*, *44*(12), 1145-1199. https://doi.org/10.1080/10934520903139811

Riddell, N., Arsenault, G., Benskin, J. P., Chittim, B., Martin, J. W., McAlees, A., & McCrindle, R. (2009). Branched perfluorooctane sulfonate isomer quantification and characterization in blood serum samples by HPLC/ESI-MS(/MS). *Environ Sci Technol*, *43*(20), 7902-7908. https://doi.org/10.1021/es901261v

Sha, B., Johansson, J. H., Tunved, P., Bohlin-Nizzetto, P., Cousins, I. T., & Salter, M. E. (2022). Sea spray aerosol (SSA) as a source of perfluoroalkyl acids (PFAAs) to the atmosphere: Field evidence from long-term air monitoring. *Environmental Science & Technology*, *56*(1), 228-238. https://doi.org/10.1021/acs.est.1c04277

Shoeib, M., Harner, T., & Vlahos, P. (2006). Perfluorinated chemicals in the Arctic atmosphere. *Environmental Science & Technology*, *40*(24), 7577-7583. https://doi.org/10.1021/es0618999

Shoeib, M., Harner, T., Wilford, B. H., Jones, K. C., & Zhu, J. (2005). Perfluorinated sulfonamides in indoor and outdoor air and indoor dust: Occurrence, partitioning, and human exposure. *Environmental Science & Technology*, *39*(17), 6599-6606. https://doi.org/10.1021/es048340y

Skaar, J. S., Ræder, E. M., Lyche, J. L., Ahrens, L., & Kallenborn, R. (2019). Elucidation of contamination sources for poly- and perfluoroalkyl substances (PFASs) on Svalbard (Norwegian Arctic). *Environ Sci Pollut Res Int*, *26*(8), 7356-7363. https://doi.org/10.1007/s11356-018-2162-4

Steenland, K., & Winquist, A. (2021). PFAS and cancer, a scoping review of the epidemiologic evidence. *Environ Res*, *194*, 110690. https://doi.org/10.1016/j.envres.2020.110690

van Deemter, J. J., Zuiderweg, F. J., & Klinkenberg, A. (1956). Longitudinal diffusion and resistance to mass transfer as causes of nonideality in chromatography. *Chemical Engineering Science*, *5*(6), 271-289. https://doi.org/https://doi.org/10.1016/0009-2509(56)80003-1

Wallington, T. J., Hurley, M. D., Xia, J., Wuebbles, D. J., Sillman, S., Ito, A., Penner, J. E., Ellis, D. A., Martin, J., Mabury, S. A., Nielsen, O. J., & Sulbaek Andersen, M. P. (2006). Formation of C7F15COOH (PFOA) and other perfluorocarboxylic acids during the atmospheric oxidation of 8:2 fluorotelomer alcohol. *Environmental Science & Technology*, *40*(3), 924-930. https://doi.org/10.1021/es051858x

Wang, W., Rhodes, G., Ge, J., Yu, X., & Li, H. (2020). Uptake and accumulation of per- and polyfluoroalkyl substances in plants. *Chemosphere*, *261*, 127584. https://doi.org/https://doi.org/10.1016/j.chemosphere.2020.127584

Yamashita, N., Kannan, K., Taniyasu, S., Horii, Y., Petrick, G., & Gamo, T. (2005). A global survey of perfluorinated acids in oceans. *Marine Pollution Bulletin*, *51*(8), 658-668. https://doi.org/https://doi.org/10.1016/j.marpolbul.2005.04.026

References

Zhang, Y.-Z., Zeng, X.-W., Qian, Z., Vaughn, M. G., Geiger, S. D., Hu, L.-W., Lu, L., Fu, C., & Dong, G.-H. (2017). Perfluoroalkyl substances with isomer analysis in umbilical cord serum in China. *Environmental Science and Pollution Research*, *24*(15), 13626-13637. https://doi.org/10.1007/s11356-017-8954-0

8   Appendix

Appendix A   Reagents, standards, materials, and instruments

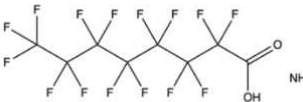***Table A.1.*** *List of reagents and chemicals (here: N/A = not available).*
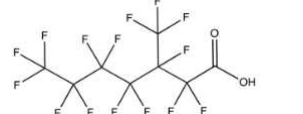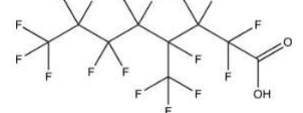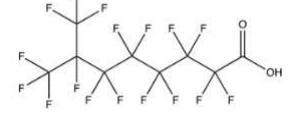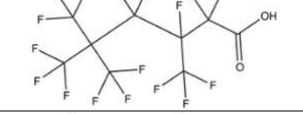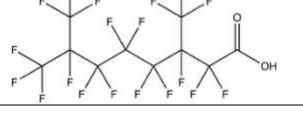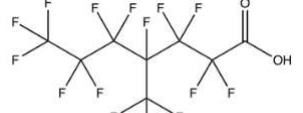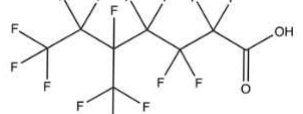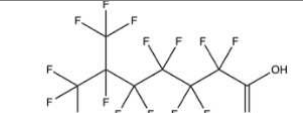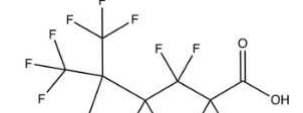
Name	Molecular formula	CAS reg. no.	Supplier	Purity/grade	Use
Methanol	CH_3OH	67-56-1	Sigma-Aldrich, St. Louis, MO, USA	>99.9%/ HPLC	Mobile phase
Ammonium acetate	$NH_4CH_3CO_2$	631-61-8	VWR, Leuven, Belgium	>99%/ LC-MS	Buffer salt for mobile phases
Formic acid	HCOOH	64-18-6	Sigma-Aldrich, St. Louis, MO, USA	≥95%/ reagent	Buffer for mobile phase
Acetonitrile	CH_3CN	75-05-8	VWR, Rosny-sous-Bois, France	>99.9%/ HPLC-MS	Mobile phase
Superclean™ Envi-Carb™	N/A	N/A	Sigma-Aldrich, St. Louis, MO, USA	N/A	Remove fat and contaminants

Table A.2. *List of hardware used for sample and standard preparation.*

Material	Manufacturer	Additional information
Purple Nitrile™ gloves	Kimberly-Clark™ KIMTECH™	PPE Category 3
Mobile phase filter	Pall Corporation, Ann Arbor, Michigan, USA	GH Polypro 0.2µm 47mm polypropylene
Centrifuge tubes	VWR, Randor, Pennsylvania, USA	Metal free 15mL
HPLC vials	VWR, Leuven, Belgium	1.5mL polypropylene 32 x 11.6mm
Screw HPLC caps	VWR, Leuven, Belgium	Polypropylene 9mm, silicone/PTFE Septa 1.0mm
Micropipette 100-1000µL	Sartorius, Göttingen, Germany	Proline® series
Micropipette 20-200µL	Sartorius, Göttingen, Germany	Proline® series
Micropipette tips	Sigma-Aldrich, St. Louis, Missouri, USA	N/A
Multipette® plus	Eppendorf, Hamburg, Germany	N/A

Combitips for Multipette			Eppendorf, Hamburg, Germany	N/A	

Table A.3. List of external and internal standards (here: N/A = not available)

Standard name	Acronym	CAS reg. no.	Supplier	Chemical purity	Chemical structure
NATIVE BRANCHED PERFLUOROALKYLCARBOXYLIC ACIDS					
Ammonium perfluorooctanoate (Technical Grade) 50.0 µg/mL	T-PFOA	3825-26-1	Wellington Laboratories, Guelph, ON, Canada	>96%	
Perfluoro-3-methylheptanoic acid 50.0 µg/mL	P3MHpA	705240-04-6	Wellington Laboratories, Guelph, ON, Canada	>98%	
Perfluoro-4-methyloctanoic acid 50.0 µg/mL	P4MOA	N/A	Wellington Laboratories, Guelph, ON, Canada	>98%	
Perfluoro-7-methyloctanoic acid 50.0 µg/mL	ipPFNA	15899-31-7	Wellington Laboratories, Guelph, ON, Canada	>98%	
Perfluoro-3,5,5-trimethylhexanoic acid 50.0 µg/mL	P355TMHxA	238403-51-5	Wellington Laboratories, Guelph, ON, Canada	>98%	
Perfluoro-3,7-dimethyloctanoic acid 50.0 µg/mL	P37DMOA	172155-07-6	Wellington Laboratories, Guelph, ON, Canada	>98%	
PFOS/PFOA ISOMERS - Mixtures					
Perfluoro-4-methylheptanoic acid 2.20 µg/mL	P4MHpA	N/A	Wellington Laboratories, Guelph, ON, Canada	N/A	
Perfluoro-5-methylheptanoic acid 1.96 µg/mL	P5MHpA	N/A	Wellington Laboratories, Guelph, ON, Canada	N/A	
Perfluoro-6-methylheptanoic acid 3.10 µg/mL	P6MHpA	N/A	Wellington Laboratories, Guelph, ON, Canada	N/A	
Perfluoro-5,5-dimethylhexanoic acid 1.95 µg/mL	P55DMHxA	N/A	Wellington Laboratories, Guelph, ON, Canada	N/A	

Perfluoro-4,5-dimethylhexanoic acid 1.22 µg/mL	P45DMHxA	N/A	Wellington Laboratories, Guelph, ON, Canada	N/A	
Perfluoro-3,5-dimethylhexanoic acid 0.60 µg/mL	P35DMHxA	N/A	Wellington Laboratories, Guelph, ON, Canada	N/A	
[$^{13}C_4$]-Perfluoroalkyl-octanoic acid	[$^{13}C_4$]-PFOA	N/A	Wellington Laboratories, Guelph, ON, Canada	N/A	N/A

Table A.4. *List of analytical instruments, systems, and software*

Name	Manufacturer/Supplier	Additional
6460 Series Triple Quadrupole LC/MS	Agilent Technologies Inc., Santa Clara, CA, USA	N/A
Agilent Series 1200 HPLC System	Agilent Technologies Inc., Santa Clara, CA, USA	N/A
Agilent 1200 Series High Performance Autosampler	Agilent Technologies Inc., Santa Clara, CA, USA	N/A
Agilent 1200 Series Binary Pump	Agilent Technologies Inc., Santa Clara, CA, USA	N/A
Agilent 1200 Series Column Compartment	Agilent Technologies Inc., Santa Clara, CA, USA	N/A
Masshunter Workstation Data Acquisition	Agilent Technologies Inc., Santa Clara, CA, USA	Version: 10.1
MassHunter Workstation Qualitative Analysis	Agilent Technologies Inc., Santa Clara, CA, USA	Version: 10.0
Quantitative Analysis (QQQ) (Quant-My-Way)	Agilent Technologies Inc., Santa Clara, CA, USA	Version: 10.1
XLSTAT (Statistical software)	Addinsoft, Paris, France	Version: 2023.1

Appendix B   Instrument parameters

Method Name	200323-PFOAstd-gradientFA-20.m
Method Path	D:\MassHunter\Methods\Ada\validering\200323-PFOAstd-gradientFA-20.m
Method Description	

Device List
- HiP Sampler
- Binary Pump
- Column Comp.
- QQQ

MS QQQ Mass Spectrometer

Ion Source	AJS ESI	Tune File	D:\MassHunter\Tune\QQQ \G6460A\atunes.TUNE.XML
Stop Mode	No Limit/As Pump	Stop Time (min)	No limit
Time Filter	On	Time Filter Width (min)	0.07

Time Segments

Index	Start Time (min)	Scan Type	Ion Mode	Div Valve	Delta EMV (-)	Store
1	0	MRM	ESI+Agilent Jet Stream	To MS	400	Yes

Time Segment 1

Scan Segments

Cpd Group	Cpd Name	ISTD?	Prec Ion	MS1 Res	Prod Ion	MS2 Res	Dwell	Frag (V)	CE (V)	Cell Acc (V)	Polarity
PFOA	P37DMOA	No	513	Unit/Enh (6490)	469	Unit/Enh (6490)	40	72	3	6	Negative
PFOA	P37DMOA	No	513	Unit/Enh (6490)	269	Unit/Enh (6490)	40	72	8	6	Negative
PFOA	P355TMHxA	No	463	Unit/Enh (6490)	443	Unit/Enh (6490)	40	46	7	4	Negative
PFOA	ipPFNA	No	463	Unit/Enh (6490)	419	Unit/Enh (6490)	40	80	4	6	Negative
PFOA	P4MOA	No	463	Unit/Enh (6490)	268	Unit/Enh (6490)	40	64	13	6	Negative
PFOA	P355TMHxA	No	463	Unit/Enh (6490)	219	Unit/Enh (6490)	40	46	7	4	Negative
PFOA	P4MOA	No	463	Unit/Enh (6490)	169	Unit/Enh (6490)	40	64	13	6	Negative
PFOA	ipPFNA	No	463	Unit/Enh (6490)	169	Unit/Enh (6490)	40	80	5	6	Negative
ISTD	MPFOA	Yes	417	Unit/Enh (6490)	372.1	Unit/Enh (6490)	40	76	0	6	Negative
PFOA	T-PFOA	No	413	Unit/Enh (6490)	369	Unit/Enh (6490)	40	86	4	5	Negative
PFOA	P3MHpA	No	413	Unit/Enh (6490)	369	Unit/Enh (6490)	40	76	2	5	Negative
PFOA	P4MHpA	No	413	Unit/Enh (6490)	369	Unit/Enh (6490)	40	121	4	4	Negative
PFOA	P5MHpA	No	413	Unit/Enh (6490)	369	Unit/Enh (6490)	40	72	4	3	Negative
PFOA	P45DMHxA P35DMHxA	No	413	Unit/Enh (6490)	369	Unit/Enh (6490)	40	69	4	6	Negative
PFOA	P6MHpA	No	413	Unit/Enh (6490)	368	Unit/Enh (6490)	40	69	4	7	Negative
PFOA	P4MHpA	No	413	Unit/Enh (6490)	279	Unit/Enh (6490)	40	121	0	4	Negative
PFOA	P45DMHxA P35DMHxA	No	413	Unit/Enh (6490)	279	Unit/Enh (6490)	40	69	0	6	Negative
PFOA	P55DMHxA	No	413	Unit/Enh (6490)	278	Unit/Enh (6490)	40	74	1	5	Negative

Continues next page.

PFOA	P55DMHxA	No	413	Unit/Enh (6490)	219	Unit/Enh (6490)	40	74	8	5	Negative
PFOA	P5MHpA	No	413	Unit/Enh (6490)	218	Unit/Enh (6490)	40	72	7	3	Negative
PFOA	P3MHpA	No	413	Unit/Enh (6490)	169	Unit/Enh (6490)	40	76	5	5	Negative
PFOA	P6MHpA	No	413	Unit/Enh (6490)	169	Unit/Enh (6490)	40	69	8	7	Negative
PFOA	P45DMHxA P35DMHxA	No	413	Unit/Enh (6490)	169	Unit/Enh (6490)	40	69	5	6	Negative
PFOA	T-PFOA	No	413	Unit/Enh (6490)	169	Unit/Enh (6490)	40	86	12	5	Negative
PFOA	P45DMHxA P35DMHxA	No	413	Unit/Enh (6490)	119	Unit/Enh (6490)	40	69	5	6	Negative

Source Parameters

Parameter	Value (+)	Value (-)
Gas Temp (°C)	300	300
Gas Flow (l/min)	5	5
Nebulizer (psi)	45	45
Sheath Gas Temp (°C)	250	250
Sheath Gas Flow (l/min)	11	11
Capillary (V)	3500	3500
Nozzle Voltage/Charging (V)	500	500

Scan Parameters

Data Stg	Threshold
Centroid	0

Chromatograms

Chrom Type	Label	Offset	Y-Range
TIC	TIC	0	10000000

Instrument Curves

Actual

Figure B.1. *Mass spectrometer parameters.*

Name: HiP Sampler   **Module: G1367C**

Auxiliary

Draw Speed	200.0 μL/min
Eject Speed	200.0 μL/min
Draw Position Offset	0.3 mm
Wait Time After Drawing	2.0 s
Sample Flush Out Factor	5.0
Vial/Well bottom sensing	No

Injection

Injection Mode	Injection with needle wash
Injection Volume	5.00 μL

Needle Wash

Needle Wash Location	Flush Port
Wash Time	5.0 s

High throughput

Automatic Delay Volume Reduction	No

Overlapped Injection

Enable Overlapped Injection	No

Valve Switching

Valve Movements	0

Valve Switch Time 1

Switch Time 1 Enabled	No

Valve Switch Time 2

Switch Time 2 Enabled	No

Valve Switch Time 3

Switch Time 3 Enabled	No

Valve Switch Time 4

Switch Time 4 Enabled	No

Stoptime

Stoptime Mode	As Pump/No Limit

Posttime

Posttime Mode	Off

Name: Binary Pump   **Module: G1312B**

Flow	0.300 mL/min
Use Solvent Types	Yes
Low Pressure Limit	0.00 bar
High Pressure Limit	600.00 bar
Maximum Flow Gradient	100.000 mL/min²

Stroke A

Automatic Stroke Calculation A	Yes

Stroke B

Automatic Stroke Calculation B	Yes

Stoptime

Stoptime Mode	Time set
Stoptime	30.00 min

Posttime

Posttime Mode	Off

Continues next page.

Solvent Composition

	Channel	Solvent 1	Name 1	Solvent 2	Name 2	Selected	Used	Percent (%)
1	A	H20	10% MeOH + 2mM NH4Ac	H20		Ch. 1	Yes	60.0 %
2	B	MeOH	0.1% Formic acid	MeOH		Ch. 1	Yes	40.0 %

Timetable

	Time (min)	A (%)	B (%)	Flow (mL/min)
1	2.00 min	60.0 %	40.0 %	--- mL/min
2	3.00 min	55.0 %	45.0 %	--- mL/min
3	5.00 min	55.0 %	45.0 %	--- mL/min
4	6.00 min	50.0 %	50.0 %	--- mL/min
5	8.00 min	50.0 %	50.0 %	--- mL/min
6	9.00 min	45.0 %	55.0 %	--- mL/min
7	11.00 min	45.0 %	55.0 %	--- mL/min
8	12.00 min	40.0 %	60.0 %	--- mL/min
9	14.00 min	40.0 %	60.0 %	--- mL/min
10	15.00 min	35.0 %	65.0 %	--- mL/min
11	17.00 min	35.0 %	65.0 %	--- mL/min
12	18.00 min	30.0 %	70.0 %	--- mL/min
13	20.00 min	30.0 %	70.0 %	--- mL/min
14	21.00 min	0.0 %	100.0 %	--- mL/min
15	23.00 min	0.0 %	100.0 %	--- mL/min
16	25.00 min	60.0 %	40.0 %	--- mL/min
17	30.00 min	60.0 %	40.0 %	--- mL/min

Figure B.2. *Liquid chromatographic parameters.*

Appendix C Worklists

Worklist Table

	Sample Name	Method	Data File	Sample Type	Level Name
1	50% MeOH	060323-PFOAstd-gradientFA-20.m	060323-meoh-wash1.d	Sample	
2	STD10ng/mL test	060323-PFOAstd-gradientFA-20.m	060323-STD10-test.d	Sample	
3	STD 0.1ng/mL	060323-PFOAstd-gradientFA-20.m	060323-valid-std0.1.d	Calibration	0.1
4	STD 0.5ng/mL	060323-PFOAstd-gradientFA-20.m	060323-valid-std0.5.d	Calibration	0.5
5	STD 1ng/mL	060323-PFOAstd-gradientFA-20.m	060323-valid-std1.d	Calibration	1
6	STD 10ng/mL	060323-PFOAstd-gradientFA-20.m	060323-valid-std10.d	Calibration	10
7	STD 50ng/mL	060323-PFOAstd-gradientFA-20.m	060323-valid-std50.d	Calibration	50
8	STD 100 ng/mL	060323-PFOAstd-gradientFA-20.m	060323-valid-std100.d	Calibration	100
9	50% MeOH	060323-PFOAstd-gradientFA-20.m	060323-meoh-wash2.d	Sample	
10	Blank	060323-PFOAstd-gradientFA-20.m	060323-valid-blk1.d	Blank	
11	Blank	060323-PFOAstd-gradientFA-20.m	060323-valid-blk2.d	Blank	
12	Blank	060323-PFOAstd-gradientFA-20.m	060323-valid-blk3.d	Blank	
13	Blind L	060323-PFOAstd-gradientFA-20.m	060323-valid-BL1.d	Sample	
14	Blind L	060323-PFOAstd-gradientFA-20.m	060323-valid-BL2.d	Sample	
15	Blind L	060323-PFOAstd-gradientFA-20.m	060323-valid-BL3.d	Sample	
16	Blind M	060323-PFOAstd-gradientFA-20.m	060323-valid-BM1.d	Sample	
17	Blind M	060323-PFOAstd-gradientFA-20.m	060323-valid-BM2.d	Sample	
18	Blind M	060323-PFOAstd-gradientFA-20.m	060323-valid-BM3.d	Sample	
19	50% MeOH	060323-PFOAstd-gradientFA-20.m	060323-meoh-wash3.d	Sample	
20	0.1ng/mL L	060323-PFOAstd-gradientFA-20.m	060323-valid-0.1L.d	Sample	
21	0.1ng/mL M	060323-PFOAstd-gradientFA-20.m	060323-valid-0.1M.d	Sample	
22	0.5ng/mL L	060323-PFOAstd-gradientFA-20.m	060323-valid-0.5L1.d	Sample	
23	0.5ng/mL L	060323-PFOAstd-gradientFA-20.m	060323-valid-0.5L2.d	Sample	
24	0.5ng/mL L	060323-PFOAstd-gradientFA-20.m	060323-valid-0.5L3.d	Sample	
25	0.5ng/mL M	060323-PFOAstd-gradientFA-20.m	060323-valid-0.5M1.d	Sample	
26	0.5ng/mL M	060323-PFOAstd-gradientFA-20.m	060323-valid-0.5M2.d	Sample	
27	0.5ng/mL M	060323-PFOAstd-gradientFA-20.m	060323-valid-0.5M3.d	Sample	
28	1ng/mL L	060323-PFOAstd-gradientFA-20.m	060323-valid-1L.d	Sample	
29	1ng/mL M	060323-PFOAstd-gradientFA-20.m	060323-valid-1M.d	Sample	
30	10ng/mL L	060323-PFOAstd-gradientFA-20.m	060323-valid-10L1.d	Sample	
31	10ng/mL L	060323-PFOAstd-gradientFA-20.m	060323-valid-10L2.d	Sample	
32	10ng/mL L	060323-PFOAstd-gradientFA-20.m	060323-valid-10L3.d	Sample	
33	10ng/mL M	060323-PFOAstd-gradientFA-20.m	060323-valid-10M1.d	Sample	
34	10ng/mL M	060323-PFOAstd-gradientFA-20.m	060323-valid-10M2.d	Sample	
35	10ng/mL M	060323-PFOAstd-gradientFA-20.m	060323-valid-10M3.d	Sample	

36	50ng/mL L	060323-PFOAstd-gradientFA-20.m	060323-valid-50L1.d	Sample	
37	50ng/mL L	060323-PFOAstd-gradientFA-20.m	060323-valid-50L2.d	Sample	
38	50ng/mL L	060323-PFOAstd-gradientFA-20.m	060323-valid-50L3.d	Sample	
39	50ng/mL M	060323-PFOAstd-gradientFA-20.m	060323-valid-50M1.d	Sample	
40	50ng/mL M	060323-PFOAstd-gradientFA-20.m	060323-valid-50M2.d	Sample	
41	50ng/mL M	060323-PFOAstd-gradientFA-20.m	060323-valid-50M3.d	Sample	
42	100ng/mL L	060323-PFOAstd-gradientFA-20.m	060323-valid-100L.d	Sample	
43	100ng/mL M	060323-PFOAstd-gradientFA-20.m	060323-valid-100M.d	Sample	
44	50% MeOH	060323-PFOAstd-gradientFA-20.m	060323-meoh-wash4-.d	Sample	
45	Matrix L	060323-PFOAstd-gradientFA-20.m	060323-valid-mL1.d	Sample	
46	Matrix L	060323-PFOAstd-gradientFA-20.m	060323-valid-mL2.d	Sample	
47	Matrix L	060323-PFOAstd-gradientFA-20.m	060323-valid-mL3.d	Sample	
48	Matrix M	060323-PFOAstd-gradientFA-20.m	060323-valid-mM1.d	Sample	
49	Matrix M	060323-PFOAstd-gradientFA-20.m	060323-valid-mM2.d	Sample	
50	Matrix M	060323-PFOAstd-gradientFA-20.m	060323-valid-mM3.d	Sample	
51	End wash	vask-prøver.m	060323-valid-endwash.d	Sample	
52	SCP_InstrumentStandby() {MH_Acq_Scripts.exe}				

Figure C.1. *Worklist for method validation.*

Worklist Table

	Sample Name	Method	Data File	Sample Type	Level Name
1	MeOH wash	200323-PFOAstd-gradientFA-20.m	120423-wash waste.d	Sample	
2	L-PFOA 500ng/mL	200323-PFOAstd-gradientFA-20.m	120423-QC1.d	QC	
3	STD 01-06 test	200323-PFOAstd-gradientFA-20.m	120423-std test.d	Sample	
4	STD 0.1	200323-PFOAstd-gradientFA-20.m	120423-STD0.1.d	Calibration	1
5	STD 1	200323-PFOAstd-gradientFA-20.m	120423-STD1.d	Calibration	2
6	STD 10	200323-PFOAstd-gradientFA-20.m	120423-STD10.d	Calibration	3
7	STD 100	200323-PFOAstd-gradientFA-20.m	120423-STD100.d	Calibration	4
8	STD 500	200323-PFOAstd-gradientFA-20.m	120423-STD500.d	Calibration	5
9	STD 1000	200323-PFOAstd-gradientFA-20.m	120423-STD1000.d	Calibration	6
10	L-PFOA 500ng/mL	200323-PFOAstd-gradientFA-20.m	120423-QC2.d	QC	
11	Method blank	110423-PFOAstd-gradientFA-20-5uL.m	120423-method-blank.d	Blank	
12	Field blank 1	110423-PFOAstd-gradientFA-20-5uL.m	120423-field-blank1.d	Blank	
13	Field blank 2	110423-PFOAstd-gradientFA-20-5uL.m	120423-field-blank2.d	Blank	
14	Field blank 3	110423-PFOAstd-gradientFA-20-5uL.m	120423-field-blank3.d	Blank	
15	NÅ-W-01A	110423-PFOAstd-gradientFA-20-5uL.m	120423-NA-W-01A.d	Sample	
16	NÅ-W-01B	110423-PFOAstd-gradientFA-20-5uL.m	120423-NA-W-01B.d	Sample	
17	NÅ-W-02A	110423-PFOAstd-gradientFA-20-5uL.m	120423-NA-W-02A.d	Sample	
18	NÅ-W-01B	110423-PFOAstd-gradientFA-20-5uL.m	120423-NA-W-02B.d	Sample	
19	NÅ-W-08A	110423-PFOAstd-gradientFA-20-5uL.m	120423-NA-W-08A.d	Sample	
20	NÅ-W-08B	110423-PFOAstd-gradientFA-20-5uL.m	120423-NA-W-08B.d	Sample	
21	NÅ-W-16	110423-PFOAstd-gradientFA-20-5uL.m	120423-NA-W-16.d	Sample	
22	NÅ-S-01	110423-PFOAstd-gradientFA-20-5uL.m	120423-NA-S-01.d	Sample	
23	NÅ-S-02	110423-PFOAstd-gradientFA-20-5uL.m	120423-NA-S-02.d	Sample	
24	MeOH wash	110423-PFOAstd-gradientFA-20-5uL.m	120423-wash waste2.d	Sample	
25	L-PFOA 500ng/mL	200323-PFOAstd-gradientFA-20.m	120423-QC3.d	QC	
26	Column wash	vask-prøver.m	120423column wash.d	Sample	
27	SCP_InstrumentStandby() {MH_Acq_Scripts.exe}				

Figure C.2. Worklist for method application: water and soil samples from Ny-Ålesund.

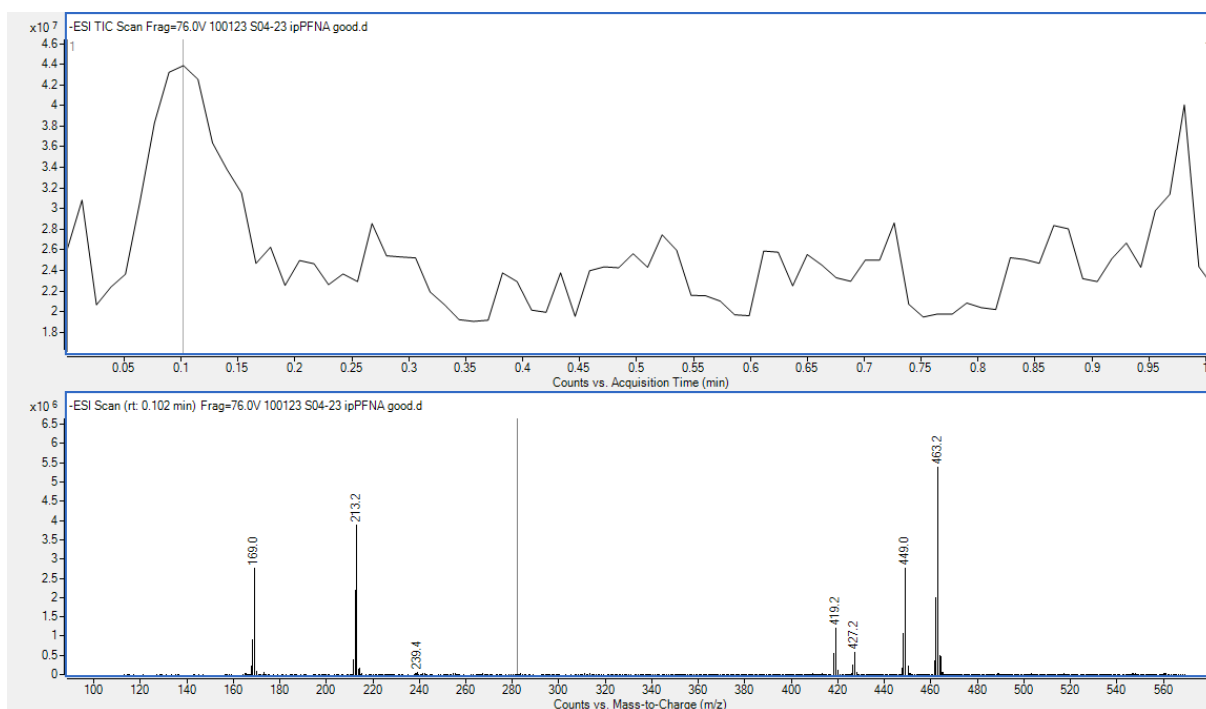## Appendix D   Chromatograms and mass spectra

Method development

Figure D.1. *MS optimization for ipPFNA. MS2-scan in negative mode to find expected precursor ion, here: m/z 463.2.*

Figure D.2. *MS optimization for ipPFNA. Product ion scan, where red chromatogram is low CE, and blank is high CE. The mass spectrum results from low CE and product ions are visible.*
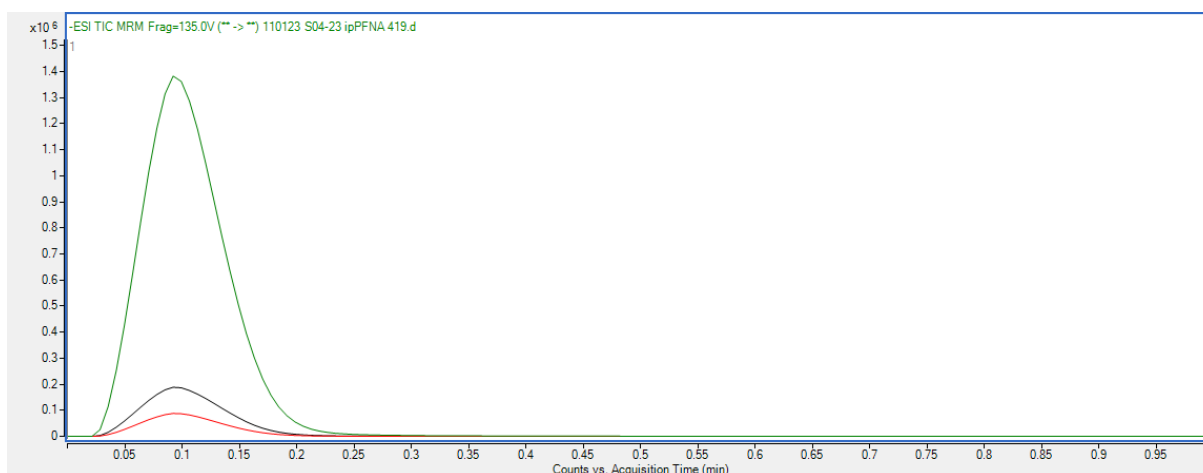
Figure D.3. *MS optimization for ipPFNA. Chromatograms for optimizing CE for each selected product ion (PI), green is PI 419, blank is PI 219, and red is PI 169.*
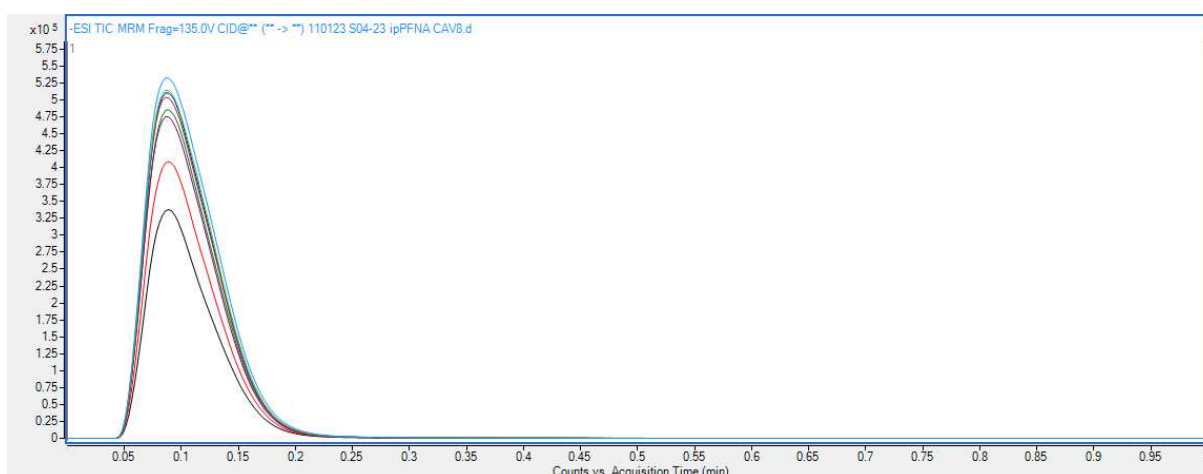

Figure D.4. *MS optimization for ipPFNA. Determination of optimized cell accelerator voltage (CAV), blue chromatogram at CAV=8 is most optimal.*
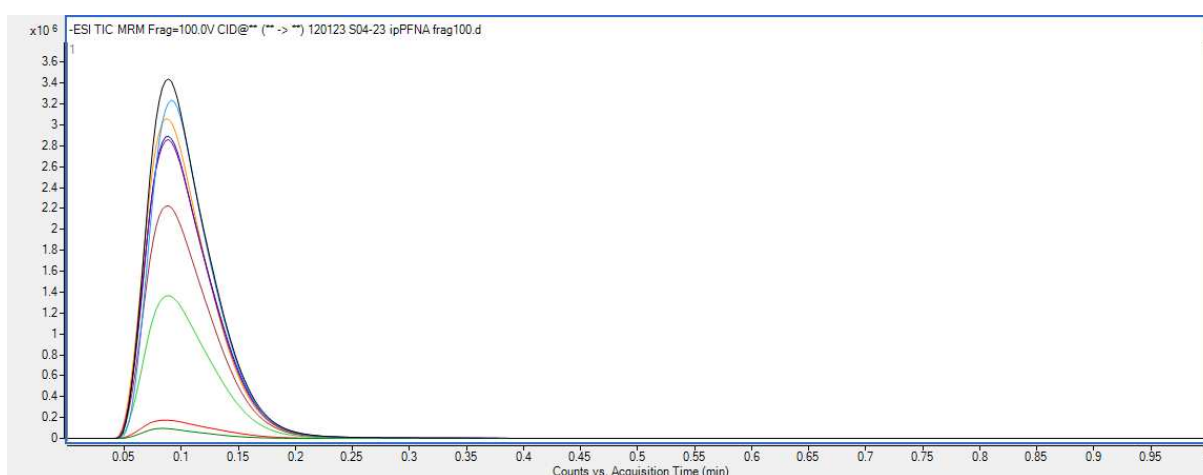

Figure D.5. *MS optimization for ipPFNA. Determination of fragmentor voltage, black chromatogram at 100 V is most optimal.*
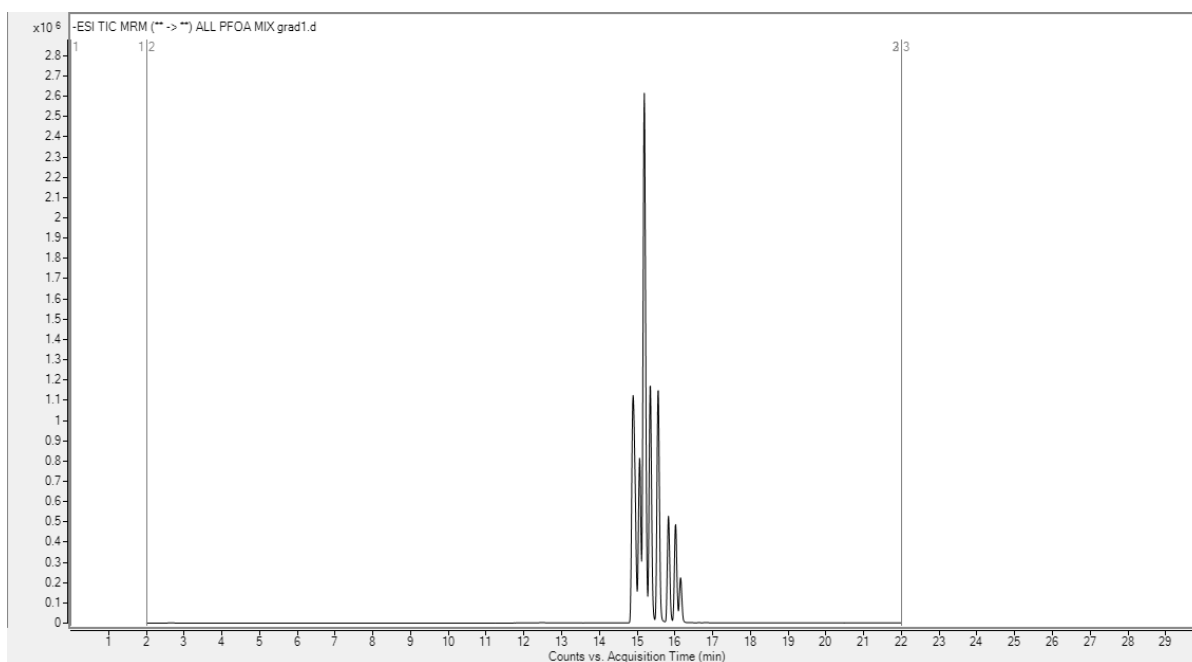
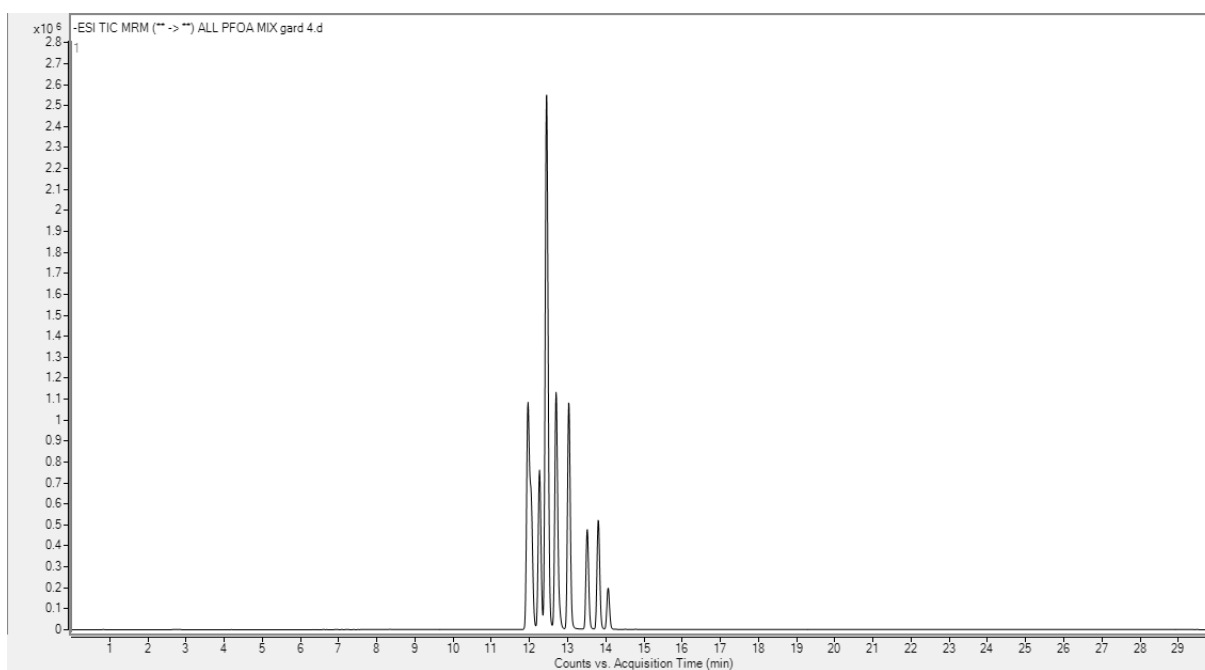***Figure D.6.****Chromatogram of stage 1 from gradient optimization.*

Figure D.7. *Chromatogram of stage 2 from gradient optimization.*
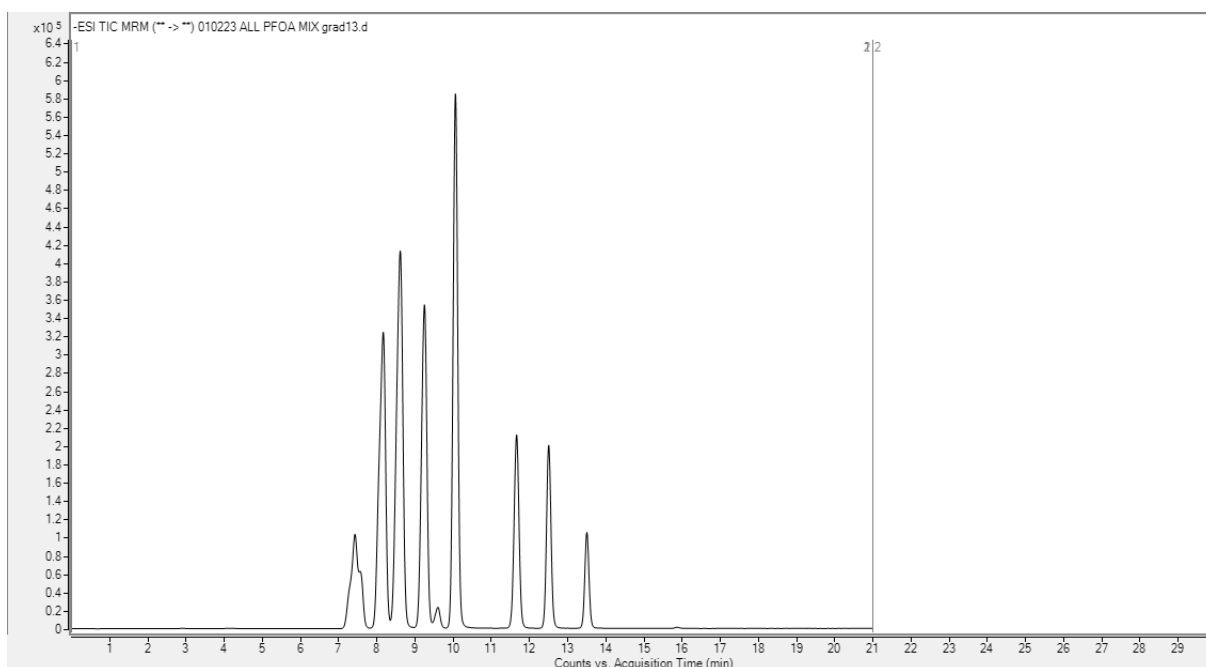
Figure D.8. *Chromatogram of stage 3 from gradient optimization.*
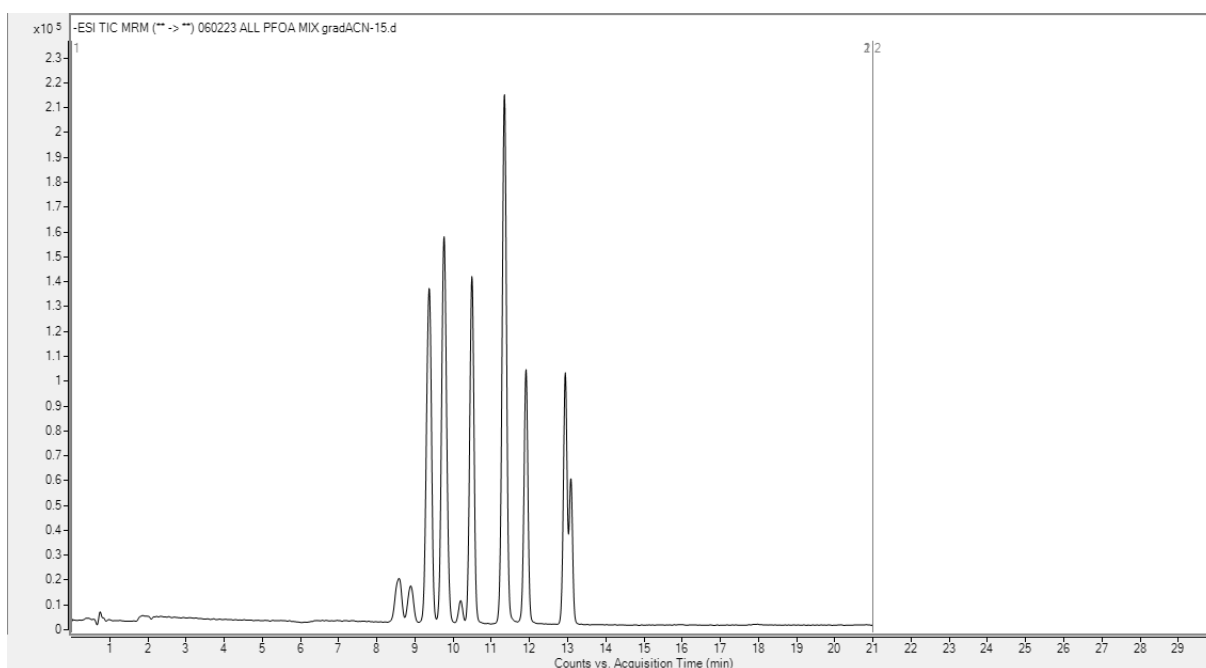
Figure D.9. *Chromatogram of stage 4 from gradient optimization.*
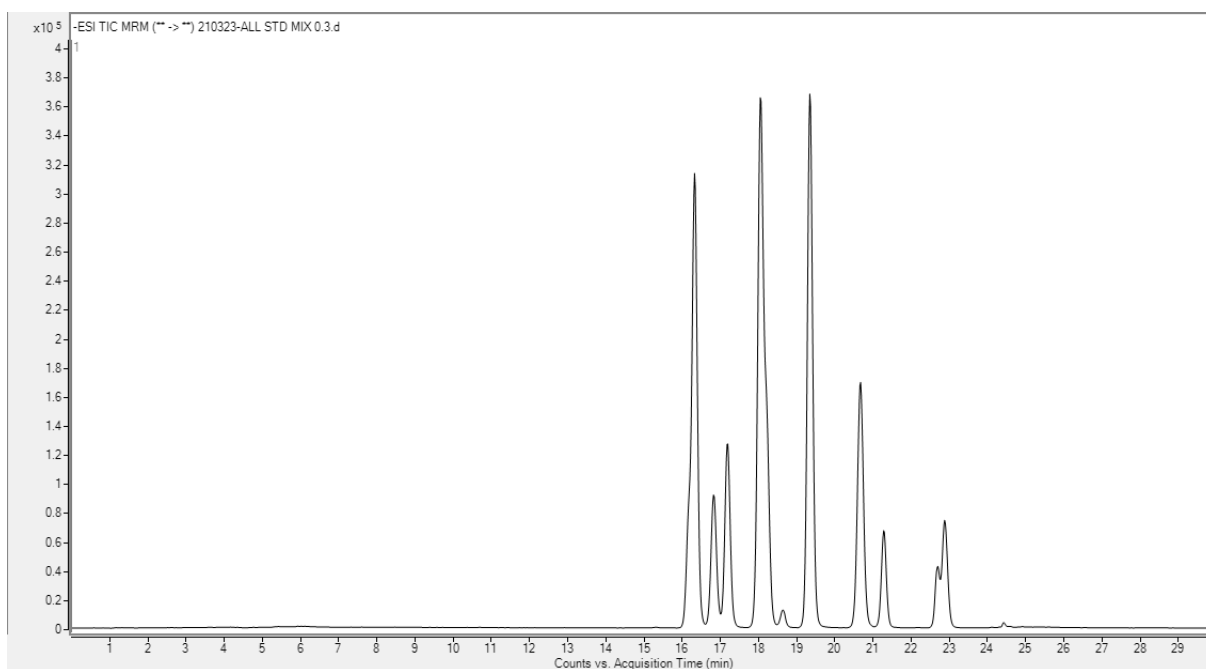
Figure D.10. *Chromatogram of stage 5 from gradient optimization.*

Ny-Ålesund samples
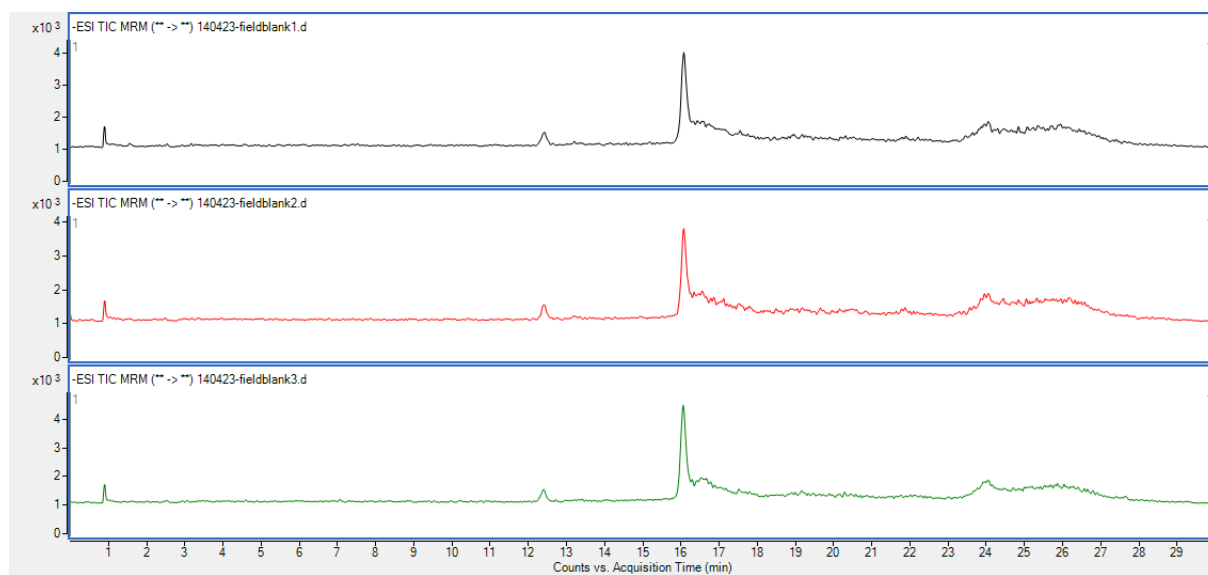
Figure D.11. *Field blanks from the Ny-Ålesund samples.*
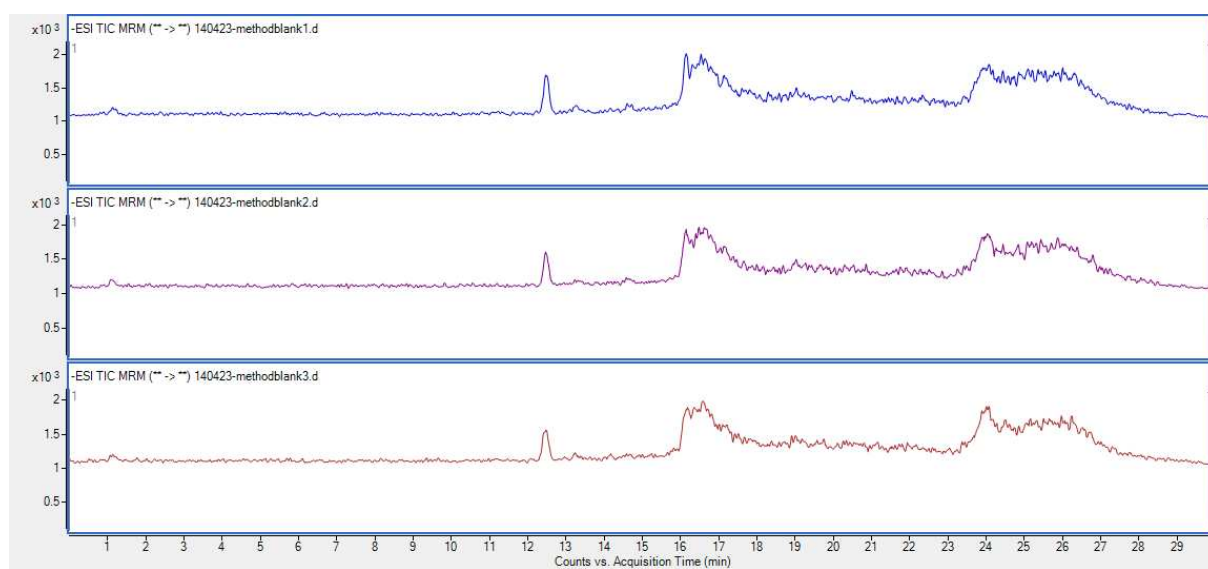
Figure D.12. *Method blanks (50% MeOH) for the Ny-Ålesund samples.*
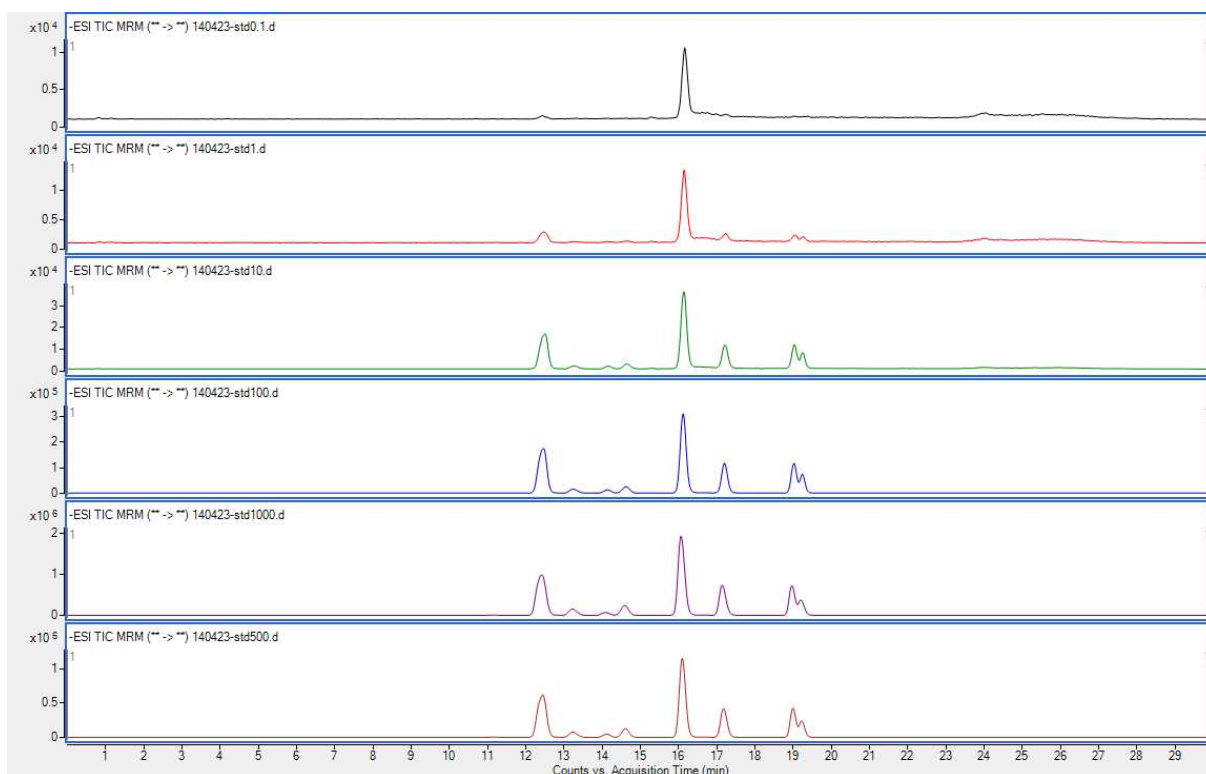
Figure D.13. *Chromatograms of calibration curve for the Ny-Ålesund samples. In order from top to bottom: 0.1, 1, 10, 100, 1000, and 500 ng/mL.*
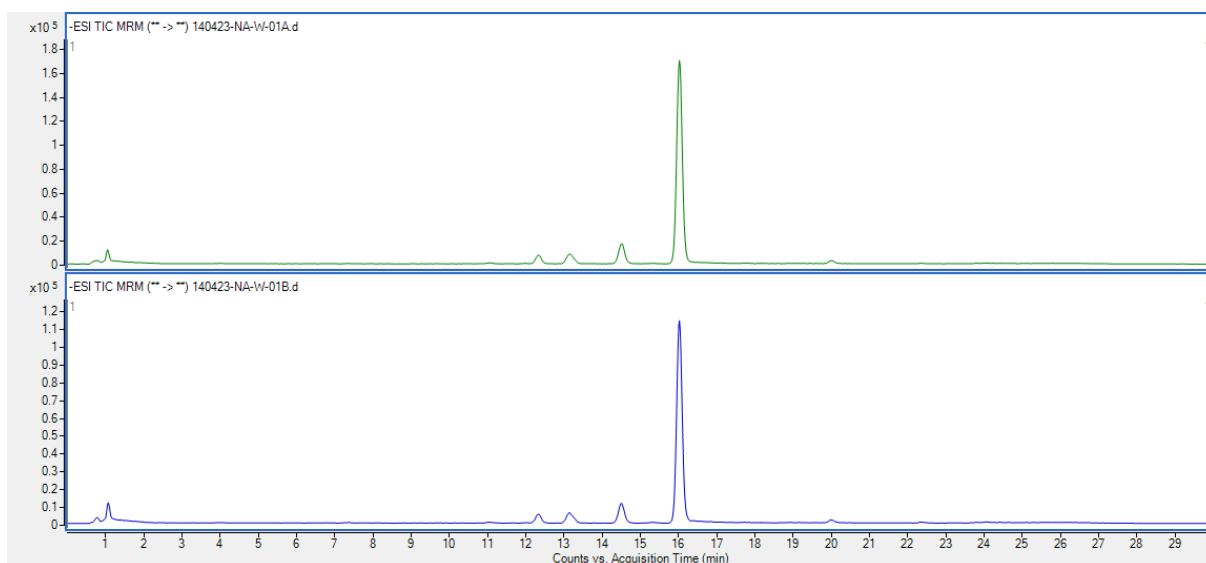
Figure D.14. *Chromatograms of NÅ-W-01A (top) and NÅ-W-01B (bottom).*
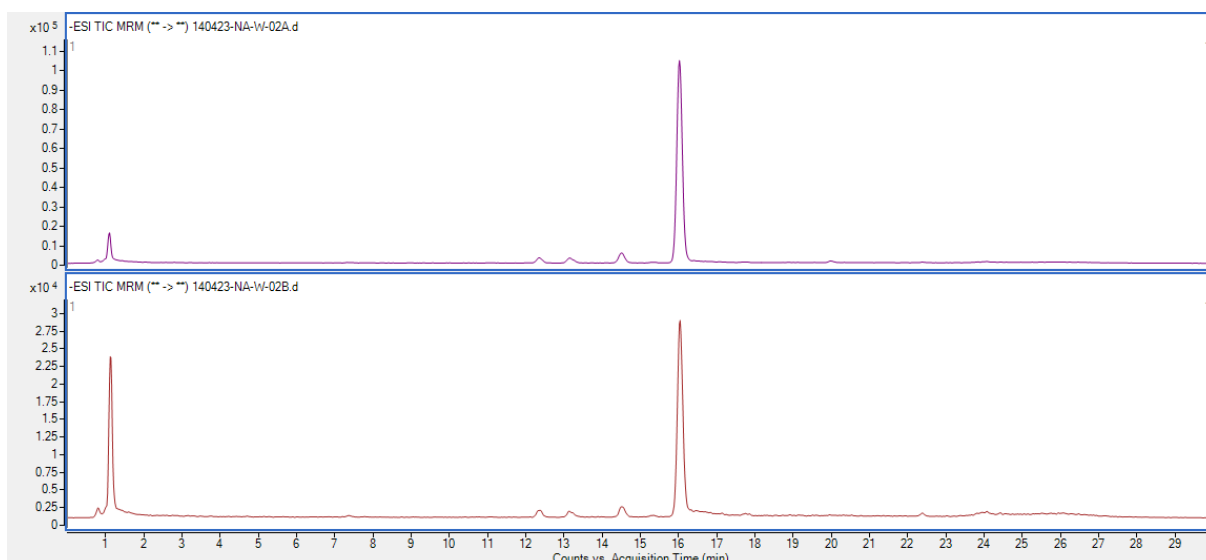
Figure D.15. *Chromatograms of NÅ-W-02A (top) and NÅ-W-02B (bottom).*
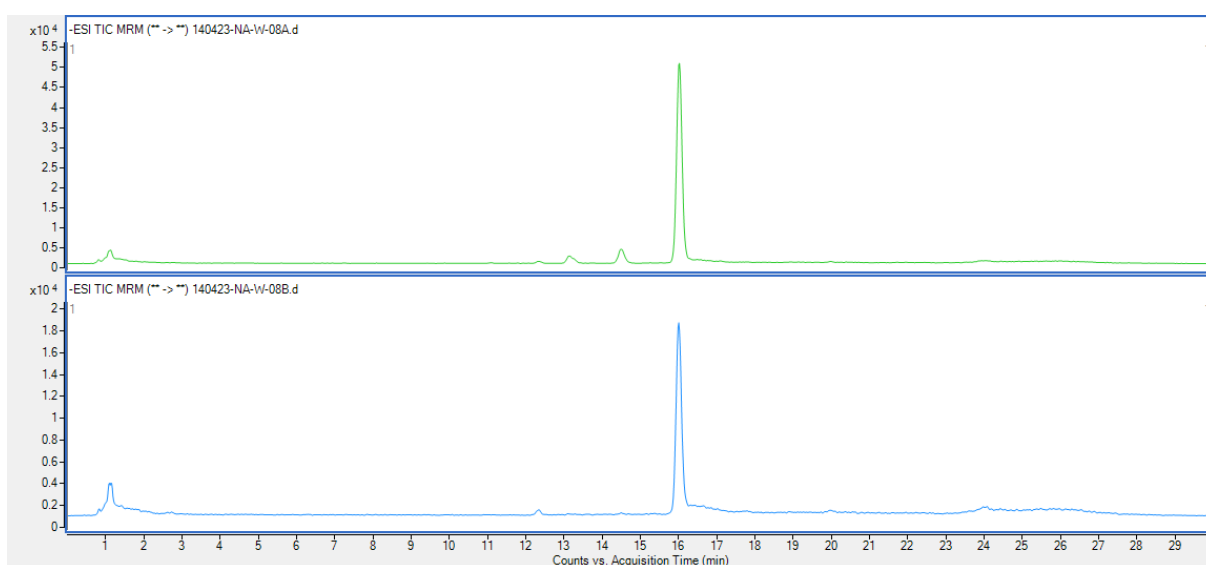
Figure D.16. *Chromatograms of NÅ-W-08A (top) and NÅ-W-08B (bottom).*
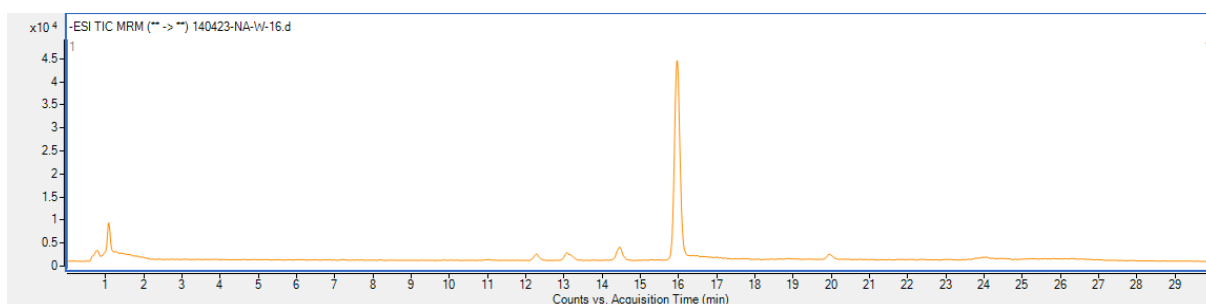
Figure D.17. *Chromatogram of NÅ-W-16.*
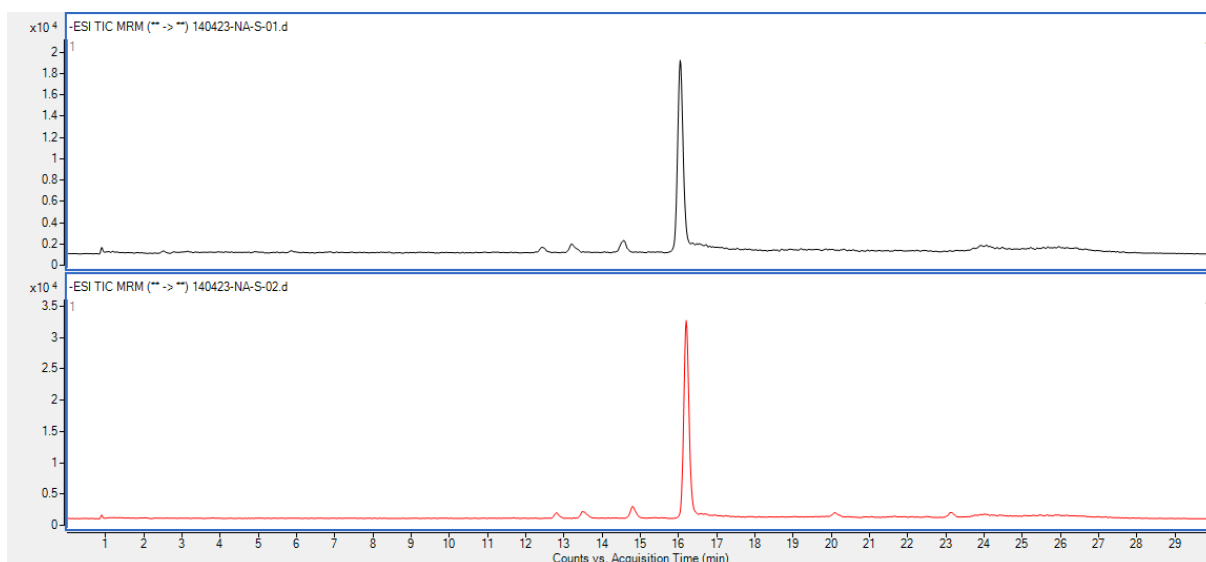
Figure D.18. *Chromatograms of NÅ-S-01 (top) and NÅ-S-02 (bottom).*

Appendix E   Calibration curves

Figure E.1. Calibration curve of L-PFOA.

Figure E.2. Calibration curve of P3MHpA.

Figure E.3. Calibration curve of P4MOA.

Figure E.4. Calibration curve of ipPFNA.

Figure E.5. Calibration curve of P355TMHxA

Figure E.6. Calibration curve of P37DMOA.

Appendix F   Raw data

Table F.1. Raw data from method validation.

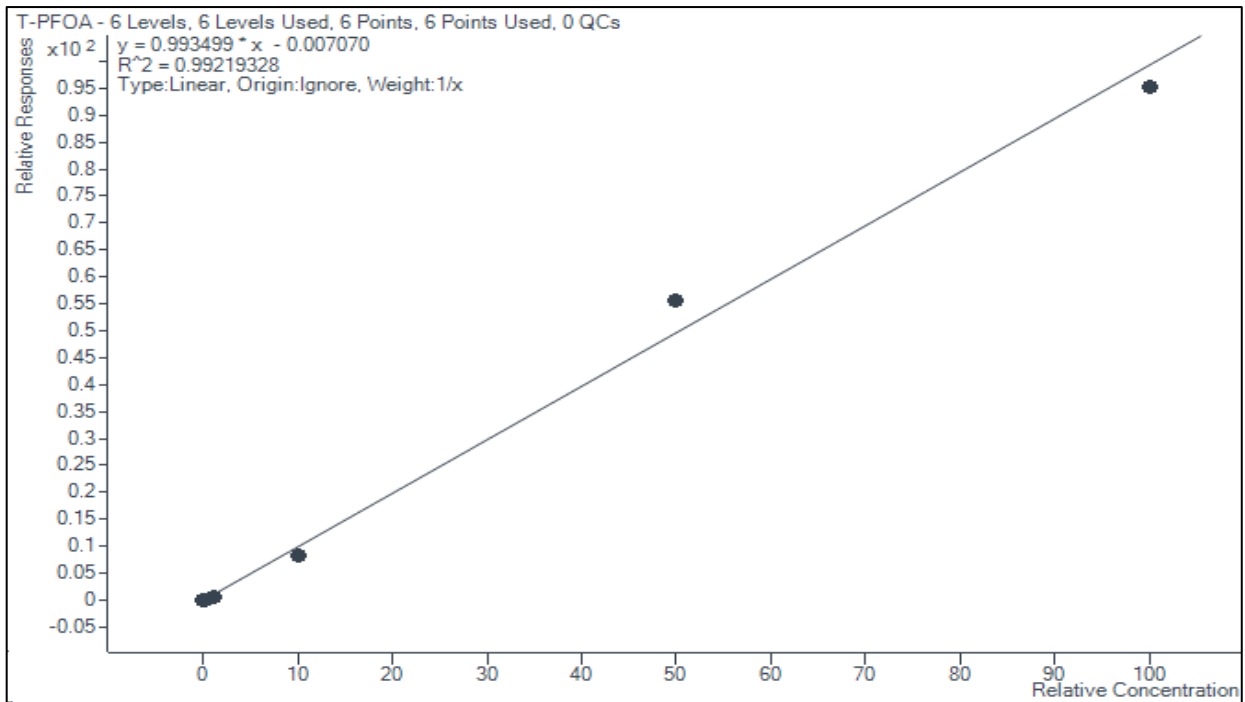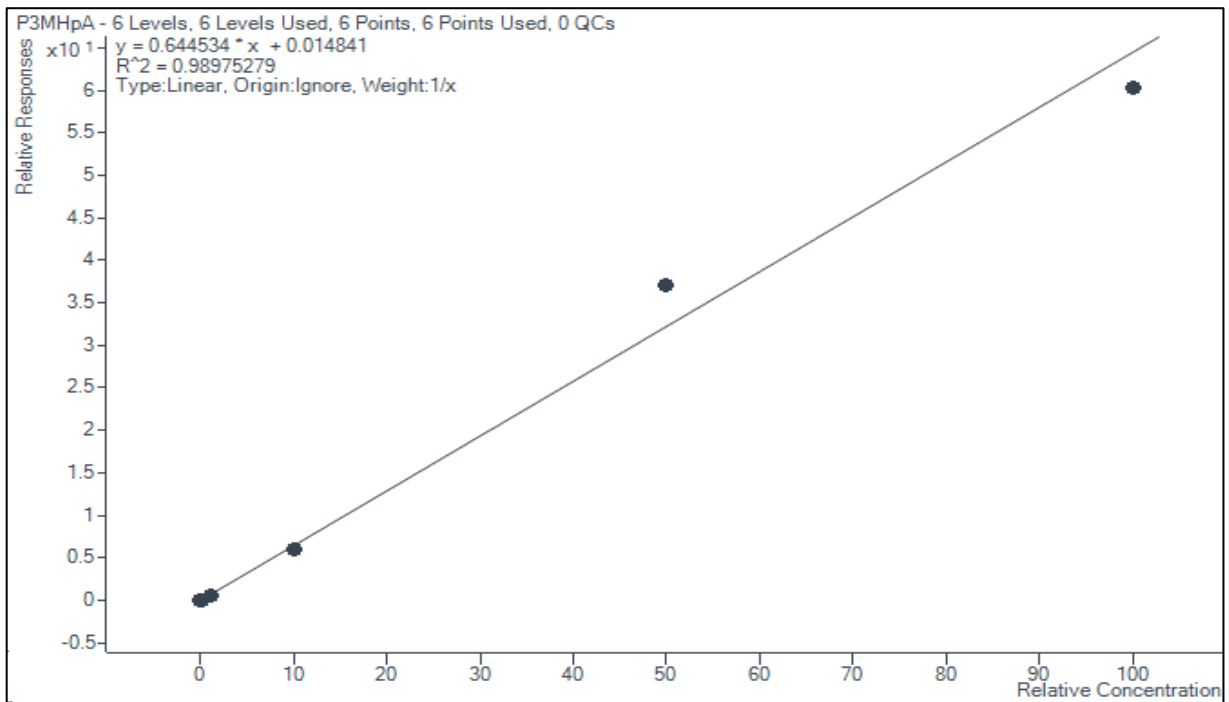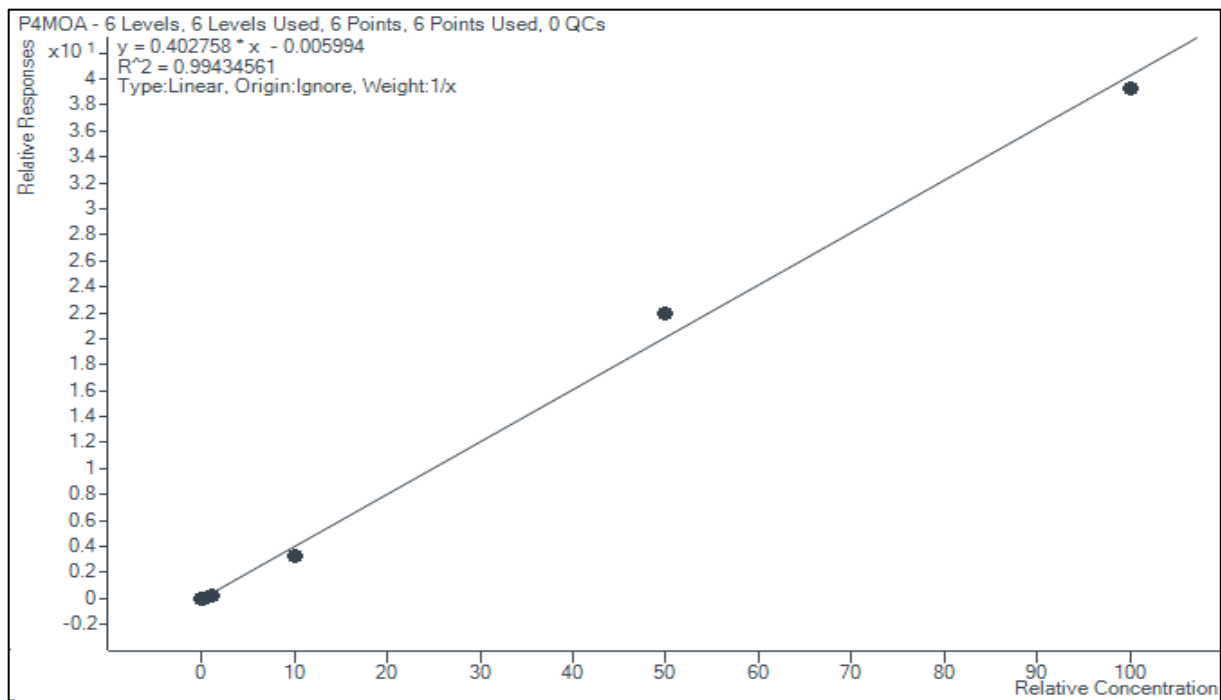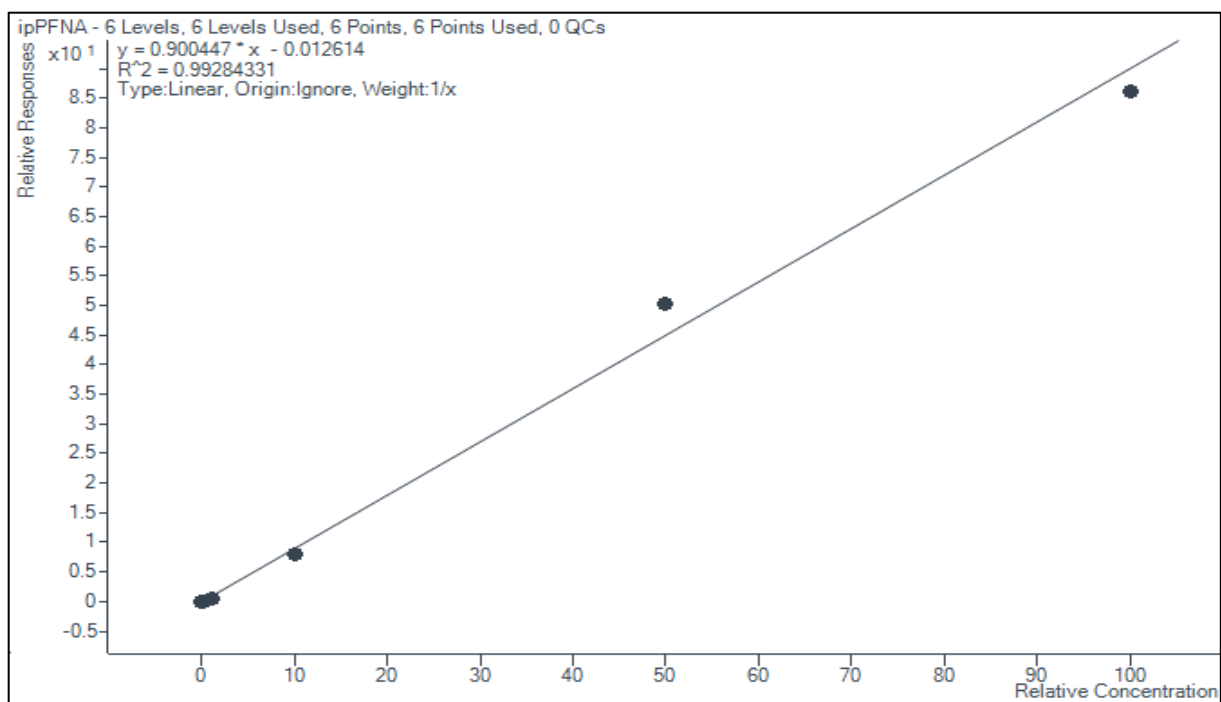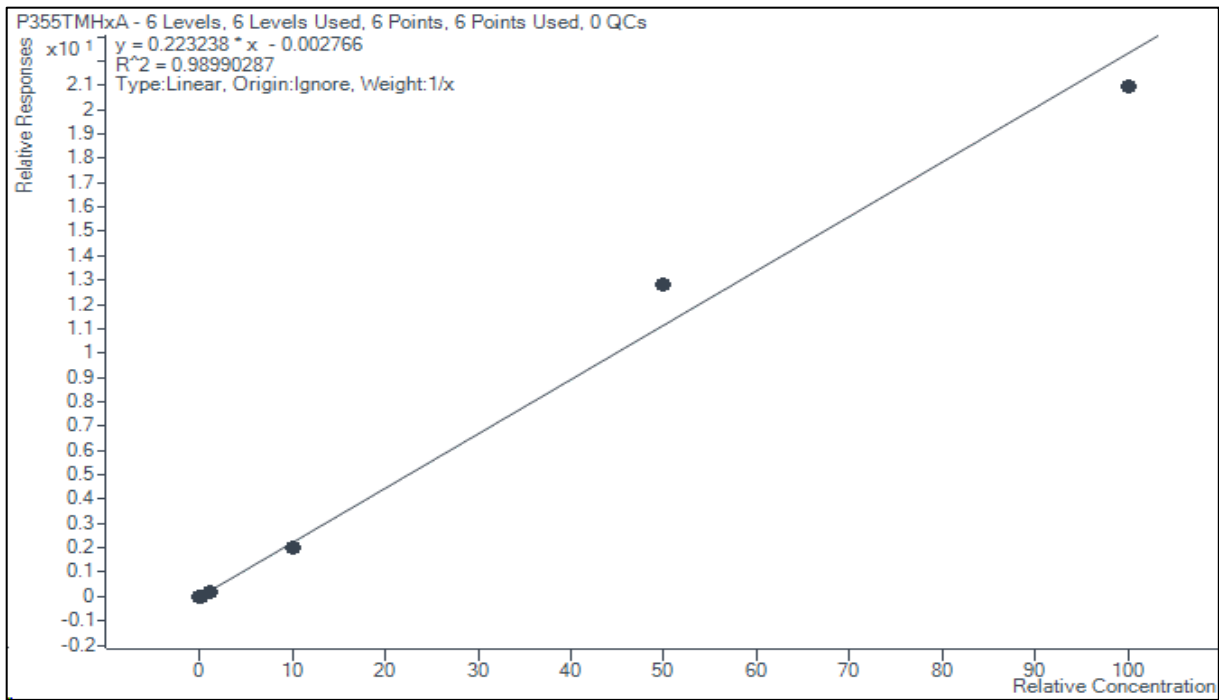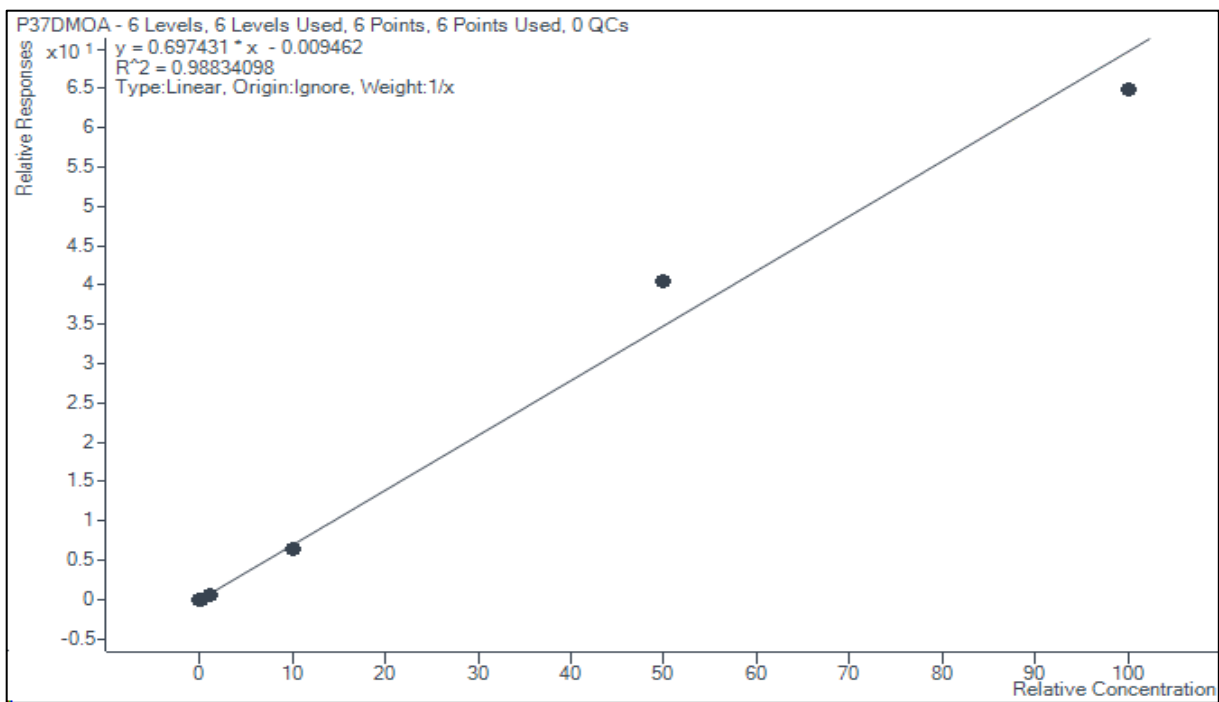| Name	Type	Level	Acq. Date-Time	P3MHpA RT	P3MHpA Area	P3MHpA Calc. Conc.	P355TMHxA RT	P355TMHxA Area	P355TMHxA Calc. Conc.	T-PFOA RT	T-PFOA Area	T-PFOA Calc. Conc.	P4MOA RT	P4MOA Area	P4MOA Calc. Conc.	P37DMOA RT	P37DMOA Area	P37DMOA Calc. Conc.	ipPFNA RT	ipPFNA Area	ipPFNA Calc. Conc.
STD 0.1ng/mL	Cal	1	22.03.2023 14:12	17,272	1395,49	0,14586182	18,582	25,3332	0,14360552	20,754	532,2638	0,1642302	21,283	58,5364	0,17407965	22,699	15,66903	0,13957225	22,932	111,671	0,16163531
STD 1ng/mL	Cal	2	22.03.2023 14:43	17,237	3589,89	0,76043181	18,671	848,372	0,79985205	20,737	3827,553	0,75642343	21,318	1257,293	0,70408969	22,752	2787,735	0,84664242	22,896	3072,918	0,74710122
STD 10ng/mL	Cal	3	22.03.2023 15:13	17,255	27960,64	7,67856928	18,706	9391,37	7,79347338	20,737	36573,03	6,78243038	21,336	14240,42	6,59481783	22,734	27884,56	7,42476318	22,932	33149,72	6,85179547
STD 100ng/mL	Cal	4	22.03.2023 15:44	17,255	339832,1	92,8421574	18,688	113404	89,797145	20,719	474275,9	84,3398822	21,336	188741	82,8714523	22,734	364883,8	92,4897133	22,932	446261	87,6250808
STD 500ng/mL	Cal	5	22.03.2023 16:15	17,219	1579493	574,998527	18,653	545978	574,208085	20,701	2372343	560,575681	21,318	936868,6	546,161909	22,699	1723080	580,062347	22,896	2145377	559,400938
STD 1000 ng/mL	Cal	6	22.03.2023 16:45	17,201	2867262	934,674453	18,653	996628	938,357839	20,683	4530777	958,481353	21,283	1867479	974,593651	22,681	3086305	930,136962	22,861	4096837	956,313449
Blank	Blank		22.03.2023 17:46	17,237	1005,819	0,07786545	18,671	77,0361	0,192028	20,737	876,7459	0,24540525	21,247	45,33278	0,17105547	22,717	162,7936	0,18175738	22,879	80,79406	0,15780751
Blank	Blank		22.03.2023 18:17	17,219	730,2178	0,00236664	18,671	62,2889	0,18118376	20,719	515,8709	0,1777775	21,283	32,39597	0,1653473	22,681	115,7844	0,16975719	22,95	150,3297	0,17437095
Blank	Blank		22.03.2023 18:48	17,237	982,445	0,06669159	18,706	50,2467	0,16774093	20,808	1465,046	0,35844121	21,283	118,1281	0,20597029	22,681	32,76806	0,14482251	22,95	126,0218	0,16735644
Blind L	Sample		22.03.2023 19:18	17,237	1042,571	0,16579501	18,671	116,185	0,25132342	20,719	337,3492	0,15430039	21,265	126,3152	0,22562177	22,752	29,47495	0,14601711	22,95	149,1204	0,18063957
Blind L	Sample		22.03.2023 19:49	17,237	1008,26	0,14691312	18,635	45,6508	0,17319701	20,665	272,1682	0,1372125	21,301	97,86545	0,20741813	22,77	56,5024	0,15520278	22,95	116,8679	0,1713844
Blind L	Sample		22.03.2023 20:20	17,219	779,2199	0,05534932	18,706	39,2395	0,16541704	20,648	374,705	0,16026118	21,247	88,28721	0,2006173	22,699	98,8047	0,16913759	22,95	151,1575	0,17974896
Blind M	Sample		22.03.2023 20:50	17,219	565,0466	0	18,688	39,4609	0,14983692	20,861	1126,883	0,23764358	21,247	104,1239	0,18677736	22,717	126,5484	0,16230189	22,879	281,9303	0,18604707
Blind M	Sample		22.03.2023 21:21	17,184	691,5905	0	18,688	57,183	0,15831098	20,665	711,2547	0,1673576	21,247	105,2568	0,18394783	22,717	138,342	0,16232289	22,896	161,346	0,16416818
Blind M	Sample		22.03.2023 21:52	17,237	481,2846	0	18,688	40,6939	0,14883706	20,648	1028,934	0,21288652	21,318	151,1749	0,2001961	22,663	271,1754	0,18887734	22,879	112,2428	0,15714919
0.1ng/mL L	Sample		22.03.2023 22:53	17,166	866,8087	0,11109661	18,688	41,5449	0,17112847	20,737	351,078	0,16085546	21,283	324,2801	0,35319609	22,628	218,7425	0,21527821	22,95	413,5134	0,25665431
0.1ng/mL M	Sample		22.03.2023 23:23	17,148	1030,48	0	18,635	216,46	0,25717905	20,648	1073,074	0,21963222	21,23	503,1353	0,32055132	22,663	532,2304	0,24057002	22,861	344,5755	0,19269367
0.5ng/mL L	Sample		22.03.2023 23:54	17,095	1612,662	0,37416409	18,617	390,729	0,54670712	20,594	2001,878	0,55791986	21,212	1323,765	0,94281242	22,628	1239,189	0,56488931	22,843	1311,902	0,49204605
0.5ng/mL L	Sample		23.03.2023 00:25	17,13	1799,269	0,55869805	18,582	413,825	0,64779643	20,559	1682,447	0,54976596	21,194	1238,4	1,01783142	22,628	898,4913	0,49976519	22,825	1300,389	0,54823981
0.5ng/mL L	Sample		23.03.2023 00:55	17,095	1868,393	0,47969044	18,546	429,928	0,59555588	20,612	2081,906	0,58437551	21,176	881,3111	0,68473907	22,628	1121,746	0,52958048	22,808	1329,091	0,50158588
0.5ng/mL M	Sample		23.03.2023 01:26	17,113	1979,318	0,2037049	18,564	541,964	0,46696437	20,594	3400,215	0,55480172	21,265	1569,328	0,69945291	22,646	2632,937	0,66915535	22,825	3245,383	0,64941238
0.5ng/mL M	Sample		23.03.2023 01:57	17,13	2002,479	0,199551	18,564	578,146	0,48217308	20,577	2891,459	0,47378906	21,176	1479,227	0,65692618	22,646	2231,112	0,57823167	22,737	2771,3	0,56586589
0.5ng/mL M	Sample		23.03.2023 02:27	17,077	1712,286	0,15714595	18,546	425,546	0,40187154	20,577	2997,621	0,51115233	21,176	1931,34	0,84810815	22,646	2495,138	0,65737793	22,754	2787,291	0,59148841
1ng/mL L	Sample		23.03.2023 02:58	17,113	2356,668	0,72090493	18,529	744,673	0,99165313	20,559	3017,833	0,8613496	21,23	1617,039	1,19326032	22,61	1682,663	0,76329193	22,825	1692,124	0,62894277
1ng/mL M	Sample		23.03.2023 03:28	17,113	2974,904	0,44257619	18,582	886,668	0,70288679	20,612	5531,6	0,88280429	21,212	2847,878	1,1795941	22,646	2849,679	0,73129912	22,754	4737,227	0,90700725
10ng/mL L	Sample		23.03.2023 03:59	17,059	14824,86	5,36855115	18,529	6680,29	7,40803243	20,559	23141,38	5,7410317	21,176	24369,7	14,8772725	22,628	17740,58	6,32748021	22,772	16885,81	4,70482009
10ng/mL L	Sample		23.03.2023 04:30	17,059	26862,57	10,1973151	18,529	7679,62	8,73091818	20,559	30411,85	7,72989998	21,176	23701,16	14,8721867	22,61	17891,65	6,55412694	22,772	24676,4	6,99663721
10ng/mL L	Sample		23.03.2023 05:00	17,059	24857,21	9,07411473	18,511	8636,48	9,45749998	20,523	33342,98	8,16804424	21,176	27359,19	16,5373409	22,574	17863,57	6,31508916	22,737	22846,46	6,26136275
10ng/mL M	Sample		23.03.2023 05:31	17,042	31528,04	6,63732946	18,493	11267,6	7,21011304	20,523	56741,82	8,08958856	21,141	43469,1	15,3015095	22,574	36506,53	7,48457158	22,737	57936,85	9,17346565
10ng/mL M	Sample		23.03.2023 06:02	17,059	34693,47	7,91911801	18,511	11115,1	7,66206268	20,559	50353,77	7,7445523	21,159	42808,08	16,2406042	22,574	38628,18	8,52110398	22,737	53993,3	9,21838818
10ng/mL M	Sample		23.03.2023 06:32	17,042	33501,35	7,01777379	18,529	11031,3	7,01459034	20,541	55264,57	7,82797623	21,159	42374,69	14,8200402	22,574	42742,49	8,68165989	22,737	59879,68	9,41319796
50ng/mL L	Sample		23.03.2023 07:03	17,024	123244,7	42,4470014	18,493	46428	46,5418789	20,506	194671,2	43,8041048	21,141	141068,1	78,3221115	22,574	103622,2	33,296522	22,754	131610,8	32,7618665
50ng/mL L	Sample		23.03.2023 07:33	17,024	136084,3	47,4066241	18,493	43685,9	44,2762963	20,506	183912,4	41,8373618	21,141	139718,9	78,4181811	22,557	104519,2	33,9480694	22,737	140271,3	35,2873798
50ng/mL L	Sample		23.03.2023 08:04	17,024	138597,5	49,7788641	18,475	46013,7	48,0595385	20,506	186488,6	43,725239	21,123	153046,5	88,5216367	22,557	113687,3	38,0453743	22,843		0
50ng/mL M	Sample		23.03.2023 08:35	17,006	163700,6	40,5918186	18,475	58964,2	42,577198	20,506	264592,3	42,8767765	21,123	235803,5	94,2503213	22,539	187743,3	43,4024019	22,719	367777,2	65,7875076
50ng/mL M	Sample		23.03.2023 09:05	16,988	173381,9	43,146755	18,458	60712,3	43,9780337	20,47	274009,1	44,5444776	21,105	240330	96,3688121	22,539	194313,6	45,0622832	22,701	371483,9	66,664909
50ng/mL M	Sample		23.03.2023 09:36	16,988	173633,1	44,0531952	18,44	59380,3	43,8488348	20,452	265482,5	43,9973598	21,105	246264,2	100,659405	22,521	185175,5	43,7809431	22,701	356740,1	65,2652653
100ng/mL L	Sample		23.03.2023 10:07	16,953	253025,1	92,7150782	18,422	85247	90,5347929	20,452	345425	82,3894765	21,088	273163,5	160,727578	22,539	203235,7	69,1292505	22,701	276272,2	72,7822973
100ng/mL M	Sample		23.03.2023 10:37	16,953	340222,7	87,9097182	18,422	116809	87,4942987	20,435	535302,8	90,0391304	21,07	470824,7	195,344582	22,503	373596,1	89,5808105	22,701	736705,5	136,752925
Matrix 50ng/mL L	Sample		24.03.2023 14:37	17,61	193530,5	57,1106585	18,99	72464,1	62,1131011	21,038	251043,6	48,3262498	21,585	100913,1	47,9968604	22,983	252508,2	69,2766258	23,163	300843,8	63,9435473
Matrix 50ng/mL L	Sample		24.03.2023 15:08	17,592	200589,3	56,2640524	18,99	76857,3	62,6209842	21,021	275438,6	50,3980952	21,585	111474,7	50,3917124	22,983	253357,8	66,0797587	23,163	327981,8	66,260355
Matrix 50ng/mL L	Sample		24.03.2023 15:38	17,592	195825,6	59,7205097	18,973	72927,3	64,5843868	21,021	268033,1	53,3055882	21,585	108856,4	53,4799659	22,983	242450,3	68,7307083	23,163	317764,8	69,7737329
Matrix 50ng/mL M	Sample		24.03.2023 16:09	17,574	207584,4	53,0988043	18,973	89443,6	66,4671072	21,021	308784,2	51,5351117	21,585	125446,3	51,7225863	22,983	259674,6	61,7871402	23,145	430431,9	79,2920489
Matrix50ng/mL M	Sample		24.03.2023 16:40	17,592	204990	56,822833	18,973	86483,8	69,6197851	21,021	293604,9	53,0849098	21,585	119967,6	53,5821088	22,983	243568,4	62,7843844	23,163	370630,5	73,9773532
Matrix 50ng/mL M	Sample		24.03.2023 17:10	17,574	205524	55,6871675	18,973	87230,5	68,6640204	21,003	289049	51,0905042	21,567	118480,9	51,7351502	22,965	245195,2	61,7868535	23,145	340631,5	66,4773465

Table F.2. *Raw data from method application, Ny-Ålesund samples.*

Sample			P3MHpA Results			P355TMHxA Results			T-PFOA Results			P4MOA Results			P37DMOA Results			ipPFNA Results		
Name	Type	Acq. Date-Time	RT	Area	Calc. Conc.	RT	Area	Calc. Conc.	RT	Area	Calc. Conc.	RT	Area	Calc. Conc.	RT	Area	Calc. Conc.	RT	Area	Calc. Conc.
STD 0.1	Cal	14.04.2023 15:19	12,424	902,5122	0,14874788	14,106	118,4787	0,12191257	16,119	1266,779	0,15632598	17,216	432,4074	0,15670834	18,916	18,21074	0,11150106	19,273	99,25484	0,14534107
STD 1	Cal	14.04.2023 15:49	12,477	4698,72	0,73851706	14,088	1895,783	0,9549072	16,19	7559,395	0,82151909	17,233	3056,578	0,82919104	19,253	5788,098	0,98962114	19,024	6123,524	0,85005831
STD 10	Cal	14.04.2023 16:20	12,53	46899,9	7,44438958	14,159	16261,52	7,81132571	16,136	62244,08	6,73051053	17,216	25964,92	6,82362847	19,253	52183,2	8,16671771	19,024	59964,4	7,25333365
STD 100	Cal	14.04.2023 16:50	12,477	527958,3	94,9343843	14,124	177838,7	96,08073	16,136	713310,1	87,2015889	17,198	290005,3	85,8842484	19,235	573253,8	100,435268	19,024	674478,3	90,8985719
STD 500	Cal	14.04.2023 17:21	12,441	2002845	572,387361	14,124	673365,7	577,89611	16,101	2851531	553,964075	17,18	1158583	545,114	19,218	2059348	572,946933	18,989	2572040	550,259202
STD 1000	Cal	14.04.2023 17:52	12,424	3289633	935,4466	14,106	1087045	928,235015	16,065	4977937	962,22598	17,145	2076928	972,292224	19,2	3354095	928,449959	18,971	4518165	961,693493
Method blank1	Blank	14.04.2023 18:53	12,477	1232,376	364,055332	14,159	212,0523	188,157863	16,19	712,0717	143,003821	17,233	60,31617	29,3742435	19,289	542,5644	156,111798	19,22	38,50687	8,64679427
Method blank2	Blank	14.04.2023 19:24	12,477	761,1246	801,008379	14,159	202,4422	639,785903	16,154	1970,729	1409,81277	17,198	310,8276	538,542121	19,235	484,7175	496,621541	19,007	421,7864	332,346241
Method blank3	Blank	14.04.2023 19:54	12,441	942,0702	310,839036	14,177	284,8612	282,286685	16,154	976,2792	218,981004	17,233	295,003	160,278397	18,916	38,49244	12,4705474	19,184	85,14476	21,1590622
Field blank 1	Blank	14.04.2023 20:25	12,406	721,7194	0,48686883	14,071	180,5774	0,42771231	16,083	878,1823	0,41757916	17,109	289,4892	0,36135675	18,827	38,92814	0,1340165	19,184	168,8632	0,21800418
Field blank 2	Blank	14.04.2023 20:55	12,388	884,1591	0,73963176	14,142	50,0099	0,1897412	16,136	1153,65	0,67066506	17,18	286,0183	0,43423289	18,827	43,81509	0,14414764	19,184	327,1145	0,33716516
Field blank 3	Blank	14.04.2023 21:26	12,424	841,8244	0,49670016	14,053	159,2379	0,3447417	16,083	2149,123	0,8734168	17,18	73,54414	0,1132491	18,987	38,54257	0,13062067	19,238	77,18476	0,1672333
NÅ-W-01A	Sample	14.04.2023 21:57	12,353	13891,65	1,28683298	14,088	68,13599	0,08365923	16,03	326728,2	20,5311363	17,091	409,772	0,10466137	19,129	272,1165	0,13311681	20,001	21276,58	1,6041692
NÅ-W-01B	Sample	14.04.2023 22:27	12,317	9815,085	1,18485729	14,106	81,27134	0,09412819	16,03	214994,5	17,6039933	17,109	293,9256	0,10058171	18,898	25,78746	0,11167399	20,001	13282,32	1,32962092
NÅ-W-02A	Sample	14.04.2023 22:58	12,353	5393,568	1,03292405	14,088	237,1521	0,200639	16,03	203264,1	26,3823296	17,091	177,8955	0,09823632	18,845	17,91398	0,11198068	18,936	430,0316	0,1948195
NÅ-W-01B	Sample	14.04.2023 23:29	12,388	1834,97	1,34859554	14,124	33,77917	0,13909849	16,048	55309,69	27,5723126	17,127	508,9693	0,65642479	19,164	358,4108	0,36432508	19,149	92,75958	0,18428716
NÅ-W-08A	Sample	14.04.2023 23:59	12,317	1045,272	0,14077096	14,142	40,10123	0,08054531	16,03	80224,03	7,165688	17,109	266,1729	0,09978919	19,147	274,6865	0,14369744	19,202	236,2335	0,15658158
NÅ-W-08B	Sample	15.04.2023 00:30	12,335	675,9335	0,06665777	14,124	40,1873	0,07599058	16,03	4535,057	0,3048313	17,02	245,3885	0,07994335	19,111	182,249	0,12515907	19,113	112,8725	0,14126794
NÅ-W-16	Sample	15.04.2023 01:01	12,299	2501,794	0,22643168	14,071	88,52621	0,08842114	15,977	54219,62	3,29827415	17,109	291,1712	0,08501793	19,093	133,0132	0,12017652	18,847	704,1367	0,18031134
NÅ-S-01	Sample	15.04.2023 01:31	12,495	1003,094	0,567298	14,071	121,6823	0,27002802	16,048	31589,34	12,0813547	17,127	178,2413	0,2072	18,987	12,91905	0,11571795	19,131	286,172	0,25373104
NÅ-S-02	Sample	15.04.2023 02:02	12,797	1619,835	1,13362657	14,142	12,55868	0,09106588	16,207	61098,98	28,9873091	16,789	13,54583	0,05791027	18,951	23,88938	0,12487254	19,042	410,18	0,34753583